A study on the mechanism whereby lysophosphatidylcholine enhances neurotrophin-induced signals

神経栄養因子シグナルに対するリゾホスファチジルコリンの増強作用に関する研究

烏漢其木格

A study on the mechanism whereby lysophosphatidylcholine enhances neurotrophin-induced signals

（神経栄養因子シグナルに対するリゾホスファチジルコリンの増強作用に関する研究）

オハンチメグ
烏漢其木格

論文題目

A study on the mechanism whereby lysophosphatidylcholine enhances neurotrophin-induced signals

（神経栄養因子シグナルに対するリゾホスファチジルコリンの増強作用に関する研究）

応用生命工学専攻
平成 22 年度博士課程入学
氏　名　烏漢其木格
指導教員名　　北本　勝ひこ

A study on the mechanism whereby lysophosphatidylcholine enhances neurotrophin-induced signals

（神経栄養因子シグナルに対するリゾホスファチジルコリンの増強作用に関する研究）

by

Wuhanqimuge

A dissertation submitted in partial fulfillment
of the requirements for the degree of
P.h. D.

Department of Biotechnology
Graduate School of Agricultural and Life Sciences
The University of Tokyo

Table of contents **Page numbers**

General introduction

Neurotrophins

Neurotrophins, including nerve growth factor (NGF) (1), brain-derived neurotrophic factor (BDNF) (2), neurotrophin-3 (NT-3) (3), and neurotrophin-4 (NT-4) (4), are a family of small secreted proteins. They are called neurotrophins (or neurotrophic factors), since this family of growth factors are able to induce the growth of new neurons and support the survival, differentiation, and functions of existing neurons. Neurotrophins, therefore, play essential roles in the nervous system through regulating the number and diverse physiological functions of various types of neurons throughout the entire life. Neurotrophins are highly conserved in sequence, with around 50% similarity in pairwise alignment, and also in their structure. Neurotrophins form and act as homodimers in solutions and tissues, but several heterodimers among neurotrophins have also been identified, such as BDNF/NT-3, BDNF/NT-4, and NGF/BDNF heterodimers (5-12).

Neurotrophins and their receptors

Neurotrophins function through two distinct classes of membrane receptors: tropomyosin-related kinase (Trk), carrying an intrinsic tyrosine kinase activity in its intracellular domain, and the receptor p75 for neurotrophins ($p75^{NTR}$) that belongs to the death receptor family. Trk receptors include TrkA, TrkB, and TrkC. Neurotrophins bind to Trk receptors with high affinity, while they bind to p75 with low affinity. For example, K_d of NGF for TrkA is ~10^{-11} M, while that for p75 is ~10^{-9} M (13). Neurotrophins selectively bind to Trk receptors: NGF specifically binds to TrkA, BDNF and NT-4 bind to TrkB, and NT-3 binds to TrkC. NT-3 also binds to TrkA and TrkB with lower affinity. In contrast, all neurotrophins bind to p75 with nearly equal affinity (Fig. 0-1, 3,6,7,14).

Neurotrophins-Trk receptors-mediated signals

Neurotrophins are often released from the target organs and bind to Trk and/or p75 receptors on the surface of axonal terminal of neurons. The axons of neurons are quite long, as axons can extend to one meter. The signaling complex (such as NGF-TrkA complex) is internalized through endocytosis after their binding, and travels in a signaling endosome for a long distance from the axonal terminal to the cell body, where they induce various signaling pathways and regulate the gene expression and cellular responses. This is known as long-distance retrograde signaling (14). Binding of neurotrophins to Trk receptors results in the phosphorylation of tyrosine residues in the intracellular domain, such as tyrosine 490, 670, 674, 675, and 785 of TrkA (analogous phosphorylation sites are present in TrkB and TrkC), and generate the binding site for the signaling molecules containing phosphotyrosine binding domain, or Src homology domain 2 (SH2). Tyrosine 490 and 785 of TrkA are known to be the major phosphorylated sites. Phosphorylation of TrkA at tyrosine 490 induces the recruitment of signaling molecule Shc through SH2, and another molecule Grb2, which recruits additional adaptor proteins Sos and Gab-1. This results in the activation of small G protein Ras, which induces the activation of mitogen-activated protein kinase (MAPK; Erk1/2) signaling cascade. Recruitment of signaling complex to the same site of Trk receptors also activates phosphatidylinositol 3-kinase (PI3K)-Akt signaling pathway. Phosphorylation of TrkA at tyrosine 785 induces the activation of phospholipase C-γ1 (PLC-γ1) pathway. Eventually, activation of these signaling cascades promotes survival, differentiation, or proliferation of neurons (Fig. 1-1, 7).

Neurotrophins-p75-mediated signals

Binding of neurotrophins to the receptor p75 triggers both survival and apoptotic pathways in different conditions. By binding to p75, neurotrophins support the cell survival mainly through nuclear factor-kappa B and Akt signaling pathways, while induce apoptotic death of cells through c-Jun N-terminal kinase (JNK)-dependent signaling pathway, generation of ceramide by acid

sphingomyelinase, or the activation of caspases by the actions of adaptor proteins, NRAGE and NADE. Activation of these apoptotic pathways inhibits the survival signals, stimulates proapoptotic inducer gene expression, or directly leads to the cell cycle arrest, thereby resulting in apoptosis (7,8).

Processing of proneurotrophins to mature neurotrophins

While all the above-mentioned discussion focused on the mature form of neurotrophins, it should be noted that neurotrophins are initially synthesized as proforms, proNGF, proBDNF, proNT-3, and proNT-4, and then processed into the mature forms by protease cleavage. For example, proNGF is mainly converted into mature NGF intracellularly by furin and other proconvertase cleavages, and secreted as a mature form in the tissues in normal condition. Furin is a protease enriched in the Golgi apparatus. It was reported that furin cleaves proNGF at its N-terminal cleavage sites. Evidence suggests that NGF is also released in its proform (proNGF), and the amount of secreted proNGF in the tissues is increased during the Alzheimer's disease. Secreted proNGF is converted into its mature form in the extracellular space mainly by plasmin cleavage at both N- and C-terminal cleavage sites. Plasmin is a serine protease present in the blood plasma, and cleaves various unprocessed proteins into their mature forms. Similar to NGF, proBDNF is converted to mature BDNF intracellularly by proconvertases including furin or extracellularly by plasmin. All the proforms of neurotrophins bind to p75 with equally high affinity and induce JNK-dependent intrinsic apoptosis, while they do not bind to Trk receptors (Fig. 0-1, 8,15-17).

Neurotrophins and neurodegenerative diseases

In a number of studies, NGF and BDNF have been implicated in the pathogenesis of several neurodegenerative diseases, such as Alzheimer's disease and Parkinson's disease, although the exact mechanism has not been fully elucidated. In the most of the patients with Alzheimer's disease, it has been found that there is an increase in proNGF and a decrease of TrkA, while p75 is not changed. Therefore, it is

hypothesized that the maturation of NGF from proNGF is prevented possibly because of the reduced level of plasmin or the inhibition of retrograde transport of signaling complex. Increased proNGF interacts with p75, and induces the apoptotic signals instead of survival signals in Alzheimer's disease (15,16). The role of BDNF in Alzheimer's disease seems to be different, since significantly reduced level of both proBDNF and BDNF was found in the patients with Alzheimer's disease (15,17). Since NGF and BDNF play essential roles in neurodegenerative diseases, therapeutic use of NGF and BDNF has been widely studied (15,17). However, neurotrophins themselves have poor pharmacokinetics, mainly because they are easy to be hydrolyzed in tissues. In addition, they have limited ability to pass through the blood-brain barrier, and their ability to distribute to the tissues is also restricted (18). These properties have caused difficulties in clinical delivery of NGF or BDNF to the correct locations where they are needed. Hence, small molecules with the ability to interact with TrkA, TrkB, and/or other survival factors for neurons are also of great interest for many therapeutic applications (18).

Secretory phospholipase A_2

Phospholipase A_2 (PLA_2) is comprised of a diverse class of enzymes which catalyze the hydrolysis of the *sn*-2 ester bond of phospholipids to liberate free fatty acids and lysophospholipids. They are mainly classified into four groups: secretory PLA_2 ($sPLA_2$), cytosolic PLA_2 ($cPLA_2$), calcium-independent PLA_2, and platelet-activating factor acetylhydrolase family. It is widely recognized that through releasing lysophospholipids and fatty acids, especially arachidonic acid (AA), PLA_2s play important roles in numerous cellular processes (19-21). In mammals, 12 isoforms of $sPLA_2$ have been found, and are named as $sPLA_2$ group IB, IIA, IIC, IID, IIE, IIF, V, X, XIIA (~20 kDa), XIIB (~20 kDa), III (~55 kDa), and otoconin (90-95 kDa). The $sPLA_2$s in group I, II, V, and X are small proteins with molecular weight ranging from 14 to 18 kDa, and are similar in structure containing Ca^{2+}-binding loop and the same catalytic site (21).

$sPLA_2$-IB is secreted in pancreatic juice and cleaved by trypsin to produce

active form in the intestine. It digests dietary and biliary phospholipids to release lysophosphilipids and free fatty acids in the intestinal tract. Inhibition of $sPLA_2$-IB was found to reduce diet-induced obesity and diabetes, possibly through preventing intestinal digestion of phospholipids, thereby improving insulin sensitivity. Low level expression of $sPLA_2$-IB was also found in other tissues, including lung and liver, but it varies among species. For example, $sPAL_2$-IB is highly expressed in the stomach of guinea pig, but not in healthy human stomach. $sPLA_2$-IB is unable to release AA by hydrolyzing phosphatidylcholine (PC) because of its poor binding affinity to PC (21,22).

$sPLA_2$-IIA is continuously expressed in paneth cells in intestine, and its expression is highly increased in various cells, including macrophages, vascular smooth muscle, and gastric epithelial cells, upon proinflammatory stimuli in a wide range of animal species. $sPLA_2$-IIA is also abundant in exocrine fluids. The antibacterial activity is the best-characterized physiological function of this enzyme. $sPLA_2$-IIA preferably bind to phosphatidylethanolamine (PE) and phosphatidylglycerol which are rich in bacterial membrane, and degrade these phospholipids, thereby protecting the host from infection. Like $sPLA_2$-IB, $sPLA_2$-IIA has weak binding affinity to PC on the cell surface, but $sPLA_2$-IIA is able to induce the release of AA intracellularly via heparan sulfate proteoglycans (HSPG)-dependent pathway, which was suggested to be involved in inflammation. In HSPG-dependent pathway, $sPLA_2$-IIA is sorted by glycosylphosphatidylinositol-anchored HSPG, internalized, and releases AA inside the cells from the perturbed microdomains in either caveolae or intracellular membranes (21,22).

Both $sPLA_2$-V and $sPLA_2$-X are expressed in bronchial epithelial cells, and their expression is remarkably increased in the patients with asthma. $sPLA_2$-V induces the release of AA through both PC-dependent and HSPG-dependent pathways. The expression of $sPLA_2$-V was also found to be induced in human lungs with inflammation, which might be attributed to the abnormal hydrolysis of lung surfactant by $sPLA_2$-V. In addition, $sPLA_2$-V is expressed in heart at high level, but its physiological functions have not been identified. Like $sPLA_2$-IB, $sPLA_2$-X is

synthesized as inactive proenzyme, and converted to its active form by protease cleavage. The expression of $sPLA_2$-X was detected in intestine, stomach, colons, spleen, thymus, and blood leukocytes, as well as in lung (21,22). Among mammalian $sPLA_2$s, $sPLA_2$-X can most efficiently bind to PC on the outer leaflet of plasma membrane, and release AA by its hydrolytic activity, while it has no affinity for heparin (22,23). Both $sPLA_2$-V and $sPLA_2$-X regulate the allergic response by mediating the release of AA, LPC, and derivatized lipid mediators. Also, high expression level of $sPLA_2$-X detected in digestive and immune organs may suggest important roles of this enzyme in phospholipid digestion and lipid mediator production. Moreover, $sPLA_2$-IIA, III, V, and X are supposed to play critical roles in atherosclerosis. Numerous studies have found that different isoforms of $sPLA_2$s play essential roles in various diseases, such as inflammatory diseases, infectious diseases, diabetes, and cancer. Therefore, identifying the biological roles of these enzymes is the most challenging theme in the filed of $sPLA_2$ (21,22).

Lysophosphatidylcholine

Lysophosphatidylcholine (LPC) is known as a bioactive lipid released from the PC of cell membrane or PC of lipoprotein by the hydrolytic activity of $sPLA_2$ in the blood (Fig. 0-2 A; 22-24). LPC can also be generated by endothelial lipase or by lecithin-cholesterol acyltransferase secreted from the liver (22-26). The concentration of LPC in human plasma separated from fresh blood is around 190 μM, but it can be up to 800 μM in blood plasma of other mammalian species (26). It is mainly present in a complex with albumin, oxidized low-density lipoproteins (Ox-LDL), or other lipoproteins (23,27,28). LPC in the plasma has several molecular species carrying saturated or unsaturated fatty acyl chains of different length, and exists as a mixture composed of LPC 16:0 (40%), 18:0 and 18:1 (10-15%), 18:2 (20%), and 20:4 (10%) in the plasma (26,28).

LPC is the main component of Ox-LDL. The level of LPC is increased at maximum by 5-fold when low density lipoprotein (LDL) is oxidized by various stimuli (22), such as UV radiation (29) and lipoxygenase treatments (30), compared to

the normal LDL. Endothelial and smooth muscle cells (31), monocytes, macrophages, and neurotrophils (30) were also reported to oxidize LDL *in vitro* to produce LPC. It is likely that the formation of LPC in Ox-LDL plays a critical role in the atherogenic effect of Ox-LDL (22,32). Besides, the increased level of LPC was reported in the site of inflammation (33) where LPC regulates the inflammation possibly through inducing the expression of proinflammatory mediator cyclooxygenase type 2 (COX-2) (34). Activation of p38, as well as the transcription factors cAMP response element-binding protein (CREB) and ATF-1 might be involved in this process (35,36). Furthermore, it was reported that LPC induces the expression of vascular cell adhesion molecule-1 and intercellular adhesion molecule-1 (37), attracts phagocytes to apoptotic cells (38), and induces chemotaxis in other types of cells (39,40). In addition, LPC was found to increase intracellular Ca^{2+} in macrophages and neurotrophils (41,42), and activate protein kinase C, activator protein-1, and c-Jun N-terminal kinase in several types of cells (43-46). By evoking various cellular responses as mentioned above, LPC plays critical roles in sepsis, rheumatoid arthritis, and multiple sclerosis, but the mechanisms seem to be complicated. A specific receptor and mechanism for the diverse biological functions of LPC has not been identified.

Other lysophospholipids

Many other lysophospholipids have been found *in vivo*, although their concentration is relatively low compared to LPC which is most abundant in the plasma. Among them, physiological and pathological roles of lysophosphatidic acid (LPA) and sphingosine 1-phosphate (S1P) are well characterized both *in vitro* and *in vivo*. LPA and S1P play essential roles in the various cellular responses through their G protein-coupled receptors (GPCR): $LPA_{1\text{-}5}$ and P2Y5 for LPA, and $S1P_{1\text{-}5}$ for S1P, respectively. LPA is produced from phosphatidic acid (PA) by PA-selective phospholipase A1 or from LPC by autotaxin, an enzyme that converts LPC to LPA. S1P is generated by the phosphorylation of sphingosine catalyzed by sphingosine kinases 1 and 2. LPA is detected in various biological fluids, such as serum, saliva,

and cerebrospinal fluid. LPA promotes the proliferation and migration of differentiated vascular smooth muscle cells, induces smooth muscle contraction and neurite retraction, and prevents apoptosis in various types of cells (47,48). LPA has also been shown to synergistically enhance NGF-induced MAPK phosphorylation in PC12 cells (49-51), which will be described in Chapter 1 in details.

Compared to studies in LPA and S1P, there are much less studies about the mechanisms and specific receptors for other lysophospholipids, such as lysophosphatidylserine (LPS) and lysophosphatidylethanolamine (LPE), although some biological actions of LPS and LPE have been found. LPS and LPE are produced from phosphatidylserine (PS) and PE by PS- or PE-selective phospholipases, respectively. LPS was reported to stimulate the degranulation of mast cells, enhances apoptotic cell engulfment by macrophages, and promotes NGF-induced neurite outgrowth in PC12 cells. GPCRs, G2A and GPR34, were found to be involved in some cellular functions of LPS (49). Studies about LPE have shown that it can increase the intracellular calcium and stimulate cellular invasion in human ovarian cancer cells. It was also reported that LPE induces the neuronal differentiation of PC12 cells. However, specific receptor(s) for LPE has not yet been reported (49).

Neurotrophin-like activity of $sPLA_2$ and LPC

Previous study in our laboratory demonstrated that $sPLA_2$ shows neurotrophin-like effects in PC12 cells (52) and in cerebellar granule neurons (CGNs) (53). PC12 cells are widely used as a model for studying the survival and differentiation of neurons, since these cells endogenously express receptors TrkA and p75, stop dividing, and differentiate into sympathetic-like neurons in response to NGF (53). Treatment of PC12 cells with $sPLA_2$ induced neuritogenesis and differentiation into a neuron-like phenotype as observed in NGF-treated PC12 cells. In addition, $sPLA_2$ rescued CGNs from apoptosis; when CGNs grown in a medium containing the depolarizing concentration of potassium are transferred to low potassium medium, cells undergo apoptosis, but this apoptosis was prevented by the addition of $sPLA_2$, mimicking the action of BDNF. Interestingly, $sPLA_2$-X, but not $sPLA_2$-IB or

$sPLA_2$-IIA, induced neurites in PC12 cells (52) and protected CGNs from apoptosis (53). Subsequent studies have shown that the neurotrophin-like activity of $sPLA_2$ is associated with the release of one of the lysophospholipids, LPC (Fig. 0-2 B). Indeed, LPC added at 100 μM and 10 μM to PC12 cells and CGNs, respectively, recapitulated the neurotrophin-like activity of $sPLA_2$, i.e. induction of neurite outgrowth in PC12 cells and protection of CGNs from apoptosis (55,56). However, the underlying mechanism remains largely unclear.

Objective

LPC was previously found to display neurotrophin-like activity in PC12 cells and in CGNs. The main objective of this study is to analyze the molecular mechanism in which LPC displays neurotrophin-like activity. It would provide important evidences for the development of a new method for combating the neurodegenerative diseases.

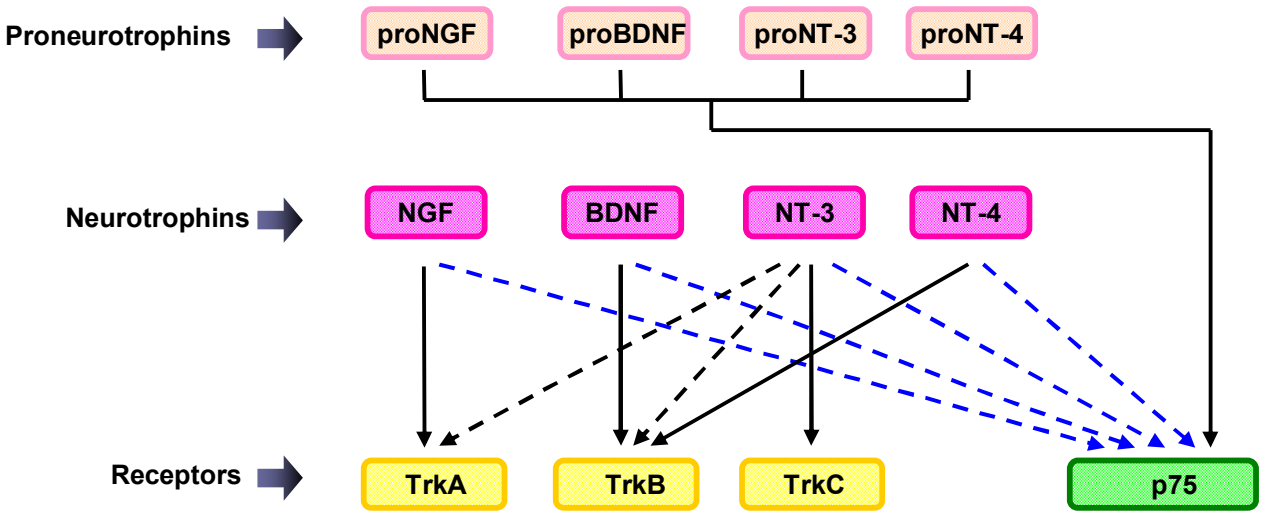

Figure 0-1 Proneurotrophins and mature neurotrophins, and their receptors

A

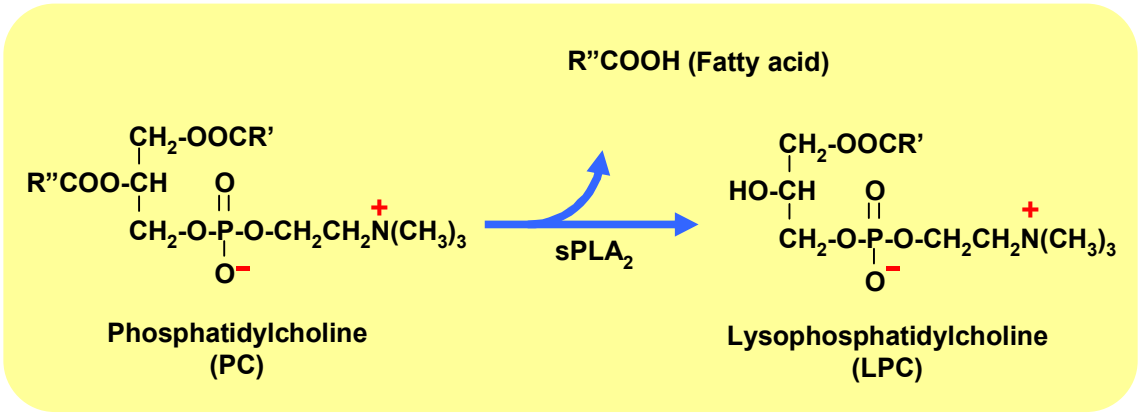

B

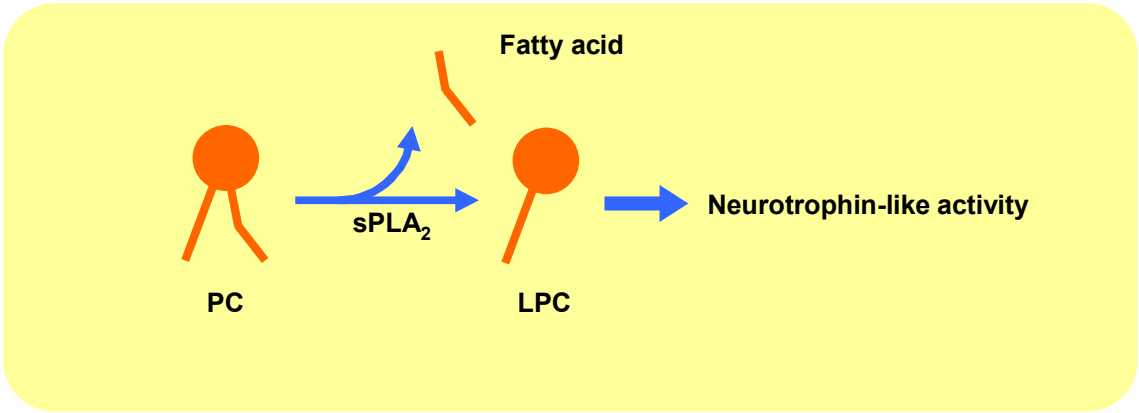

Figure 0-2 Generation of lysophosphatidylcholine by $sPLA_2$ from phosphatidylcholine shown in chemical structure in A, and in scheme in B

Chapter 1. Lysophosphatidylcholine enhances NGF-induced MAPK and Akt signals by enhancing the activation of TrkA in PC12 cells

1.1 Introduction

Nerve growth factor

Nerve growth factor (NGF) was initially found 60 years ago as a molecule that regulates the development of sensory and sympathetic neurons in the peripheral nervous system (PNS) (6). Critical biological functions of NGF in the central nervous system (CNS) have also been extensively characterized. NGF, the most extensively-characterized neurotrophin, is known to be generated from nonneuronal cells of target tissues, such as skin, muscle, testis, and salivary glands (5,6). NGF has two receptors, TrkA (with high affinity) and p75 (with low affinity). Binding of NGF to TrkA induces kinase activity of TrkA and its autophosphorylation at tyrosine residues. Phosphorylation of TrkA at tyrosine 490 recruits the signaling molecules such as Shc, and induces the activation of Ras-MAPK signaling cascade which is essential for neuronal differentiation (6,7,57,58). Activated TrkA also transmits signals to the PI3K-Akt signaling cascade which is important for cell survival. Phosphorylation of TrkA at tyrosine 785 leads to the activation of phospholipase C-γ1 pathway (6,7,58). These pathways eventually lead to the expression of immediate early genes, such as c-*fos* and *NGF-IA*, which are critical for cell proliferation, differentiation, and survival (Fig. 1-1) (59). Besides, by binding to the receptor p75, NGF induces the proapoptotic and prosurvival pathways. Studies found that activated TrkA can suppress p75-mediated

apoptotic pathways. On the other hand, p75 increases the binding specificity of NGF to TrkA, and promotes the retrograde transport of NGF-TrkA signaling complex. However, activated p75 was also reported to inhibit NGF-induced TrkA autophosphorylation. The interaction between TrkA and p75 appears to vary in different conditions and neurons (6).

Rat pheochromocytoma cells (PC12)

Rat pheochromocytoma PC12 is a cell line established from a solid tumor of chromaffin cells in the adrenal medulla. PC12 cells stop dividing and start differentiation in response to NGF, and show neuron-like properties. PC12 cells also respond to other growth factors that use the same signaling cascade, which leads to distinct outcomes. For example, epidermal growth factor (EGF) stimulation causes the proliferation, instead of differentiation, of PC12 cells. These properties make PC12 cells become a suitable model for studying the cellular responses of growth factors at the molecular level (60-63).

In this Chapter, I have examined the effect of LPC on MAPK and Akt phosphorylation in PC 12 cells, and found that LPC specifically enhanced NGF-induced MAPK and Akt phosphorylation. In accordance, NGF-induced expression of immediate early genes, c-*fos* and *NGF-IA*, was up-regulated by LPC. Phosphorylation of the upstream components, MEK and the NGF receptor TrkA, was also enhanced by LPC. In contrast, LPC did not affect EGF- or basic fibroblast growth factor (bFGF)-induced MAPK phosphorylation, and insulin-like growth factor-1 (IGF-1)-induced Akt phosphorylation. In addition, LPC did not enhance EGF-induced EGF receptor (EGFR) phosphorylation, which is in line with the fact that LPC does not promote EGF-induced

signal.

1.2 Objective

The specific objective of the work in this Chapter is to examine whether or not a cross-talk between NGF- and LPC-induced signals exists in PC12 cells, and to elucidate how the signals from LPC affect the signals from NGF.

1.3 Results

1.3.1 LPC enhances NGF-induced MAPK phosphorylation in PC12 cells

As mentioned in the Introduction, it was previously found that both $sPLA_2$ and LPC produced by the hydrolysis of phosphatidylcholine by $sPLA_2$ induced neuronal differentiation of PC12 cells (52,55), mimicking the action of NGF. It is well-known that the activation of Ras-MAPK signaling pathway is necessary for NGF-initiated differentiation of PC12 cells (7,64). NGF induces MAPK signaling cascade through its receptor TrkA, while $sPLA_2$ is known to activate L-type Ca^{2+} channel, thereby also activating MAPK signaling pathway. Since NGF and LPC evoke the similar cellular responses but employ distinct pathways, it is of interest to examine whether a signaling cross-talk between NGF and LPC occurs in PC12 cells. To test this, PC12 cells were serum-starved for 1.5 h, and treated with NGF or LPC alone, or NGF and LPC together at specified concentrations for 10 min. Then, the amounts of phosphorylated MAPK (p-MAPK) and total MAPK (t-MAPK) were analyzed by Western blotting. The general experimental strategy is shown in Fig. 1-2. PC12 cells express two similar MAPKs, Erk1 (44 kDa) and Erk2 (42 kDa), which are phosphorylated on specific threonine 202 and tyrosine 204 residues upon NGF treatment. As shown in Figs. 1-3 A and B, treatment of cells with NGF (10 and 50 ng/ml) elicited modest level of MAPK phosphorylation, whereas treatment of cells with LPC alone (C16:0; 0.1 and 1 μM) did not induce MAPK phosphorylation. Interestingly, significant increase in MAPK phosphorylation was observed when the cells were treated with NGF and LPC together; at the highest, LPC (1 μM) enhanced NGF (50 ng/ml)-induced phosphorylation of MAPK by three- to four-fold compared to that in cells treated with NGF (50 ng/ml) alone. This increase was dose-dependent of LPC used, as the enhanced NGF-induced

MAPK phosphorylation by LPC at 0.1 μM was further increased at 1 μM. This result implicates that a cross-talk between NGF and LPC signaling pathways exists in PC12 cells.

1.3.2 LPC, but not other lysophospholipids tested, displays significant enhancement of NGF-induced MAPK phosphorylation in PC12 cells

The result shown in Fig. 1-3 prompted me to examine whether other lysophospholipids bearing different headgroups, such as LPA, LPE, and LPS, display similar enhancement of NGF-induced MAPK phosphorylation. As shown in Figs. 1-4 A and B, PC12 cells were treated with various lysophospholipids or NGF alone, or NGF together with various lysophospholipids for 10 min as indicated. Then, the amounts of p-MAPK and t-MAPK were analyzed by Western blotting, and p-MAPK/t-MAPK ratio was quantified. The result in Figs. 1-4 A and B shows that no significant phosphorylation of MAPK was seen in cells stimulated with these lysophospholipids alone at 1 μM. The result also shows that none of these lysophospholipids enhanced NGF-induced MAPK phosphorylation to comparable level of LPC. This result suggests a specific role of LPC on NGF-induced signaling in PC12 cells.

In my experimental condition, LPA (1 μM) alone dissolved in methanol did not induce MAPK phosphorylation (Fig. 1-4). This observation caught my attention, since it has been demonstrated that LPA alone is able to induce the phosphorylation of TrkA and MAPK through LPA receptor 1 (LPA_1) in PC12 cells. Also, LPA and NGF synergistically stimulate phosphorylation of MAPK and nuclear translocation of their receptors in PC12 cells (50). Constitutively active LPA_1 form a complex with TrkA, which enhances NGF-induced signals in PC12 cells expressing LPA_1 (51). In these

reports, LPA was dissolved in phosphate-buffered saline (PBS) containing different percentages of fatty acid-free bovine serum albumin (BSA). Thus, I tested the effect of LPA when it was dissolved in PBS containing 1% fatty acid-free BSA, instead of routinely-used methanol. I found that LPA (1 μM) alone induced MAPK phosphorylation, and synergistically enhanced NGF-induced MAPK phosphorylation to the similar level of LPC (Fig. 1-4). Dissolving LPA in methanol in my experiment might have impaired the activity of LPA to some extent.

1.3.3 LPC 14:0, 16:0, 18:0 and 18:1, but not 12:0, show significant enhancement of NGF-induced MAPK phosphorylation in PC12 cells

It has been reported that LPC species carrying different acyl chains in length and the degree of saturation play different biological roles. For example, LPC 16:0 and 18:0 reduced the background generation of reactive oxygen species (ROS), whereas LPC 16:1, 18:1, and 18:2 induced the intracellular production of ROS in human polymorphonuclear leukocytes (PMNs; 26). In neutrophils, saturated LPC 16:0 and 18:0 increased intracellular Ca^{2+} to much higher level than unsaturated LPC 18:1 (26). In primary human aortic endothelial cells (HAEC), LPC 16:0, 18:1, and 20:4 promoted the production of prostacyclin by 1.4-, 3-, and 8.3-fold, respectively. However, LPC 18:2 did not induce the production of prostacyclin in HAEC (65). Therefore, I examined if LPC 12:0, 14:0, 16:0, 18:0, and 18:1 have different effect on NGF-induced MAPK phosphorylation. Figs. 1-5 A and B show that LPC species carrying fatty acyl chains 14:0, 16:0, 18:0, and 18:1 effectively promoted NGF-induced MAPK phosphorylation to a similar extent, whereas LPC 12:0 was ineffective. Since LPC 16:0 is the most abundant component among these species in the human blood plasma as mentioned in

the General introduction, LPC 16:0 was used in all the following experiments.

1.3.4 LPC up-regulates the expression of NGF-induced immediate early genes, c-*fos* and *NGF-IA*, in PC12 cells

c-*fos* and *NGF-IA* are two of the major immediate early genes which are rapidly transcribed in response to many extracellular stimuli, including NGF, and are early components of a series of transcriptional events necessary for the initiation and maintenance of differentiation (59,66-69). To examine whether LPC also affects the NGF-induced expression of c-*fos* and *NGF-IA* at the downstream of MAPK in PC12 cells, cells stimulated with NGF in the presence or absence of LPC for 30 min were lysed, total RNA was isolated, and cDNA was synthesized by reverse transcription. Finally, the expression of both c-*fos* and *NGF-IA* genes was measured by semi-quantitative and quantitative RT-PCR (Figs. 1-6 and 1-7). Consistent with the result shown in Fig. 1-3, NGF (50 ng/ml) slightly induced the expression of c-*fos* and *NGF-IA*, and the addition of LPC (1 μM) significantly elevated the expression of both genes, while LPC alone failed to induce the expression (Figs. 1-7 A-D). This result shows that enhanced MAPK phosphorylation by LPC results in the up-regulation of c-*fos* and *NGF-IA* expression, suggesting again a functional role of LPC on NGF-induced signaling pathway.

1.3.5 LPC promotes NGF-induced MEK phosphorylation in PC12 cells

To pinpoint the cellular component at which the NGF signal is augmented by LPC, I next examined MEK1/2 (MEK) phosphorylation, which is just upstream of MAPK activation. Western blot analysis shows that phosphorylation of MEK triggered

by NGF was significantly enhanced by LPC (Figs. 1-8 A and B), indicating that LPC acts on or at the upstream of MEK.

1.3.6 LPC potentiates NGF-induced MAPK phosphorylation through enhancing the phosphorylation of receptor TrkA in PC12 cells

Next, I tested whether the enhancement of NGF-induced MAPK and MEK phosphorylation by LPC occurs via augmentation of TrkA activation. PC12 cells were stimulated with NGF in the presence or absence of LPC, and the phosphorylation of TrkA was analyzed by Western blotting using the antibody that recognizes TrkA phosphorylated at tyrosine 490; phosphorylation of TrkA at this site is known to be essential for NGF-induced MAPK and Akt activation in PC12 cells (7,70). Since the amount of endogenous TrkA is low, 6-cm dishes, instead of 24-well plates, were used to culture the cells to obtain clear image by Western blotting. As shown in Fig. 1-9, NGF (50 ng/ml) led to a slight phosphorylation of TrkA, which was significantly increased by the addition of LPC. Taken together, results obtained from Figs. 1-3 to 1-9 indicate that LPC promotes NGF-induced signaling through TrkA/MEK/MAPK pathway by enhancing the activation of TrkA in PC12 cells.

1.3.7 LPC also enhances Akt phosphorylation induced by NGF, but not by IGF-1, in PC12 cells

By binding to TrkA, NGF also activates PI3K-Akt pathway (Figs. 1-1 and 1-10). I next asked if LPC also enhances NGF-induced Akt phosphorylation in PC12 cells. To test this, PC12 cells stimulated with NGF in the presence or absence of LPC were analyzed for Akt phosphorylation using antibodies against phospho-Akt (Ser473) and

total Akt. As shown in Figs. 1-11 A and B, NGF-induced Akt phosphorylation was significantly increased by LPC, whereas the effect of LPC alone on Akt phosphorylation was minimal.

IGF-1 is a polypeptide trophic factor playing important roles in the survival and differentiation of both neuronal and non-neuronal cells. It has been shown that IGF-1 induces the phosphorylation of Akt and its survival pathway in PC12 cells (Fig. 1-10, 71). Since LPC enhanced NGF-induced Akt phosphorylation (Fig. 1-11), I tested if LPC has the similar effect on IGF-1-induced Akt phosphorylation. However, no significant enhancement of IGF-1-induced Akt phosphorylation was observed by LPC addition (Figs. 1-12 A and B). Thus, LPC does not affect IGF-1-induced Akt signaling. This result suggests that the effect of LPC is specific to NGF-TrkA pathway.

1.3.8 LPC elevates NGF-induced, but not EGF- or FGF-induced, MAPK phosphorylation in PC12 cells

Ras-MAPK cascade can also be triggered by various growth factors besides NGF, such as epidermal growth factor (EGF) and basic fibroblast growth factor (bFGF), and is essential for the effect of these growth factors (Fig. 1-13, 7,72-75). To test if LPC enhances MAPK phosphorylation induced by these growth factors, MAPK phosphorylation in PC12 cells stimulated with EGF, bFGF, and NGF in the presence or absence of LPC was analyzed in the time-course experiments in Figs.1-14, 1-15, and 1-16. As shown in Figs. 1-14 A and B, LPC significantly enhanced NGF-induced MAPK phosphorylation, and this effect was observed for as long as 30 min. In contrast, no increased phosphorylation of MAPK by LPC was detected in cells treated with EGF (Figs. 1-15 A and B) or bFGF (Figs. 1-16 A and B). These data pose again an interesting

possibility that LPC acts specifically on NGF-TrkA signaling pathway.

1.3.9 LPC does not affect EGF-induced EGF receptor phosphorylation in PC12 cells

To analyze why LPC did not enhance EGF-induced MAPK phosphorylation, I next tested the effect of LPC on EGF-induced EGF receptor (EGFR) phosphorylation. In line with the result showing that EGF-elicited MAPK phosphorylation was not enhanced by LPC (Fig. 1-15), EGF-induced autophosphorylation of EGFR at Tyr1173, which is involved in MAPK activation, was not affected by LPC (Figs. 1-17 A and B). Considering the possibility that EGF at 25 ng/ml used in Fig. 1-15 and 1-17 might have maximally induced the phosphorylation of MAPK and EGFR, so that no further increase of MAPK phosphorylation by LPC was detected, the effect of LPC on EGF-induced phosphorylation of MAPK and EGFR was also tested at lower concentrations of EGF (Fig. 1-18 A). Also, the effect of LPC on EGF-induced EGFR phosphorylation was examined in the time-course experiment (Fig. 1-18 B). In both experiments, similar results were observed to those obtained in Figs. 1-15 and 1-17; LPC did not enhance EGF-induced MAPK and EGFR phosphorylation in PC12 cells. Phosphorylation of MAPK and EGFR triggered by EGF was very rapid and transient, which is consistent with the well-known fact that EGF induces transient, but not sustained, phosphorylation of EGFR and MAPK in PC12 cells (63,75). These results confirmed that LPC does not affect EGF-induced signal in PC12 cells.

1.3.10 Effect of LPC on NGF-induced neurite outgrowth and morphological changes in PC12 cells.

To evaluate the effect of LPC on NGF-induced differentiation of PC12 cells, neurite outgrowth was assayed in PC12 cells cultured in the serum-free medium containing NGF and/or LPC for 48 h. Results in Figs. 1-19 A and B show that LPC added alone at 1 μM does not induce neurite outgrowth. In an agreement with the well-established observation, NGF added at 50 ng/ml induced neurite outgrowth. No significant increase was seen by the co-addition of LPC (1 μM), although a slight increase was seen. In this neurite outgrowth assay, only cells having neurites longer than the diameter of cell body were counted as positive. In fact, increased number of cells with enlarged cell body showing the tendency of differentiation (bearing short neurites) was observed when the cells were stimulated with NGF plus LPC, compared to the treatment with NGF alone. This suggests that LPC potentiates the NGF-induced initial differentiation of PC12 cells. Since LPC added at 10 μM displayed toxicity to the cells in the serum-free medium, the effect of LPC at higher concentrations was not tested.

1.4 Discussion

In this Chapter, I have demonstrated the effect of LPC on NGF-induced MAPK and Akt signaling pathways in PC12 cells and further characterized its signaling mode by which LPC enhances NGF-induced MAPK phosphorylation. Lysophospholipids with different headgroups (LPA, LPE, and LPS dissolved in methanol) also enhanced NGF-induced MAPK phosphorylation, but at a lower level than LPC (Fig. 1-4). Interestingly, similar headgroup specificity of lysophospholipid was observed in our previous studies wherein neurite outgrowth in PC12 cells and the cell survival of CGNs were examined; only LPC, but not other lysophospholipids, induced neurites in PC12 cells (52) and rescued CGNs from apoptosis (56). As mentioned earlier, LPA is known to synergistically stimulate NGF-induced MAPK phosphorylation through its receptor LPA_1 in PC12 cells (51). However, the signaling mechanism of LPC on NGF-induced MAPK phosphorylation still needs to be analyzed.

LPC species with the fatty acyl chains of 14:0, 16:0, 18:0, and 18:1, but not 12:0, enhanced NGF-induced MAPK phosphorylation. Again, similar results were obtained in our previous studies; LPC species containing the acyl chains of 14:0, 16:0, and 18:0, but not 12:0, were effective in neurite outgrowth of PC12 cells and survival of CGNs (55,56). Acyl chain-dependent effect of LPC on human neutrophils (26) and endothelial prostacyclin production (65) was previously described. Recently, distinct effect of different species of LPC on COX-2 expression in endothelial cells was also reported. In this report, LPC 16:0 and 20:0 increased both COX-2 mRNA and protein production, while LPC 18:1 showed only a weak increase in COX-2 mRNA. Interestingly, LPC 18:2 promoted COX-2 protein production without affecting mRNA level (35). These findings, together with the result in this study (Fig. 1-5), suggest the existence of LPC species-dependent effects in neuronal systems.

To identify the most upstream cellular component(s) affected by LPC, I examined the phosphorylation of MEK and TrkA. Interestingly, in addition to MEK, TrkA phosphorylation induced by NGF was significantly enhanced by LPC. Consistent with increased TrkA phosphorylation, NGF-induced Akt phosphorylation,

located at the downstream of TrkA, was also elevated by LPC. In contrast, EGF-induced phosphorylation of EGFR and MAPK was not affected by LPC. I also observed that bFGF-induced MAPK phosphorylation and IGF-1-induced Akt phosphorylation were not elevated by LPC. Collectively, these results clearly demonstrate that the effect of LPC is specific to NGF-TrkA system. Moreover, neurite outgrowth assay suggested that LPC, at least partially, affected NGF-induced neurite outgrowth, indicating that potentiation of NGF-TrkA signal by LPC functionally resulted in the differentiation phenotype of PC12 cells.

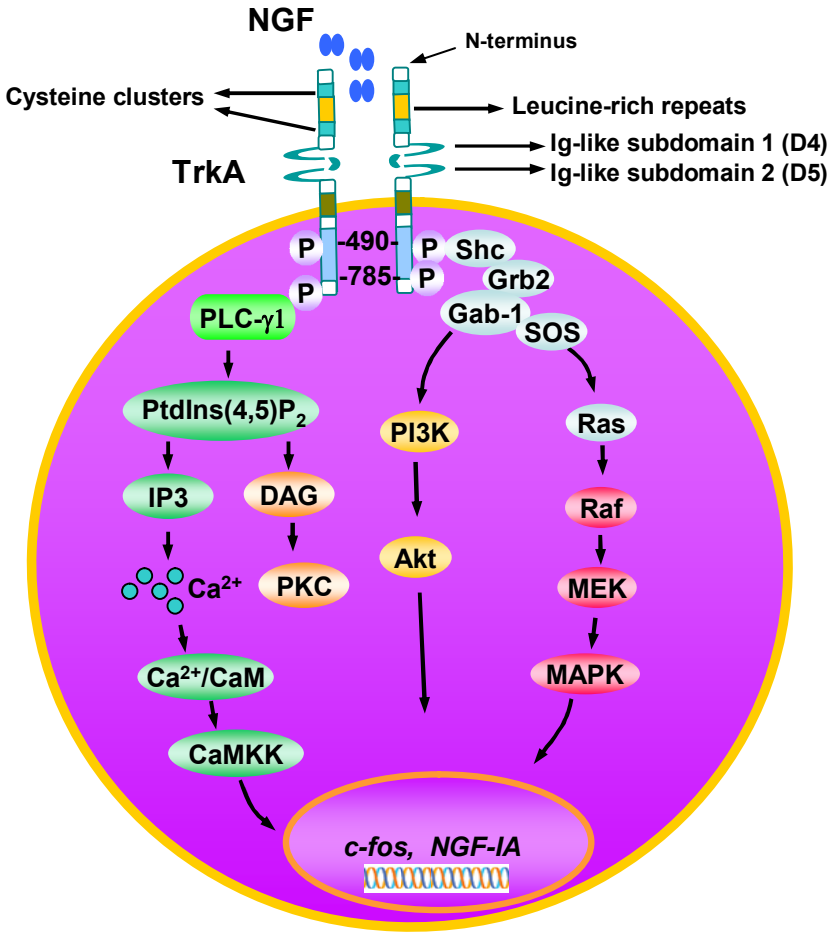

Figure 1-1 Major NGF-TrkA mediated signaling pathways

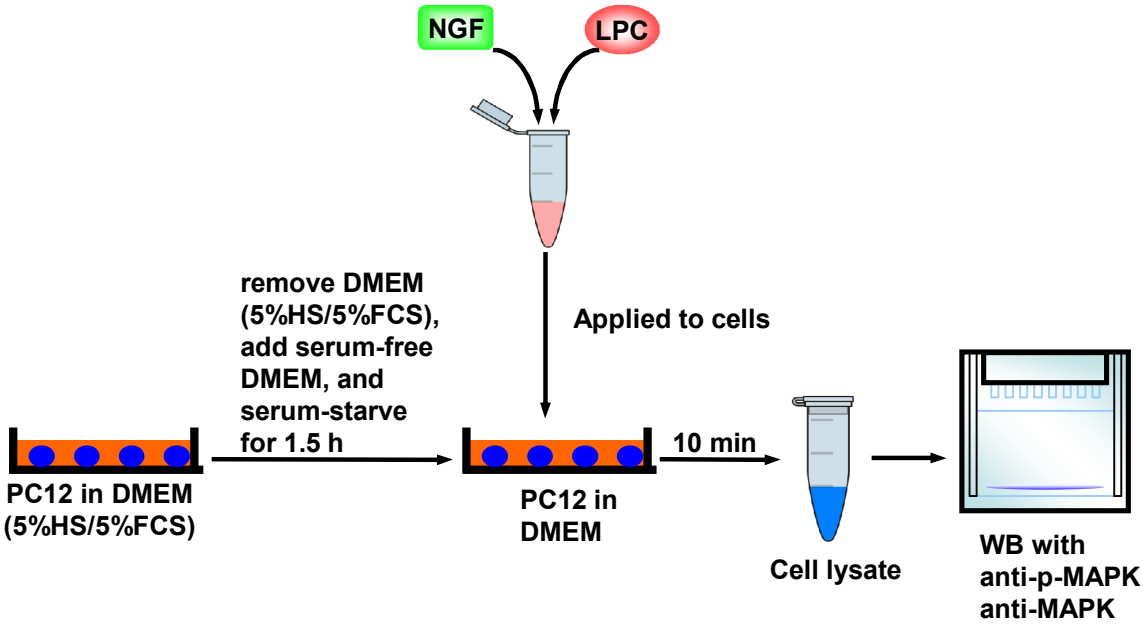

Figure 1-2 General experimental strategy for the detection of the effect of LPC on MAPK phosphorylation in PC12 cells. PC12 cells cultured on collagen-coated plates or dishes were serum-starved for 1.5 h, and then the cells were treated with vehicle control (DMEM plus methanol), NGF or LPC alone, or NGF and LPC together for 10 min or indicated times as described in the figure legend. Cells were lysed with 1×SDS sample buffer and boiled for 3 min. Equal amount of each sample was subjected to Western blotting. Phosphorylated MAPK (p-MAPK) and total MAPK (t-MAPK) were analyzed by Western blotting using phospho-p44/42 (Thr202/Tyr204) MAP Kinase and p44/42 MAP Kinase primary antibodies, respectively. In this figure, the experiment in which the cells are stimulated with NGF and LPC together is shown.

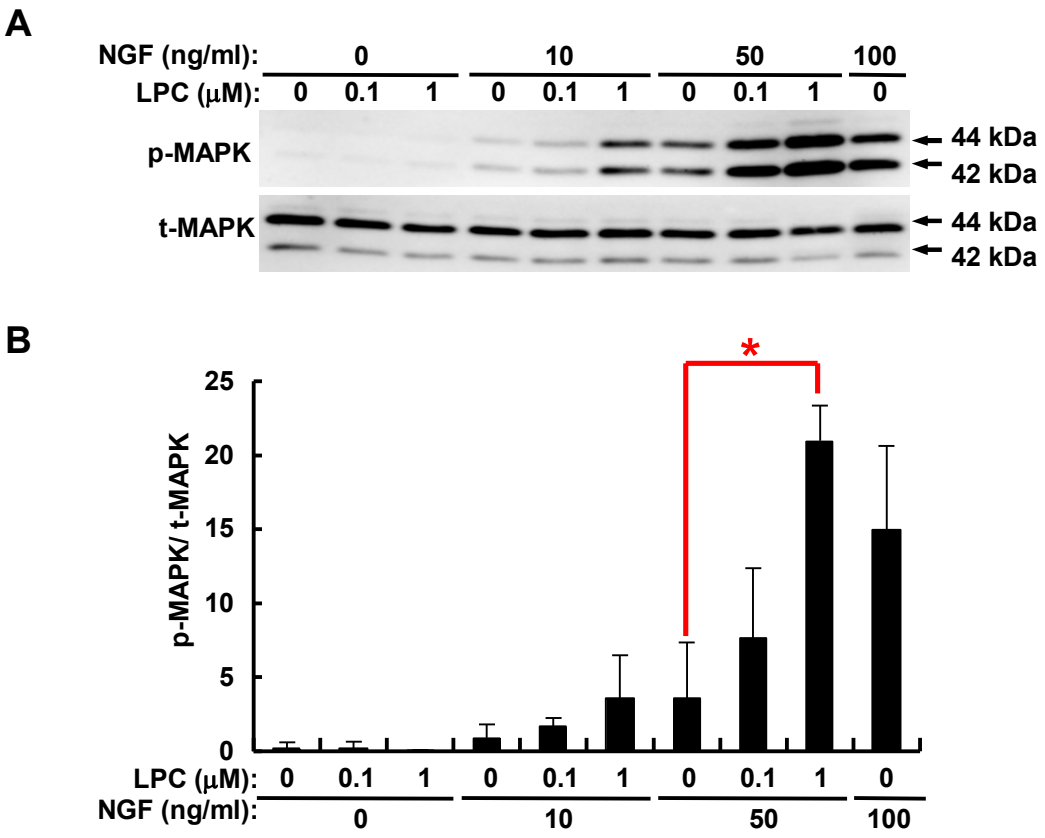

Figure 1-3 LPC enhances NGF-induced MAPK phosphorylation in PC12 cells. PC12 cells cultured in 24-well plate were serum-starved for 1.5 h, and treated with vehicle control (DMEM plus methanol), NGF (10, 50, and 100 ng/ml) or LPC (0.1 and 1 μM) alone, or NGF and LPC together as indicated for 10 min. Cells were lysed by adding 50 μl/well of 1 × SDS sample buffer and boiled for 3 min. Equal volume of each sample was subjected to Western blotting. **A**, phosphorylated MAPK (p-MAPK) and total MAPK (t-MAPK) were analyzed by Western blotting using phospho-p44/42 (Thr202/Tyr204) MAP Kinase and p44/42 MAP Kinase primary antibodies, respectively. The image shown is the representative of three independent experiments which gave similar results. **B**, the amounts of p-MAPK and t-MAPK were quantified and the relative ratio of p-MAPK vs t-MAPK in each condition was calculated. Data are means ± SD of three independent experiments. *, $p<0.01$ by one-way ANOVA.

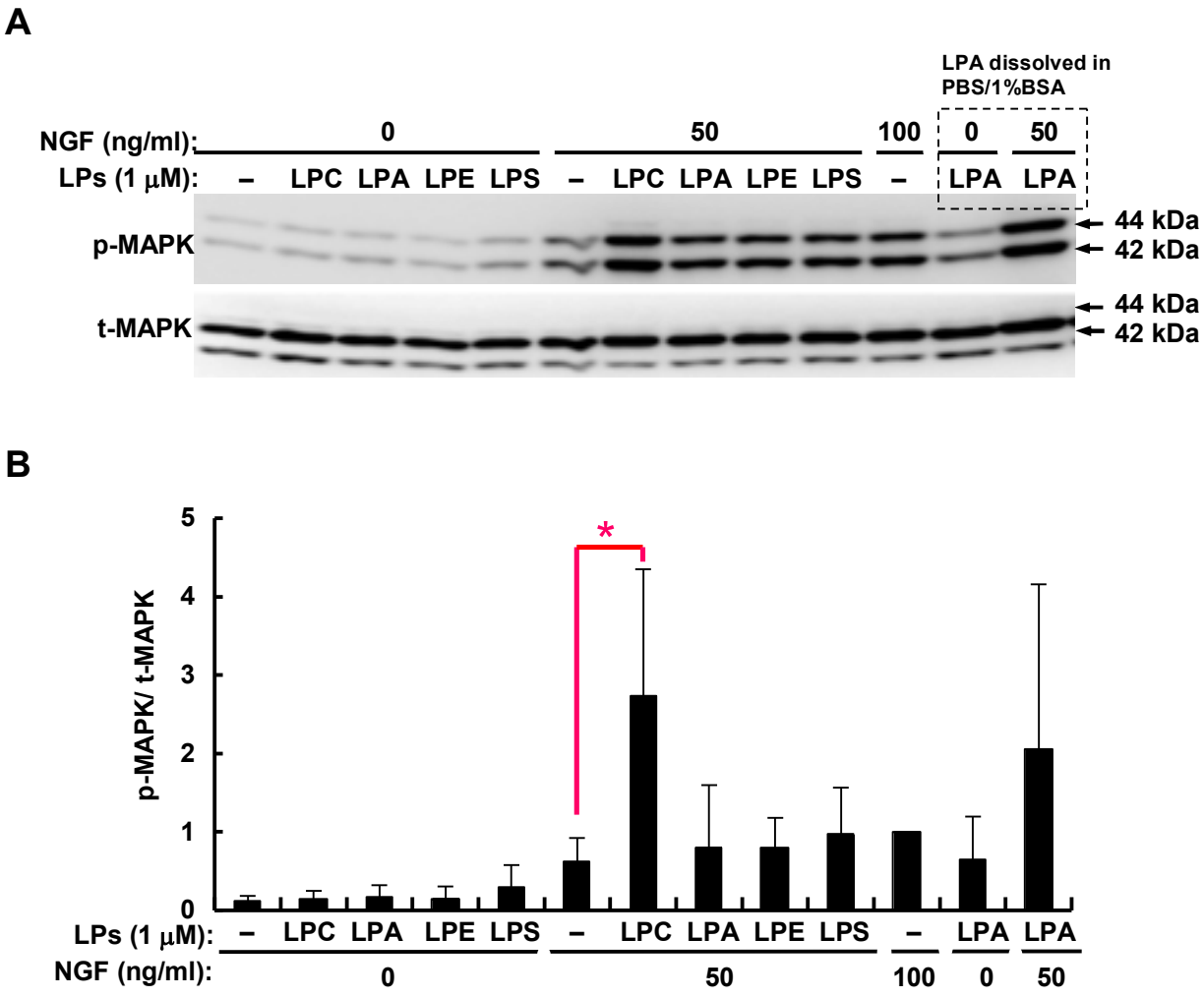

Figure 1-4 LPC, but not other lysophospholipids, displays significant enhancement of NGF-induced MAPK phosphorylation in PC12 cells. PC12 cells cultured in 24-well plate were serum-starved for 1.5 h, and treated with vehicle control (DMEM plus methanol), NGF (50 and 100 ng/ml) or lysophospholipids (LPC, LPA, LPE, and LPS at 1 μM) alone, or NGF and lysophospholipids together as indicated for 10 min. Cells were also treated with LPA (1 μM; dissolved in PBS containing 1% fatty acid-free BSA) alone or together with NGF for 10 min. Cells were lysed by adding 50 μl/well of 1×SDS sample buffer and boiled for 3 min. Equal volume of each sample was subjected to Western blotting as described in Materials and Methods. **A**, phosphorylated MAPK (p-MAPK) and total MAPK (t-MAPK) were analyzed by Western blotting using phospho-p44/42 (Thr202/Tyr204) MAP Kinase and p44/42 MAP Kinase primary antibodies, respectively. The image shown is the representative of three independent experiments which gave similar results. **B,** the amounts of p-MAPK and t-MAPK were quantified and the relative ratio of p-MAPK vs t-MAPK in each condition was calculated. Data are means ± SD of three independent experiments. *, $p<0.01$ by one-way ANOVA. PBS, phosphate-buffered saline; BSA, bovine serum albumin.

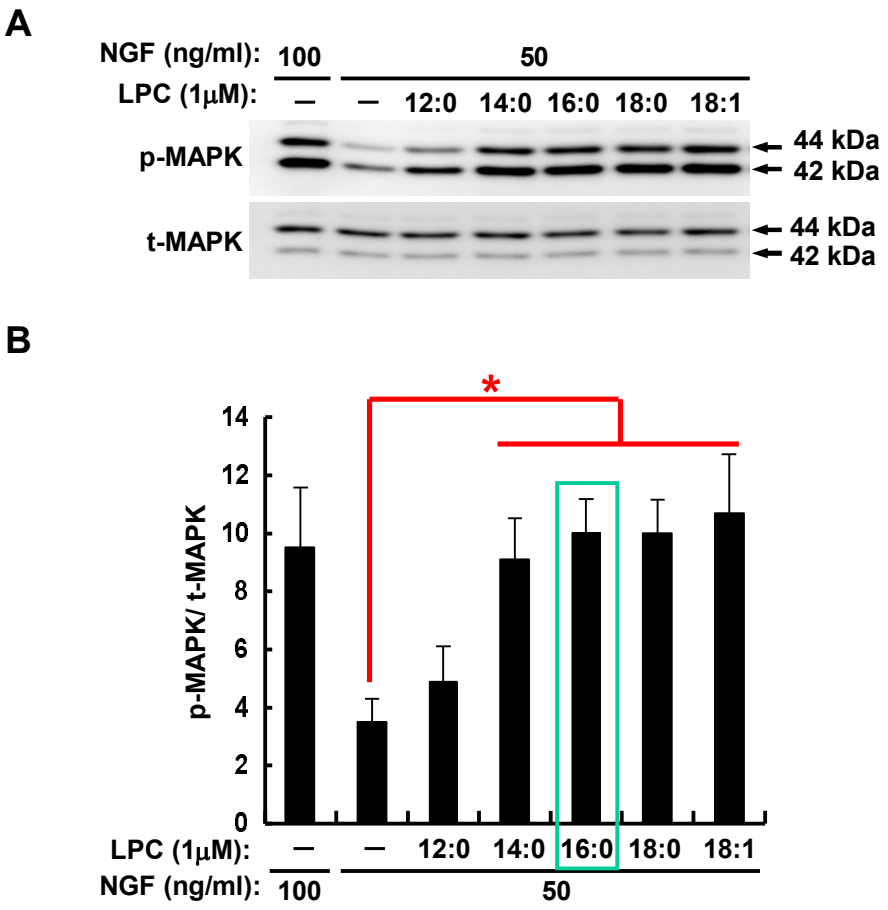

Figure 1-5 LPC 14:0, 16:0, 18:0, and 18:1, but not 12:0, show significant enhancement of NGF-induced MAPK phosphorylation in PC12 cells. PC12 cells cultured in 24-well plate were serum-starved for 1.5 h, and treated with NGF (50 and 100 ng/ml) alone, or NGF and various species of LPC (LPC 12:0, 14:0, 16:0, 18:0, and 18:1 at 1 μM) together as indicated for 10 min. Cells were lysed with 50 μl/well of 1×SDS sample buffer and boiled for 3 min. Equal volume of each sample was subjected to Western blotting as described in Materials and Methods. **A**, phosphorylated MAPK (p-MAPK) and total MAPK (t-MAPK) were analyzed by Western blotting using phospho-p44/42 (Thr202/Tyr204) MAP Kinase and p44/42 MAP Kinase primary antibodies, respectively. The image shown is the representative of three independent experiments which gave similar results. **B**, the amounts of p-MAPK and t-MAPK were quantified and the relative ratio of p-MAPK vs t-MAPK in each condition was calculated. Data are means ± SD of three independent experiments. *, $p<0.01$ by one-way ANOVA.

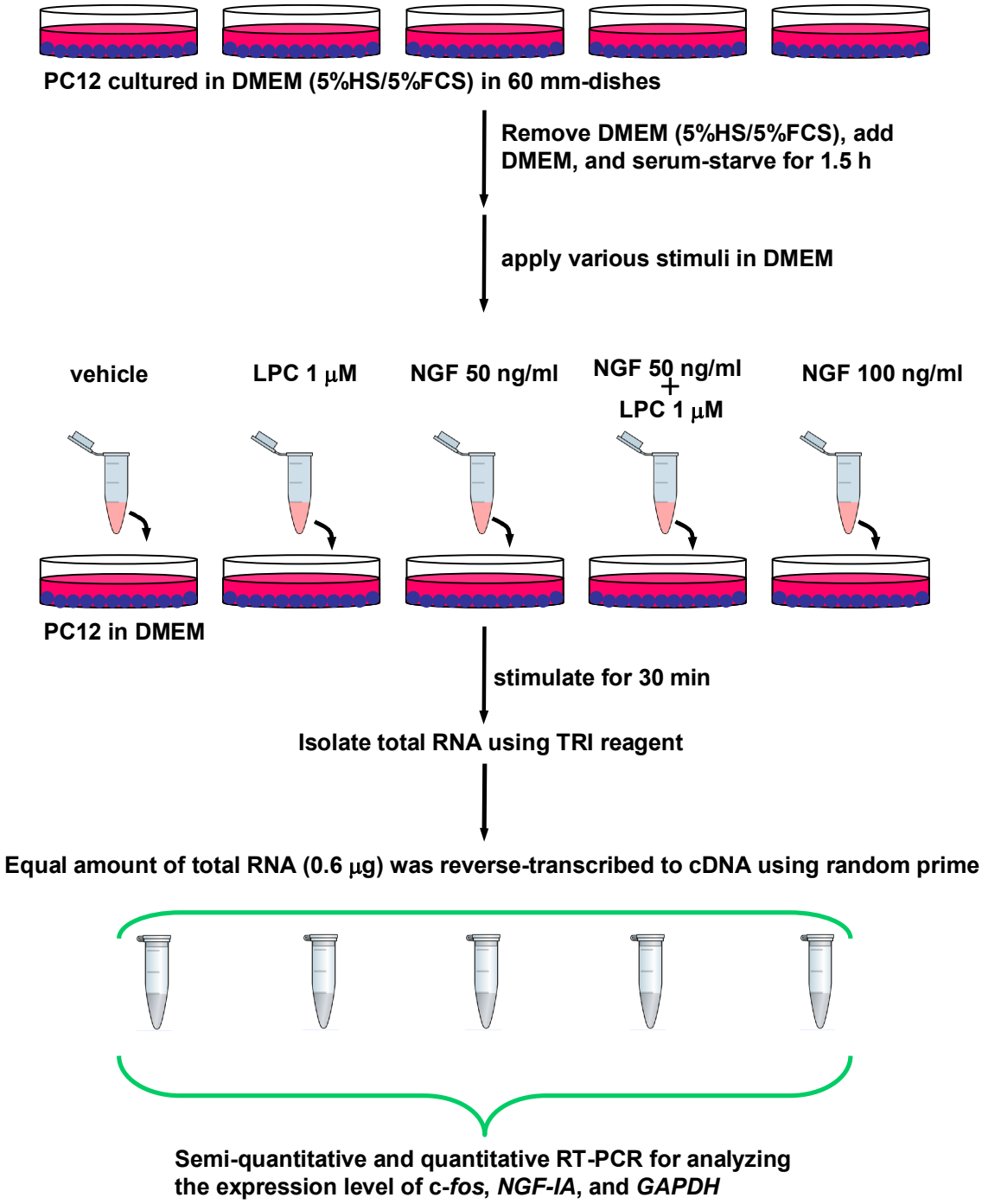

Figure 1-6 Experimental process for the analysis of the effect of LPC on the expression level of NGF-induced immediate early genes, c-*fos* and *NGF-IA*, in PC12 cells. PC12 cells cultured in 60 mm-dishes were serum-starved for 1.5 h, and the cells were treated with vehicle control, NGF or LPC alone, or NGF and LPC together for 30 min. The concentration of NGF and LPC shown in the figure is the final concentration.

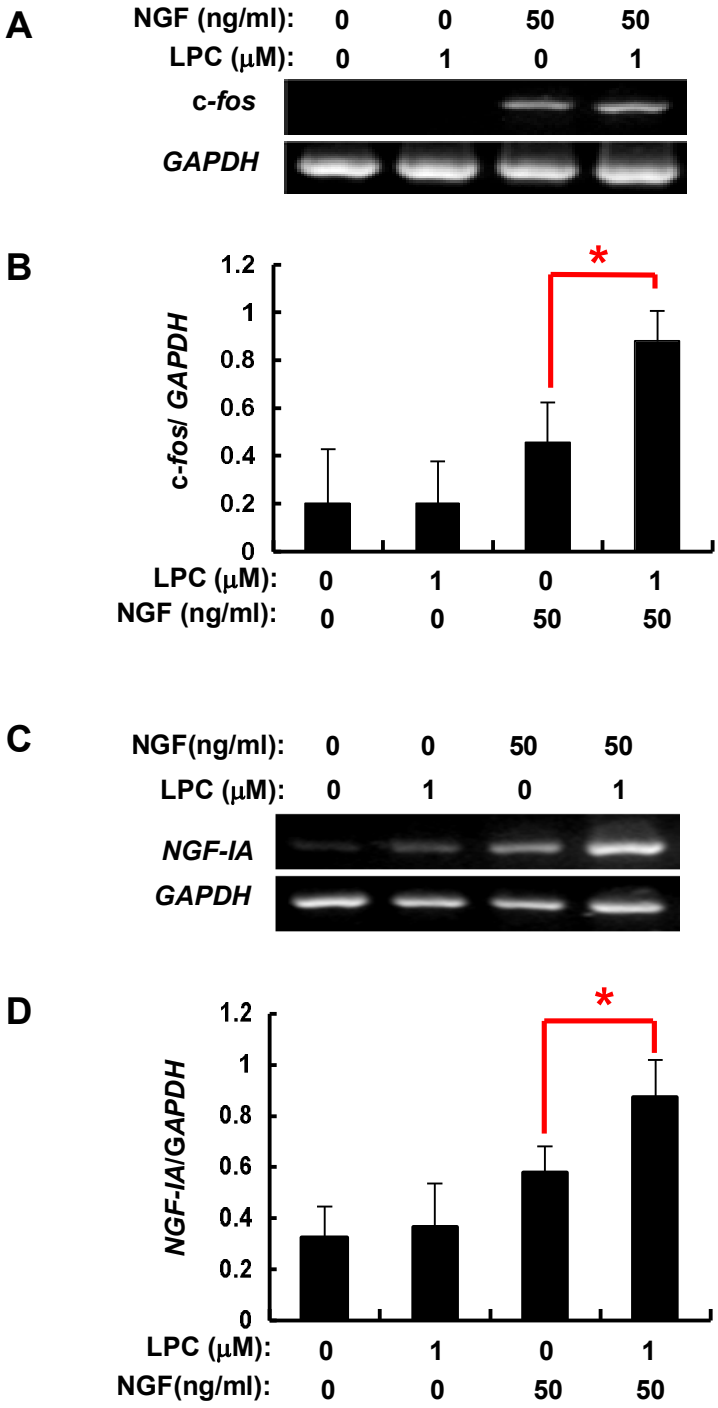

Figure 1-7 LPC up-regulates the expression of NGF-induced immediate early genes, *c-fos* and *NGF-IA*, in PC12 cells. PC12 cells were treated with vehicle control (DMEM plus methanol), LPC (1 μM) or NGF (50 and 100 ng/ml) alone or NGF (50 ng/ml) together with LPC for 30 min. Total RNA was isolated and reverse-transcribed using the random primer. **A** and **C**, the expression levels of c-*fos*, *NGF-IA*, and *GAPDH* were analyzed by semi-quantitative RT-PCR. **B** and **D**, the expression levels of c-*fos*, *NGF-IA*, and *GAPDH* were measured by quantitative real-time PCR. The amounts of transcripts for c-*fos* or *NGF-IA* relative to *GAPDH* were calculated by setting the value for NGF (100 ng/ml; not shown) at 1. Data are means ± SD of three independent experiments. *, $p<0.05$ by one-way ANOVA.

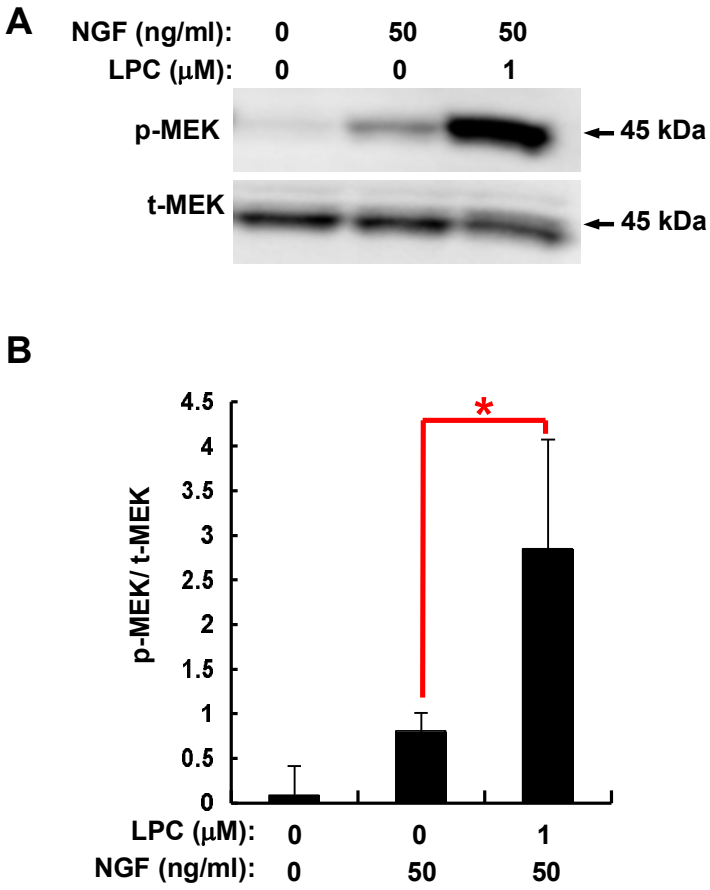

Figure 1-8 LPC promotes NGF-induced MEK (MEK 1/2) phosphorylation in PC12 cells. PC12 cells cultured in 60-mm dishes were serum-starved for 1.5 h, and then treated with vehicle control (DMEM plus methanol), or NGF (50 ng/ml) in the absence or presence of LPC (1 μM) for 5 min. Cells were lysed with 300 μl/well of 1 × SDS sample buffer and boiled for 3 min. Equal volume of each sample was subjected to Western blotting. **A**, phosphorylated MEK (p-MEK) and total MEK (t-MEK) were analyzed using anti-phospho-MEK1/2 (Ser 217/221) and anti-MEK1/2 antibodies, respectively. The image shown is the representative of five independent experiments which gave similar results. **B**, the amounts of p-MEK and t-MEK were quantified and the relative ratio of p-MEK vs t-MEK was calculated. Data are means ± SD of five independent experiments. *, $p<0.05$ by one-way ANOVA.

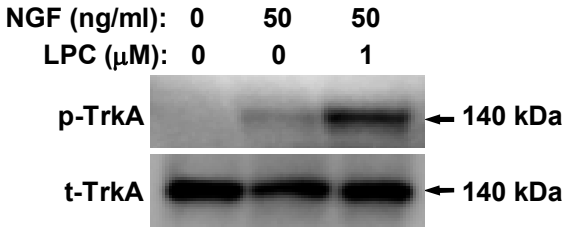

Figure 1-9 LPC potentiates NGF-induced MAPK phosphorylation through enhancing the phosphorylation of receptor TrkA in PC12 cells. PC12 cells cultured in 60-mm dishes were serum-starved for 1.5 h, and then treated with vehicle control (DMEM plus methanol), NGF (50 ng/ml) alone, or NGF plus LPC (1 μM) for 5 min. Cells in each dish were lysed with 300 μl/well of 1 × SDS sample buffer and boiled for 3 min. Equal volume of each sample was subjected to Western blotting. Phosphorylated TrkA (p-TrkA) and total TrkA (t-TrkA) were analyzed using anti-phospho-TrkA (Tyr490) and anti-TrkA antibodies, respectively. The image shown is a representative of four independent experiments which essentially gave similar results.

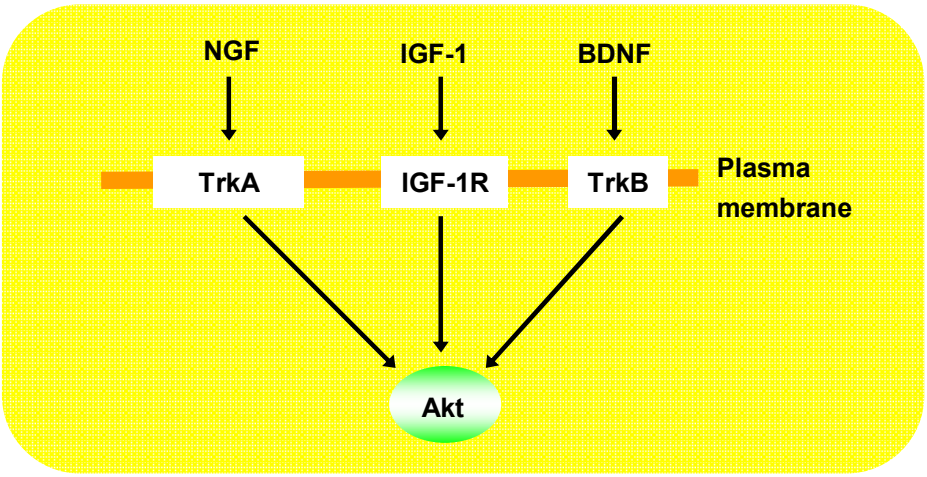

NGF: nerve growth factor; TrkA: NGF receptor,

IGF-1: insulin-like growth factor-1; IGF-1R: IGF-1 receptor,

BDNF: brain-derived neurotrophic factor; TrkB: BDNF receptor

Figure 1-10 Scheme showing that Akt can be phosphorylated by NGF, IGF-I, and BDNF

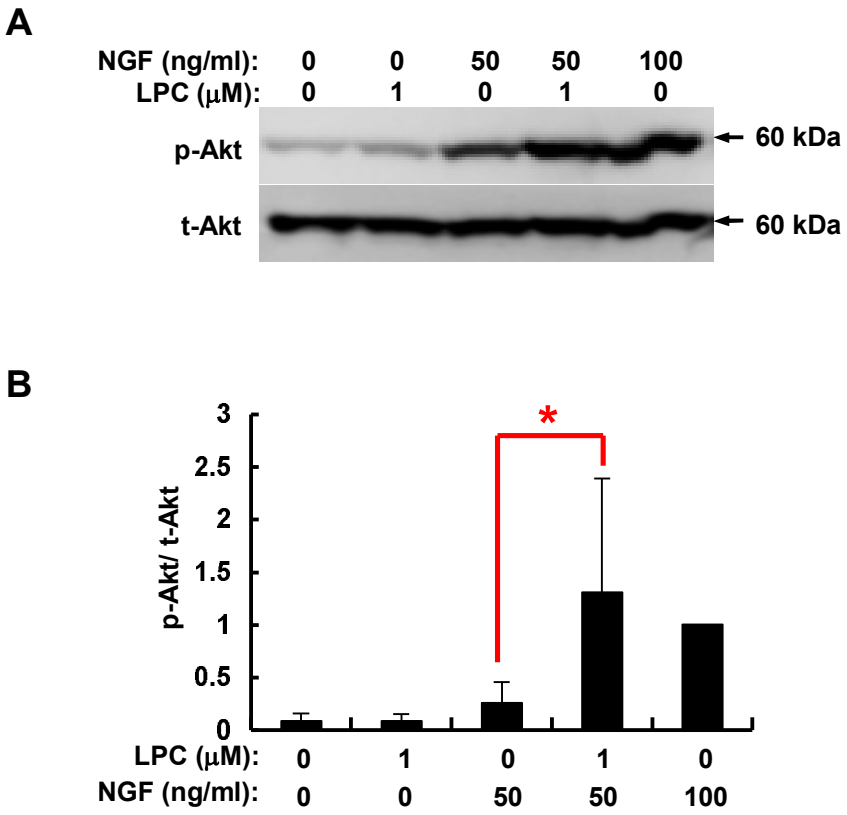

Figure 1-11 LPC also enhances NGF-induced Akt phosphorylation in PC12 cells. PC12 cells cultured in 24-well plate were serum-starved for 1.5 h, and the cells were treated with vehicle control (DMEM plus methanol), NGF (50 and 100 ng/ml) or LPC (1 μM) alone, or NGF (50 ng/ml) together with LPC for 10 min. **A**, phosphorylated Akt (p-Akt) and total Akt (t-Akt) were analyzed by Western blotting using anti-phospho-Akt (Ser473) and anti-Akt primary antibodies, respectively. The image shown is the representative of five independent experiments which gave similar results. **B**, the amounts of p-Akt and t-Akt were quantified and the relative ratio of p-Akt vs t-Akt was calculated by setting the value for NGF (100 ng/ml) at 1. Data are means ± SD of five independent experiments. *, $p<0.05$ by one-way ANOVA.

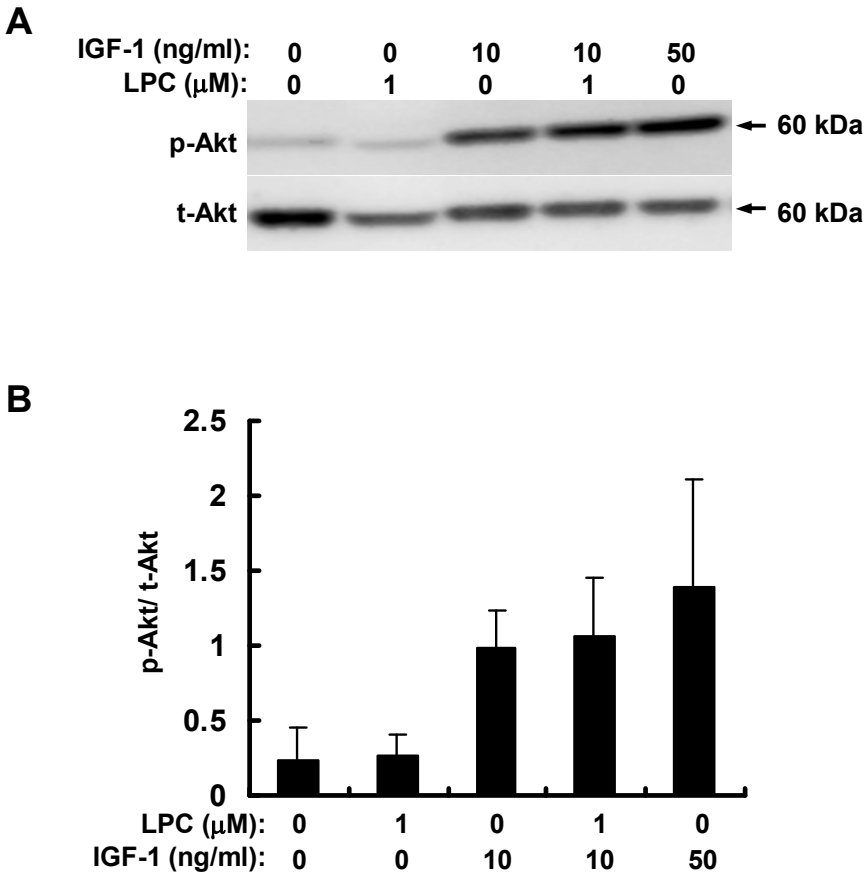

Figure 1-12 LPC does not affect IGF-1-induced Akt phosphorylation in PC12 cells. PC12 cells cultured in 24-well plate were serum-starved for 1.5 h, and the cells were treated with vehicle control (DMEM plus methanol), IGF-1 (10 and 50 ng/ml) or LPC (1 μM) alone, or IGF-1 (10 ng/ml) plus LPC for 30 min. **A**, phosphorylated Akt (p-Akt) and total Akt (t-Akt) were analyzed by Western blotting using anti-phospho-Akt (Ser473) and anti-Akt primary antibodies, respectively. The image shown is the representative of three independent experiments which gave similar results. Each experiment was done in duplicate. **B**, the amounts of p-Akt and t-Akt were quantified and the relative ratio of p-Akt vs t-Akt was calculated. Data are means ± SD of three independent experiments.

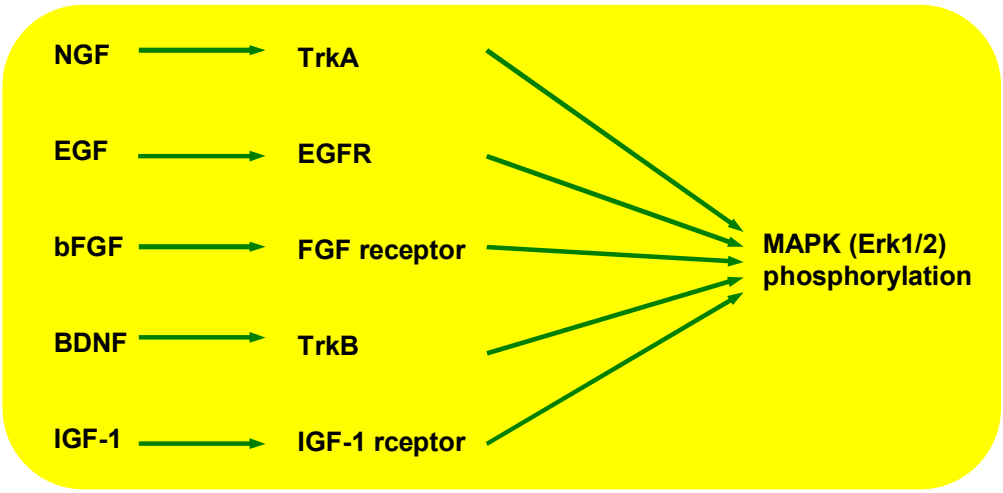

Figure 1-13 Scheme showing that MAPK can be phosphorylated by various growth factors

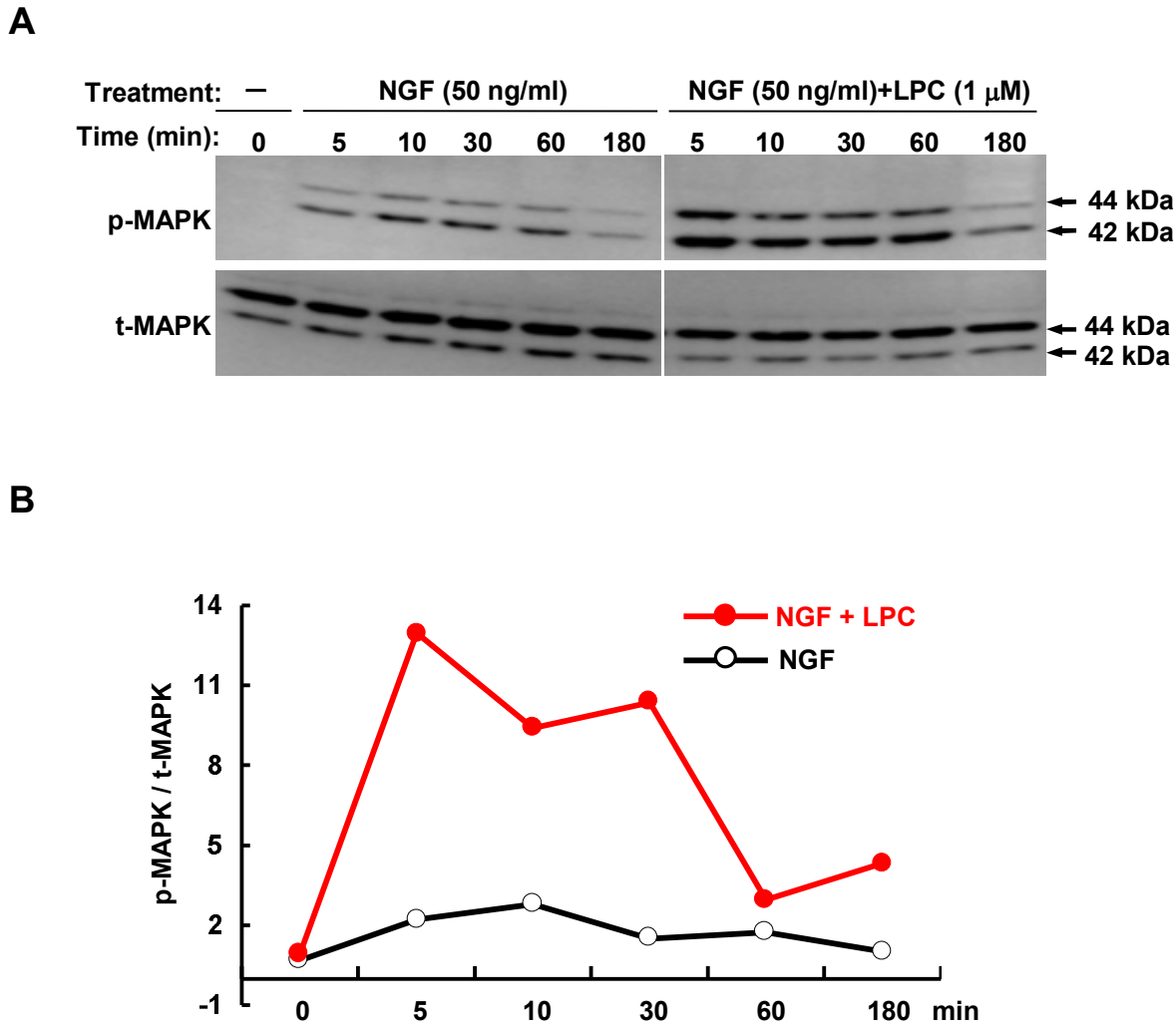

Figure 1-14 LPC enhances NGF-induced MAPK phosphorylation in PC12 cells. PC12 cells cultured in 24-well plate were serum-starved for 1.5 h, and the cells were stimulated with vehicle control (DMEM plus methanol), NGF (50 ng/ml) alone, or NGF plus LPC (1 μM) in the time-course experiment as indicated. **A**, phosphorylated MAPK (p-MAPK) and total MAPK (t-MAPK) were analyzed by Western blotting using phospho-p44/42 (Thr202/Tyr204) MAP Kinase and p44/42 MAP Kinase primary antibodies, respectively. **B**, the amounts of p-MAPK and t-MAPK were quantified and the relative ratio of p-MAPK vs t-MAPK in each condition was calculated. The result shown is the representative of three independent experiments which gave similar results.

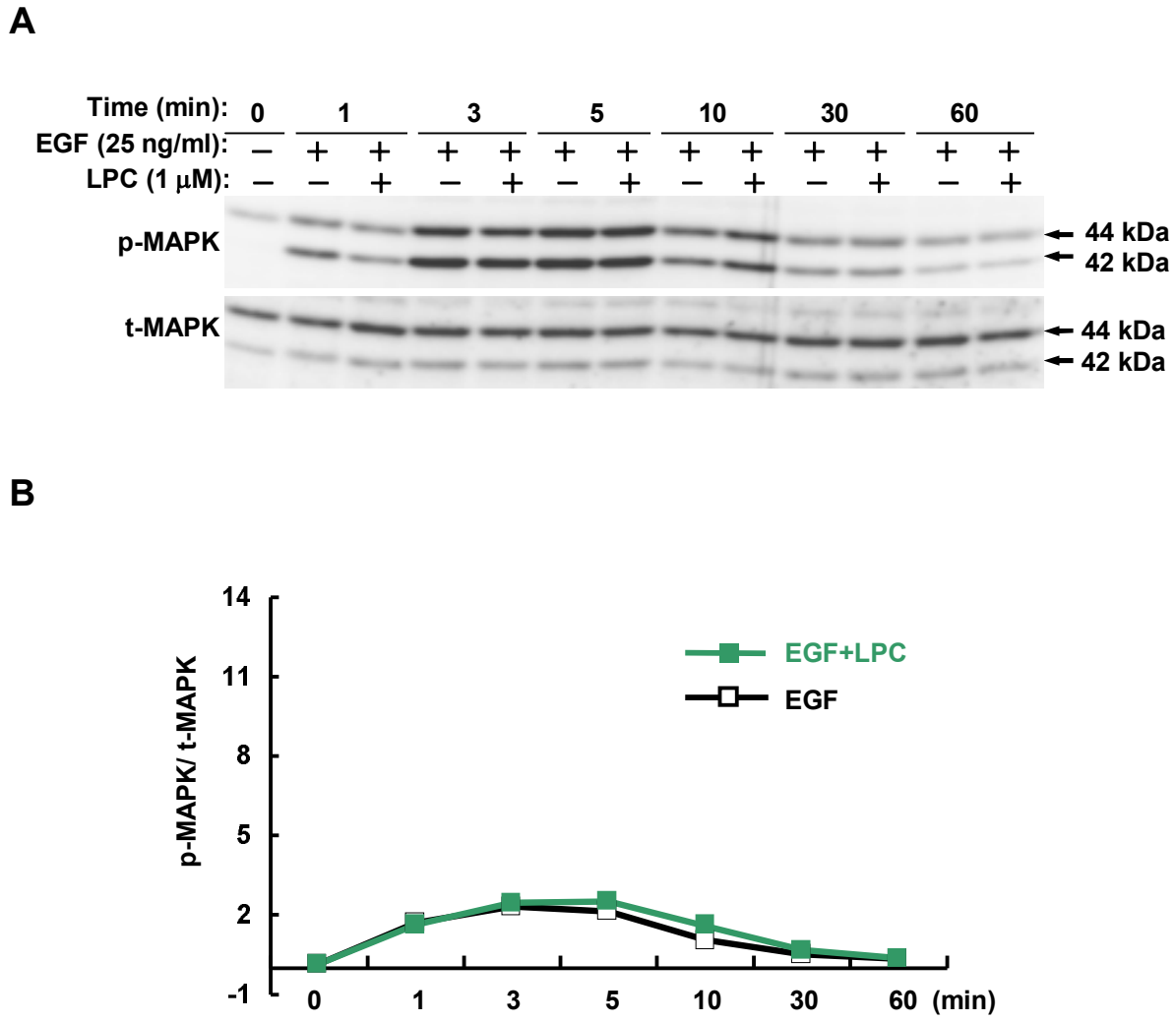

Figure 1-15 LPC does not enhance EGF-induced MAPK phosphorylation in PC12 cells. PC12 cells cultured in 24-well plate were serum-starved for 1.5 h, and the cells were stimulated with vehicle control (DMEM plus methanol), EGF (25 ng/ml) alone, or EGF plus LPC (1 μM) in the time-course experiment as indicated. **A**, phosphorylated MAPK (p-MAPK) and total MAPK (t-MAPK) were analyzed by Western blotting using phospho-p44/42 (Thr202/Tyr204) MAP Kinase and p44/42 MAP Kinase primary antibodies, respectively. **B**, the amounts of p-MAPK and t-MAPK were quantified and the relative ratio of p-MAPK vs t-MAPK in each condition was calculated. The result shown is the representative of three independent experiments which gave similar results.

A

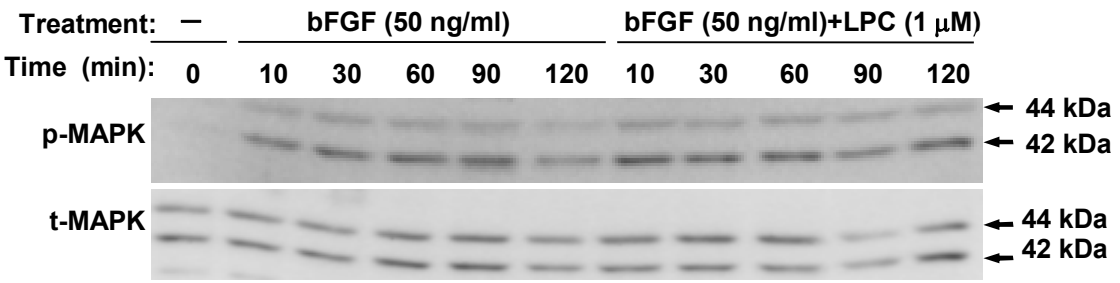

B

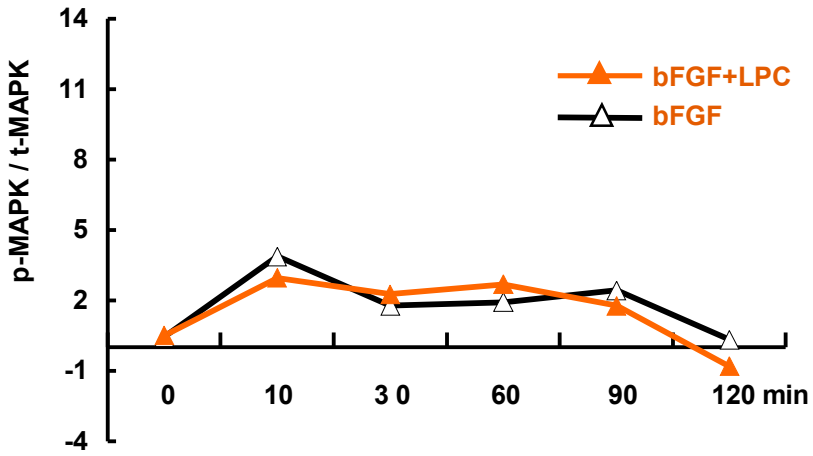

Figure 1 - 16 LPC does not enhance b F GF-induced MAPK phosphorylation in PC12 cells. PC12 cells cultured in 24-well plate were serum-starved for 1.5 h, and the cells were stimulated with vehicle control (DMEM plus methanol), bFGF (50 ng/ml) alone, or bFGF plus LPC (1 μM) in the time-course experiment as indicated. **A**, phosphorylated MAPK (p-MAPK) and total MAPK (t-MAPK) were analyzed by Western blotting using phospho-p44/42 (Thr202/Tyr204) MAP Kinase and p44/42 MAP Kinase primary antibodies, respectively. **B**, the amounts of p-MAPK and t-MAPK were quantified and the relative ratio of p-MAPK vs t-MAPK in each condition was calculated. The result shown is the representative of three independent experiments which gave similar results.

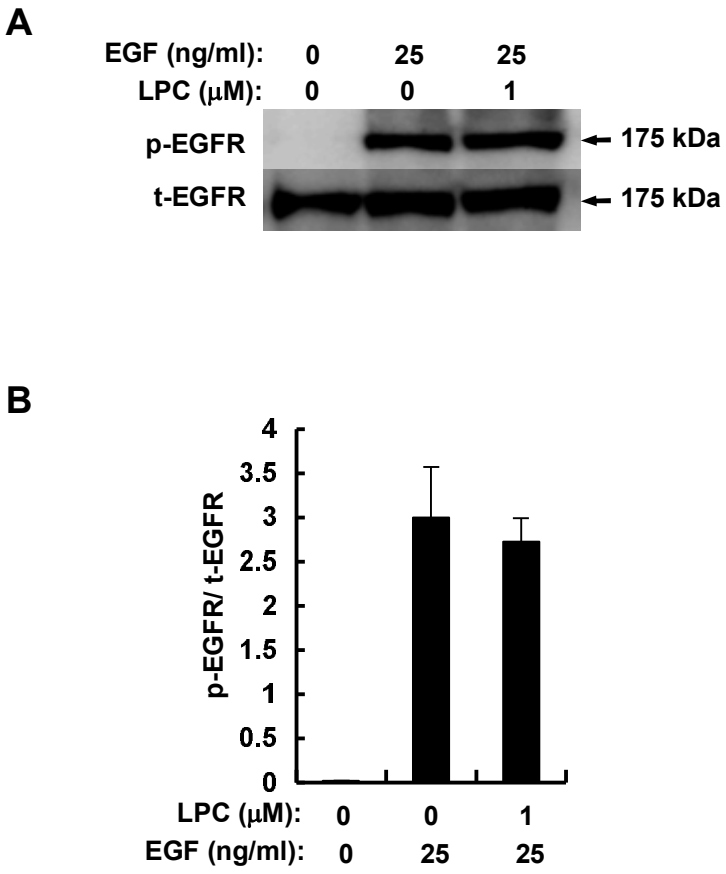

Figure 1-17 LPC does not affect EGF-induced EGF receptor phosphorylation in PC12 cells. PC12 cells cultured in 6-well plate were serum-starved for 1.5 h, and the cells were treated with vehicle control (DMEM plus methanol), EGF (25 ng/ml) alone, or EGF and LPC (1 μM) together for 2 min. **A**, phosphorylated EGF receptor (p-EGFR) and total EGFR (t-EGFR) were analyzed by Western blotting using anti-phospho-EGFR (Tyr1173) and anti-EGFR primary antibodies, respectively. **B**, The amounts of p-EGFR and t-EGFR were quantified and the relative ratio of p-EGFR vs t-EGFR was calculated. Data are means ± SD of two independent experiments.

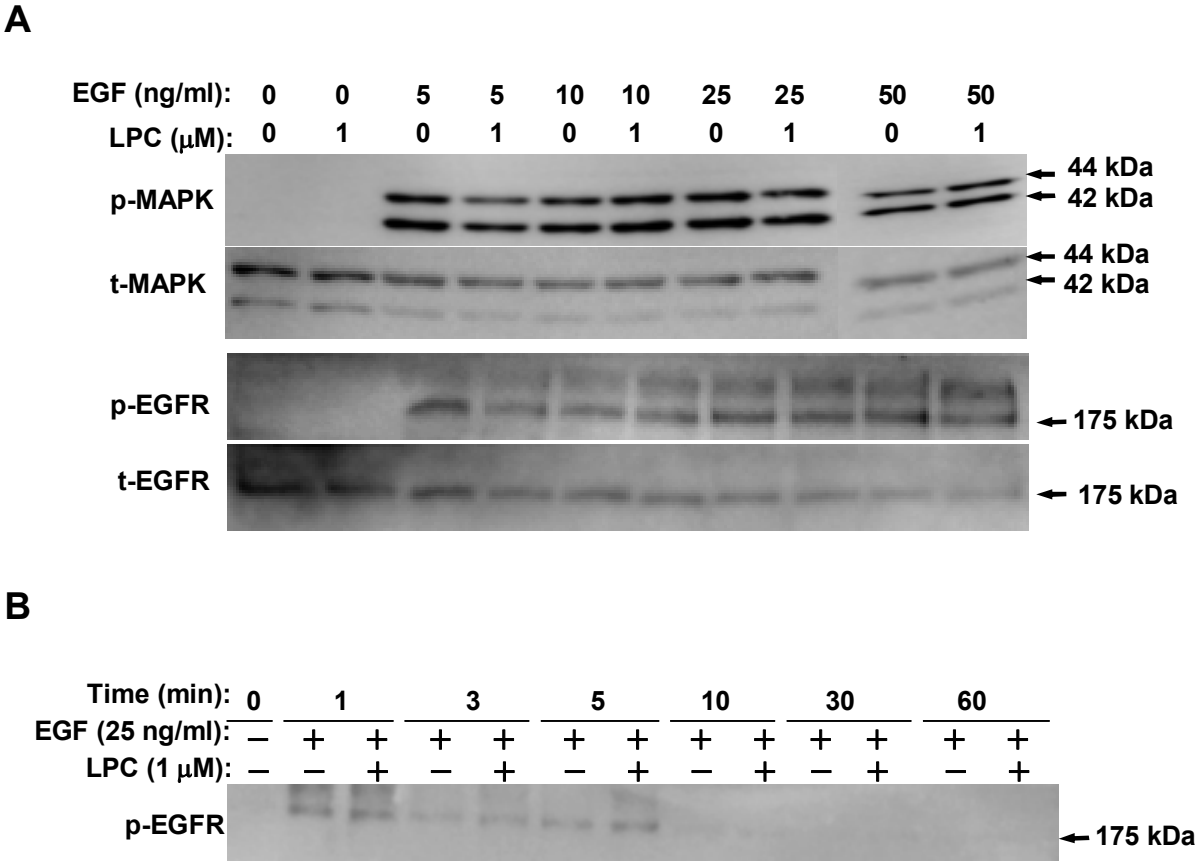

Figure 1-18 LPC does not enhance EGF-induced EGF receptor phosphorylation in PC12 cells. PC12 cells cultured in 24-well plate were serum-starved for 1.5 h, and the cells were stimulated with vehicle control (DMEM plus methanol), EGF (5, 10, 25, and 50 ng/m) alone or together with LPC (1 μM) for 3 min in **A**. In **B**, cells were stimulated with vehicle control, EGF (25 ng/ml) alone or together with LPC (1 μM) in the time-course as indicated. **A**, phosphorylated MAPK (p-MAPK) and total MAPK (t-MAPK) were analyzed by Western blotting using phospho-p44/42 (Thr202/Tyr204) MAP Kinase and p44/42 MAP Kinase primary antibodies, respectively. **B**, phosphorylated EGF receptor (p-EGFR) and total EGFR (t-EGFR) were analyzed by Western blotting using anti-phospho-EGFR (Tyr1173) and anti-EGFR primary antibodies, respectively. The images are the representative of two independent experiments which gave similar results.

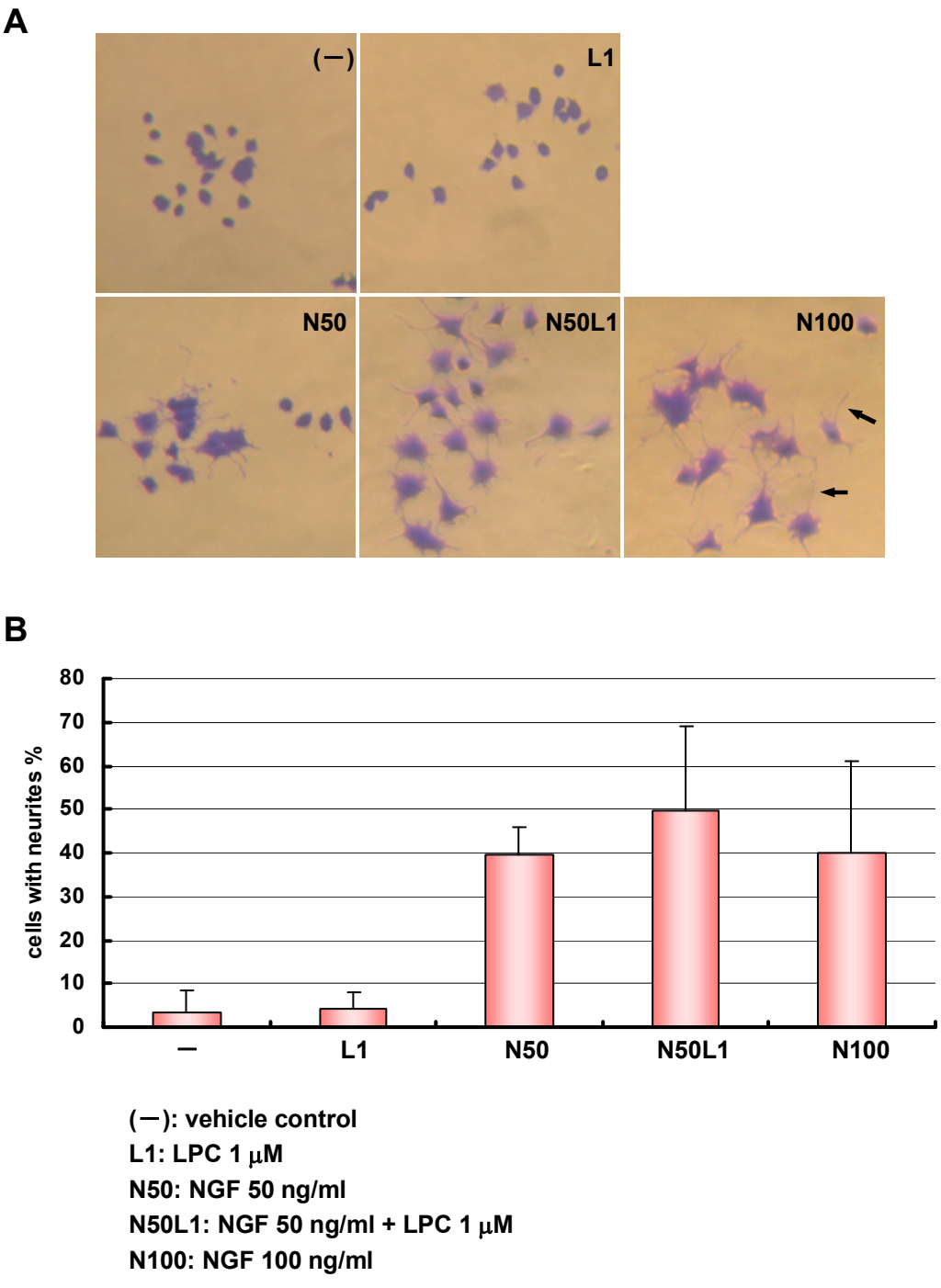

Figure 1-19 Effect of LPC on NGF-induced neurite outgrowth and morphological changes in PC12 cells. PC12 cells were incubated in the serum-free DMEM supplemented with vehicle control (DMEM plus methanol), LPC (1 μM), NGF (50 ng/ml), NGF together with LPC, or NGF (100 ng/ml) for 48 h. The cells were fixed with 4% paraformaldehyde, and stained with CBB. Cells were observed by phase-contrast microscopy. Arrows indicate neurites in **A**. Cells with neurites longer than the diameter of cell body were counted as positive and the percentage of total number of cells was calculated in each treatment. Error bars represent the means ± SD of five independent experiments in **B**.

Chapter 2. Lysophosphatidylcholine potentiates BDNF-induced MAPK and Akt signals by enhancing the activation of TrkB in cerebellar granule neurons

2.1 Introduction

Brain-derived neurotrofic factor

As mentioned in the General introduction, brain-derived neurotrophic factor (BDNF) is a member of the neurotrophin family growth factors. BDNF was initially found as a survival factor for peripheral neurons, but also has emerged as a critical factor that regulates the synaptic plasticity and development of neurons in the CNS, and supports their survival and differentiation (17). BDNF has been widely studied as a key drug target for neurodegenerative diseases, since the involvement of BDNF in neurological disorders, especially in Huntington's disease, has been found: the transcriptional level of BDNF was reduced during the early stage and development of Huntington's disease brains (17). BDNF has also been implicated in Alzheimer's and Parkinson's diseases. For example, significant decreases of BDNF mRNA and protein levels were observed in the hippocampus and cerebral cortex in Alzheimer's disease, which might be associated with the memory dysfunction of patients with this disease. The progressive loss of synapses and neurons in Alzheimer's disease is closely associated with the role of BDNF in the synaptic plasticity and survival of hippocampal neurons. However, the exact contribution of BDNF to the pathogenesis of these neurodegenerative diseases has still not been fully understood (17,76-78).

BDNF is abundantly expressed in the developing and adult mammalian brain,

particularly in the hippocampus, in almost all the cortical area, and the spinal cord regions, where it supports the survival of hippocampal, cerebellar granule, and other types of neurons (15,78). BDNF was found to be released through both constitutive and activity-dependent pathways from neurons (76). Similar to NGF, the cellular actions of BDNF are mediated through two receptors: TrkB and p75. BDNF exerts its survival effects by binding to TrkB and inducing two key signaling pathways (Fig. 2-1). One way is that the phosphorylation of TrkB at tyrosine 515 (analogous to tyrosine 490 in TrkA) activates the Ras-MAPK signaling cascade, which induces the phosphorylation of CREB and various transcription factors that facilitate the cell survival. Another way is that phosphorylated TrkB at tyrosine 515 also induces the activation of PI3K-Akt pathway, which can inhibit proapoptotic signals thereby supporting the survival of cells. Activated TrkB at tyrosine 816 (analogous to tyrosine 785 in TrkA) can also recruit and phosphorylate phospholipase Cγ-1 (PLCγ-1) and induce the activation of protein kinase C, which modulate the synaptic plasticity. Activated PLCγ-1 increases the release of Ca^{2+} from intracellular stores to the cytoplasm, and induces Ca^{2+}/calmodulin-dependent kinase (Ca^{2+}/CaM) activation and eventually promotes cell survival (76-78).

Cerebellar granule neurons

Cerebellar granule neurons (CGNs) are the smallest but the most abundant neurons in the brain. In humans, the total number of CGNs on average is around 50 billion, which constitute 3/4 of neurons in the brain. Cell bodies of CGNs are intensively packed in the bottom layer of cerebellar cortex. CGNs in the packed layer grow dendrite to the target upper layers of cortex to exert excitatory effect on the target. Cultured CGNs have been widely used as a model for studying the cell survival and

differentiation for several reasons. First, CGNs can be easily prepared from mouse postnatal cerebellum because of their abundance and homogeneity. Second, membrane depolarization by high concentration of potassium is necessary for their survival: when cells are shifted from the culture medium containing high potassium (25 mM) to the culture medium containing low potassium (5 mM), cells undergo programmed cell death with typical characteristics of cell shrinkage, nuclear condensation and fragmentation (78-82).

BDNF, but not NT-3, was shown to be the survival factor for CGNs, although CGNs express receptors TrkB and TrkC for BDNF and NT-3, respectively (81,82). Similar to BDNF, IGF-1 is also able to activate IGF-1 receptor to promote the survival of CGNs (80). Further studies have shown that both BDNF and IGF-1 can protect CGNs from low potassium-induced apoptosis through activating Ras-MAPK and PI3K-Akt signaling cascades, respectively (83,84). Besides, IGF-1 also induces the activation of L-type voltage-dependent Ca^{2+} channel, and Ca^{2+}/CaM activation to promote the cell survival (85-87).

As described in the General introduction, $sPLA_2$ and LPC showed NGF-like activity by inducing differentiation of PC12 cells, and BDNF-like activity by protecting CGNs from low extracellular potassium-induced apoptosis. In Chapter 1, I have tested and shown that LPC can promote NGF-induced MAPK and Akt pathways in PC12 cells via TrkA. In this Chapter, whether or not LPC has similar effect on BDNF-induced MAPK and Akt signaling pathways in TrkB-transfected CHO-K1 cells and primary cultured CGNs will be studied.

2.2 Objective

Ras-MAPK and PI3K-Akt signaling pathways are critical for the survival effect of BDNF and IGF-1 in CGNs. In the previous studies, LPC has been found to show survival factor-like effect in CGNs. In Chapter 1, it has been demonstrated that LPC promotes NGF-induced Ras-MAPK and PI3K-Akt pathways in PC12 cells. The objective in this Chapter is to investigate whether or not LPC has similar effect on BDNF- or IGF-1-induced Ras-MAPK and PI3K-Akt signaling pathways in CGNs, which will be important to understand the signaling mechanism of neurotrophin-like activity triggered by LPC in CGNs.

2.3 Results

2.3.1 Construction of the plasmid for expression of TrkB

A cDNA fragment encoding the full-length mouse TrkB (GeneBank accession No. NP_001020245.1), 821 amino acid-long, was amplified by PCR, and was cloned into *Eco*R I site of pEGFP-N1 (EGFP-N1, GeneBank accession No. U55762) expression vector; in this construct, the intracellular, C-terminal end of TrkB was fused with EGFP (TrkB-EGFP-N1; Fig. 2-2).

2.3.2 BDNF and LPC do not induce MAPK phosphorylation in the wild type and vector-transfected CHO-K1 cells

Before examining the effect of BDNF and LPC on MAPK phosphorylation in TrkB-transfected CHO-K1 cells, I tested MAPK phosphorylation in response to BDNF and/or LPC treatments in the wild type and EGFP-N1 vector-transfected CHO-K1 cells. As shown in Fig. 2-3, in the wild type and vector-transfected CHO-K1 cells, MAPK was not phosphorylated upon BDNF (5 ng/ml) and/or LPC (1 μM) stimuli, indicating that CHO-K1 cells are suitable for testing the effect of BDNF and/or LPC on transfected TrkB.

2.3.3 LPC enhances BDNF-induced MAPK phosphorylation in TrkB-transfected CHO-K1 cells

To examine whether LPC can also potentiate BDNF-TrkB signaling, TrkB was expressed in CHO-K1 cells and the ability of LPC to increase MAPK phosphorylation triggered by BDNF was assessed. Western blot analysis shown in Figs. 2-4 A and B demonstrates that LPC (1 μM) significantly potentiated BDNF-induced MAPK

phosphorylation, suggesting that LPC displays similar effect on BDNF-TrkB signaling in addition to its potentiation on NGF-TrkA signaling.

2.3.4 Dephosphorylation of MAPK in the low potassium medium and the effect of BDNF and LPC on MAPK phosphorylation in CGNs

To test the effect of LPC on BDNF-TrkB signaling in the *in vivo*-like model system, the primary culture of CGNs from mouse cerebella which express endogenous TrkB as well as the receptor for IGF-1 was used. MAPK is highly phosphorylated in the medium containing high concentration of potassium (25 mM; HK), which causes membrane depolarization and cell survival. When the culture medium was changed to the medium containing normal concentration of potassium (5 mM; LK), MAPK is dephosphorylated and the majority of cells undergo apoptotic death. To test how long serum-starvation in LK can sufficiently reduce MAPK phosphorylation in HK, I checked MAPK phosphorylation in a time-course experiment after the cells were shifted to LK. Cells were serum-starved in LK for 1, 3, and 5 h, and MAPK phosphorylation was analyzed. The result in Fig. 2-5 A shows that after one hour of serum-starvation in LK, the level of phosphorylated MAPK was still high (upper, lane 2), although there was a small decrease compared to that in HK (upper, lane 1). The result in Figs. 2-5 B and C (upper, lanes 1′, 2′, 1″, and 2″) shows that culturing the cells in LK for 3 to 5 hours can sufficiently reduce MAPK phosphorylation. In Figs. 2-5 A-C (upper, lanes 3-8, 3′-8′, and 3″-8″), the effect of BDNF and LPC on MAPK phosphorylation in cells serum-starved for 1, 3, and 5 h was tested. The effects of BDNF and LPC were not clearly seen in cells cultured in LK for 1 h, because of high level of MAPK phosphorylation remaining in LK (Fig. 2-5 A). As shown in Figs. 2-5 B and C, when the

cells were cultured for 3 or 5 h in LK, BDNF induced MAPK phosphorylation (upper, 5′ and 5″), which was enhanced by the addition of LPC (1 and 10 μM; upper, lanes 6′, 7′, 6″, and 7″). In the following experiments, cells were cultured in LK for 3 or 5 h before subjected to various stimuli.

2.3.5 LPC enhances BDNF-induced MAPK phosphorylation in CGNs

To confirm the result obtained in Figs. 2-5 B and C, the effect of LPC on BDNF-induced MAPK phosphorylation was tested in cells cultured for 3 h in LK and challenged with different concentrations of BDNF. MAPK phosphorylation induced by BDNF added at 5 and 10 ng/ml was enhanced by the addition of LPC compared to that by BDNF alone (Fig. 2-6 A, upper, lanes 6-11). Since BDNF added at 25 ng/ml induced maximal phosphorylation of MAPK, there was no further increase by LPC (Fig. 2-6 A, upper, lanes 12-14). This result was confirmed again in Fig. 2-6 B where CGNs cultured in 6-well plates, instead of 24-well plates as in Figs. 2-6 A, were used. To test the significance of this increase in BDNF-induced MAPK phosphorylation by LPC, this experiment in which cells were cultured in LK for 3 and 5 h before BDNF/LPC treatment was repeated five times. Then, the difference in MAPK phosphorylation upon treatments with BDNF alone or BDNF plus LPC was statistically analyzed (Fig. 2-7). Western blot analysis showed that BDNF added at 5 ng/ml slightly induced MAPK phosphorylation (Figs. 2-7 A and C, upper, lanes 5 and 5′), which was enhanced by LPC (Figs. 2-7 A and C, upper, lanes 6, 7, 6′, and 7′), while LPC alone added at 1 and 10 μM did not induce MAPK phosphorylation (Figs. 2-7 A and C, upper, lanes 3, 4, 3′, and 4′). Quantification of the results of Western blot analysis shown in Fig. 2-7 D demonstrates that the enhancement by LPC (1 and 10 μM) of BDNF (5 ng/ml)-induced MAPK

phosphorylation was significant when the data were analyzed by one-way ANOVA, although this was significant only when analyzed by Student's *t*-test, not by one-way ANOVA in Fig. 2-7 B. Nevertheless, I concluded that the results obtained in Figs. 2-6 and 2-7 collectively demonstrate that LPC enhances BDNF-induced MAPK phosphorylation.

2.3.6 LPC does not affect IGF-1-induced MAPK phosphorylation in CGNs

CGNs express IGF-1 receptor, and binding of IGF-1 to its receptor induces MAPK phosphorylation as described in Fig. 1-13. Whether or not LPC has any effect on MAPK phosphorylation induced by IGF-1, similar to that induced by BDNF, was examined in CGNs after being cultured for 3 h in LK. IGF-1 (10 ng/ml) triggered the phosphorylation of MAPK, but it was not further elevated by LPC (Figs. 2-8 A, lanes 3 and 4, and B). To obtain more conclusive data, the effect of LPC (1 μM) on MAPK phosphorylation triggered by IGF-1 at lower concentration (5 ng/ml) was also tested. IGF-1 (5 ng/ml)-induced MAPK phosphorylation was not affected by LPC (Fig. 2-8 C, lanes 3 and 4). Again, IGF-1 (10 ng/ml)-induced MAPK phosphorylation was not enhanced by LPC (Fig. 2-8 C, lanes 5 -7). These results indicate that LPC is ineffective on IGF-1-induced MAPK phosphorylation in CGNs.

2.3.7 LPC promotes BDNF-induced, but not IGF-1-induced, Akt phosphorylation in CGNs

Next, the effect of LPC on another BDNF- or IGF-1-induced pathway, Akt phosphorylation, was examined. In the same way, after being cultured for 3 h in LK, CGNs were treated with BDNF, IGF-1, and/or LPC, and the effect of LPC on Akt

phosphorylation was examined. Addition of either BDNF (Fig. 2-9 A, lane 5) or IGF-1 (Fig. 2-9 B, lane 3) triggered Akt phosphorylation, and BDNF-induced Akt phosphorylation was further enhanced by LPC (Fig. 2-9 A, lanes 6 and 7). However, IGF-1-induced Akt phosphorylation was not affected by LPC (Fig. 2-9 B, lane 4). Taken together, results in Figs. from 2-6 to 2-9 demonstrate that LPC enhances BDNF-induced, but not IGF-1-induced, MAPK and Akt signals in CGNs.

2.3.8 LPC potentiates BDNF-induced MAPK and Akt phosphorylation through enhancing the phosphorylation of TrkB in CGNs

To address if the increase in BDNF-induced MAPK and Akt phosphorylation by LPC is the consequence of enhanced TrkB activation, TrkB phosphorylation in CGNs treated with BDNF and/or LPC was analyzed. Phosphorylation of TrkB by BDNF at 5 ng/ml was minimal (Fig. 2-10, lane 5). When LPC (1 and 10 μM) was added together with BDNF, an increase in BDNF-induced TrkB phosphorylation was observed (Fig. 2-10, lanes 6 and 7). This, together with the results in Figs. from 2-6 to 2-10, suggests that LPC potentiates BDNF-induced both MAPK and Akt signaling pathways through promoting the activation of receptor TrkB.

2.3.9 LPC at high concentration induces MAPK phosphorylation in the absence of BDNF in CGNs

LPC added alone at 1 or 10 μM did not induce MAPK phosphorylation in CGNs in LK (Figs. 2-5 and 2-7). Here, I tested if LPC added alone at 100 μM in LK induces MAPK phosphorylation. Consistent with the result in Figs. 2-5 and 2-7, LPC added at 1 and 10 μM did not induce MAPK phosphorylation (Fig. 2-11). However, LPC added at

100 μM induced phosphorylation of MAPK at a similar level to that in BDNF (25 ng/ml)-treated cells, suggesting that LPC added at high concentration induces a different signal.

2.3.10 LPC added alone at 10 μM sufficiently protect CGNs from LK-induced apoptosis

Finally, to further understand the relationship between BDNF and/or LPC-induced MAPK activation and the survival of CGNs in LK, the ability of LPC to inhibit LK-induced apoptosis of CGNs was tested. Cells were kept in HK or LK supplemented with various stimuli as shown in Figs. 2-12 A-I for 24 h. Then the cells were fixed and the nuclei were stained with Hoechst 33258 dye. In HK, most of the cells (>80%) were alive as judged by the morphology of nuclei (Figs. 2-12 A and I), while 70% of cells displayed apoptotic phenotype characterized by condensed and shrunken nuclei in LK (Figs. 2-12 B and I). In LK supplied with LPC at 1 μM, apoptosis was slightly inhibited (Figs. 2-12 C and I). In LK supplied with LPC at 10 μM, apoptosis was significantly inhibited; survival rate in this condition was around 70% (Figs. 2-12 D and I), which was even higher than the percentage of surviving cells by BDNF added at 10 ng/ml (~60%, Figs. 2-12 H and I). BDNF added at 5 ng/ml modestly promoted the survival of cells (Figs. 2-12 E and I), but it was not significantly enhanced by LPC (1 and 10 μM) (Figs. 2-12 F, G, and I). Since LPC added at 10 μM did not induce MAPK phosphorylation (Figs. 2-5, 2-7, and 2-11), but rescued CGNs from apoptosis, this result implies a mechanism independent of BDNF-TrkB-induced MAPK phosphorylation involved in the neurotrophin-like effect of LPC. LPC added alone at 100 μM showed toxicity to CGNs in the serum-free medium. Thus, the effect of LPC at

this concentration was not further examined.

2.4 Discussion

Results obtained in this Chapter confirmed that LPC potentiates BDNF-TrkB signaling in CGNs. LPC (1 and 10 μM) significantly enhanced the phosphorylation of MAPK and Akt induced by BDNF in CGNs, while LPC added alone did not induce the phosphorylation of both. In contrast, LPC did not show any effect on IGF-1-induced signals in CGNs. These results, together with the findings in Chapter 1, suggest that LPC has a special role on Trk receptors (TrkA and TrkB) and on their ligand-induced downstream signals.

Although LPC exhibited similar effect on BDNF-TrkB system, as on NGF-TrkA system, some differences were observed. First, the fold-increase in BDNF-induced MAPK phosphorylation by LPC (Fig. 2-7 D) obtained by analyzing all the data from five independent experiments was less than 2-fold on average. This fold-increase by LPC was not as high as that by LPC in NGF-induced MAPK phosphorylation in PC12 cells, which was on average around 3-4 fold. This indicates that NGF-TrkA pathway is more sensitive to LPC than BDNF-TrkB pathway. Another difference is that LPC (10 μM) added alone slightly induced MAPK phosphorylation in PC12 cells, whereas it did not induce MAPK phosphorylation in CGNs.

In the previous study, LPC added alone at 10 μM protected CGNs from LK-induced apoptosis (56). Here, I tested the effect of LPC added alone at 1 or 10 μM on the protection of CGN from LK-induced apoptosis. Consistent with the previous finding, LPC added at 10 μM effectively rescued the cells from LK-induced apoptosis, and LPC 1 μM also showed a slight protecting effect. However, LPC added alone at 1 or 10 μM did not induce the activation of TrkB, and the downstream signals, Akt and MAPK (Figs. 2-7, 2-9, and 2-10). These results suggest that LPC (10 μM) protects CGNs from LK-induced apoptosis through a pathway that does not involve MAPK and Akt cascades. In a recent study, LPC was found to cause the activation of a G protein-coupled receptor, G2A, and the release of G protein subunits $G_{\alpha i\text{-}1}$ and $G_{\alpha q\text{-}11}$, which can increase intracellular Ca^{2+} in primary PMNs (42). As described in the Introduction, IGF-1-induced release of Ca^{2+} from the intracellular stores induces the

activation of Ca^{2+}/CaM, thereby supporting the survival CGNs. These facts suggest that LPC might exert neurotrophin-like activity by increasing intracellular Ca^{2+} and Ca^{2+}/CaM in CGNs. Further study is still required to elucidate the precise mechanism of LPC-mediated survival of CGNs.

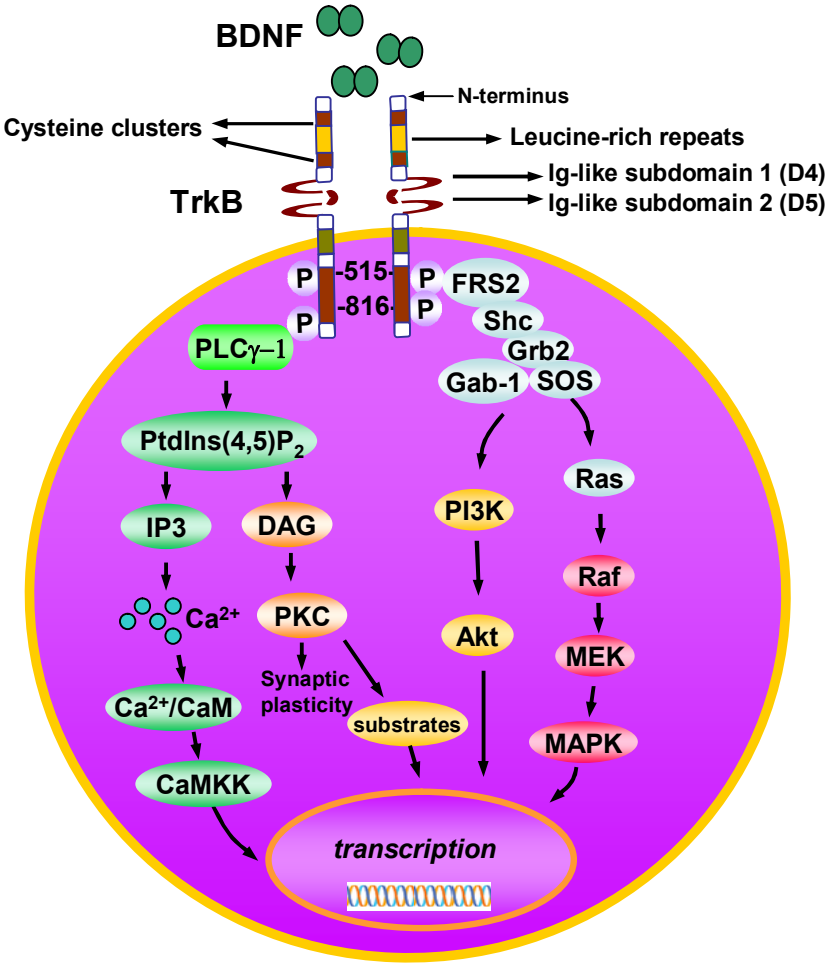

Figure 2-1 Major BDNF-TrkB mediated signaling pathways

A

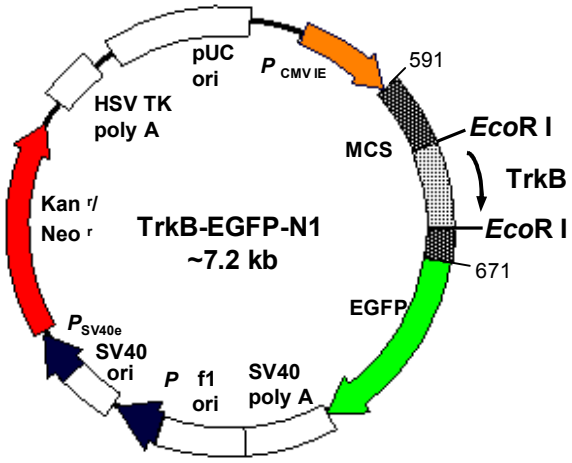

B

MCS 591~671:

591 601 611 621 631 641 651

G CTA GCG CTA CCG GAC TCA GAT CTC GAG CTC AAG CTT CGA ATT CTG CAG TCG ACG GTA CCG CGG

Bgl II *Xho* I *Hind* III *EcoR* I *Pst* I *Sal* I *Kpn* I

661 671

GCC CGG GAT CCA CCG GTC GCC ACC **ATG GTG**

Sma I *Bam*H I EGFP

Figure 2-2 The map of the plasmid TrkB-EGFP-N1 for expression of TrkB. **A**, a PCR product encoding full-legth TrkB was inserted into the *Eco*R I site of expression vector pEGFP-N1. C-terminus of TrkB was fused with EGFP. **B**, restriction sites in the multiple cloning site of the vector are shown.

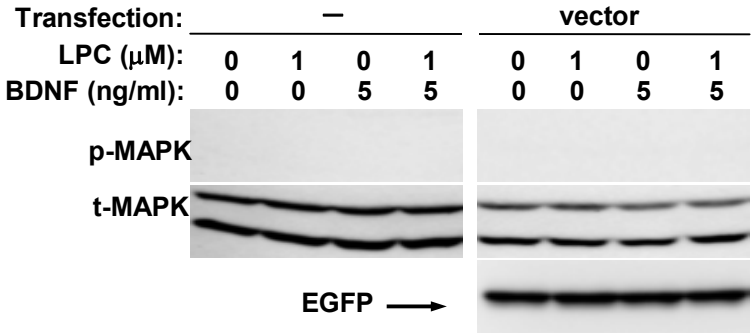

Figure 2-3 BDNF and LPC do not induce MAPK phosphorylation in wild type and vector-transfected CHO-K1 cells. CHO-K1 cells cultured in 24-well plate were untransfected (—) or transiently transfected with EGFP-N1 vector (vector, 0.8 μg/well) by Lipofectamine 2000 (1.5 μl/well) for 18-24 h. Cells were then serum-starved for 1.5 h, and treated with vehicle control (DMEM plus methanol), LPC (1 μM), BDNF (5 ng/ml), or BDNF together with LPC for 10 min. Cells were lysed with 1XSDS sample buffer (50 μl/well) and boiled for 3 min. Phosphorylated and total MAPK (p-MAPK and t-MAPK) were analyzed by Western blotting using anti-phospho-p44/42 MAPK and anti-44/42 MAPK antibodies, respectively. Expression of EGFP was detected by anti-GFP antibody.

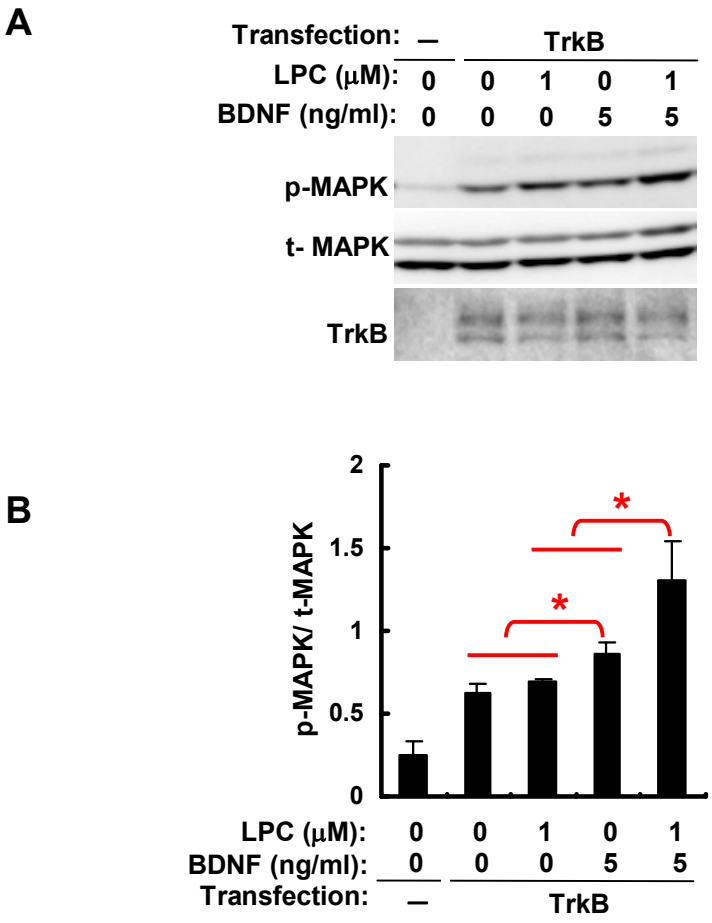

Figure 2-4 LPC enhances BDNF-induced MAPK phosphorylation in TrkB-transfected CHO-K1 cells. CHO-K1 cells cultured in 24-well plate were untransfected (—) or transiently transfected with TrkB-EGFP-N1 (TrkB, 0.8 μg/well) by Lipofectamine 2000 for 18-24 h. Cells were then serum-starved for 1.5 h and treated with vehicle control (DMEM plus methanol), BDNF (5 ng/ml), LPC (1 μM), or BDNF together with LPC as indicated for 10 min. **A**, Phosphorylated and total MAPK (p-MAPK and t-MAPK) were analyzed by Western blotting using anti-phospho-p44/42 MAPK and anti-44/42 MAPK antibodies, respectively. The expression of TrkB-EGFP was detected by anti-GFP-antibody. **B**, the amounts of p-MAPK and t-MAPK were quantified and the relative ratio of p-MAPK vs t-MAPK in each condition was calculated. Data are means ± SD of three independent experiments. *, $p<0.05$ by one-way ANOVA.

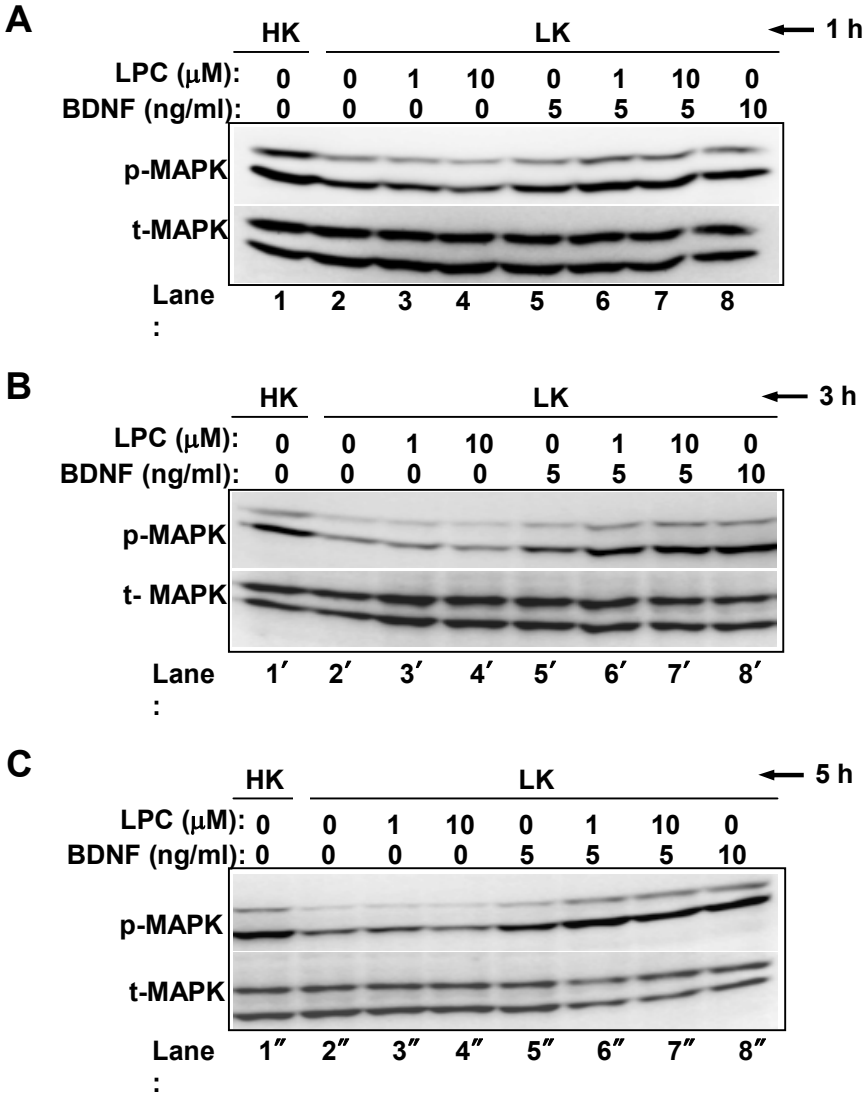

Figure 2-5 Dephosphorylation of MAPK in the low patassium medium and the effect of BDNF and LPC on MAPK phosphorylation in CGNs. CGNs cultured for 5 days *in vitro* were serum-starved in HK (DMEM containing 25 mM potassium) or LK (DMEM containing 5 mM potassium) for 1 h in **A**, 3 h in **B**, and 5 h in **C**. Cells were treated with vehicle control (DMEM plus methanol), BDNF (5 and 10 ng/ml) or LPC (1 and 10 μM) alone, or BDNF (5 ng/ml) together with LPC for 10 min. Phosphorylated and total MAPK (p-MAPK and t-MAPK) were analyzed by Western blotting using anti-phospho-p44/42 MAPK and anti-44/42 MAPK antibodies, respectively. The images shown are the representatives of at least three independent experiments which gave similar results.

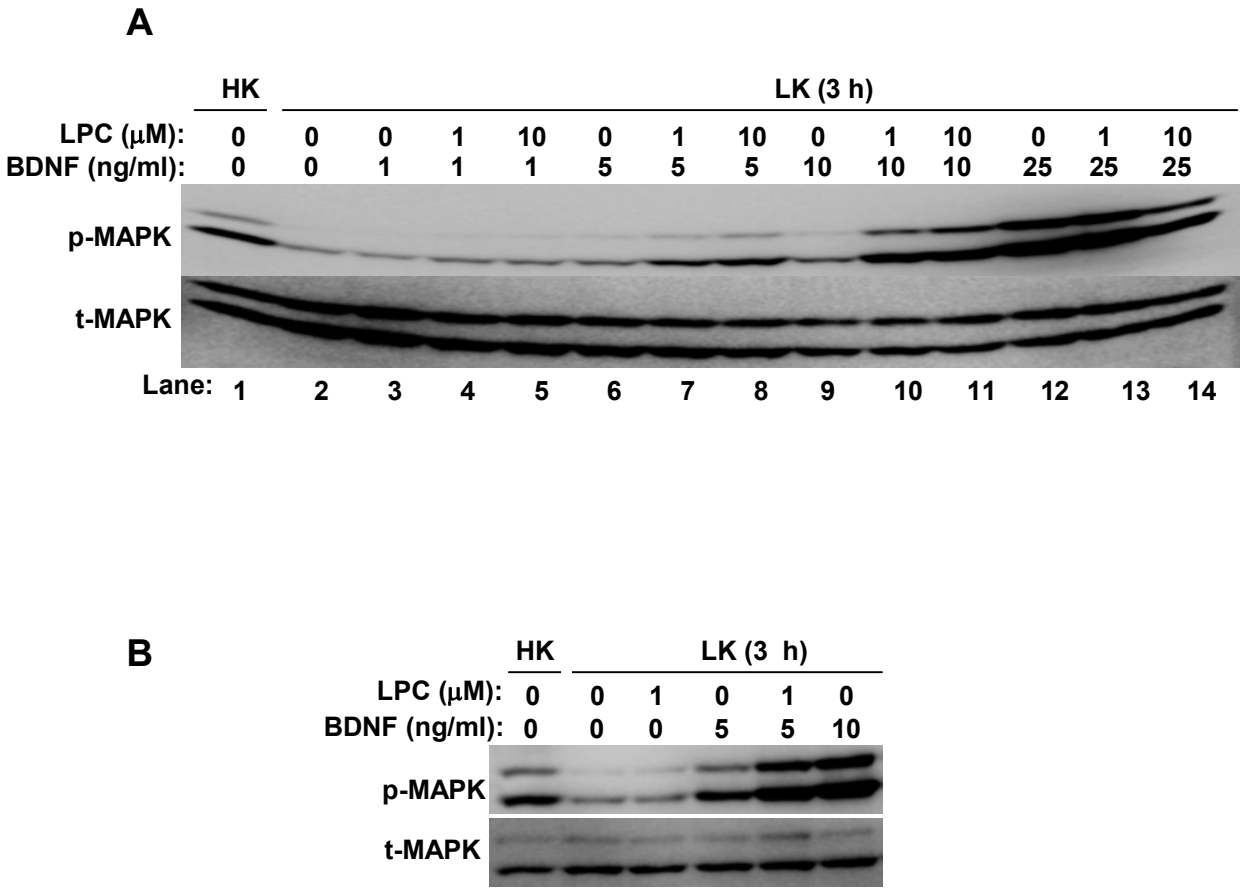

Figure 2-6 LPC enhances BDNF-induced MAPK phosphorylation in CGNs. CGNs cultured for 5 days *in vitro* (24-well plate in **A**, 6-well plate in **B**) were serum-starved in HK (DMEM containing 25 mM potassium) or LK (DMEM containing 5 mM potassium) for 3 h. Cells were treated with vehicle control (DMEM plus methanol), BDNF (1, 5, 10, and 25 ng/ml) or LPC (1 μM) alone, or BDNF together with LPC (1 and 10 μM) for 10 min. Phosphorylated and total MAPK (p-MAPK and t-MAPK) were analyzed by Western blotting using anti-phospho-p44/42 MAPK and anti-44/42 MAPK antibodies, respectively.

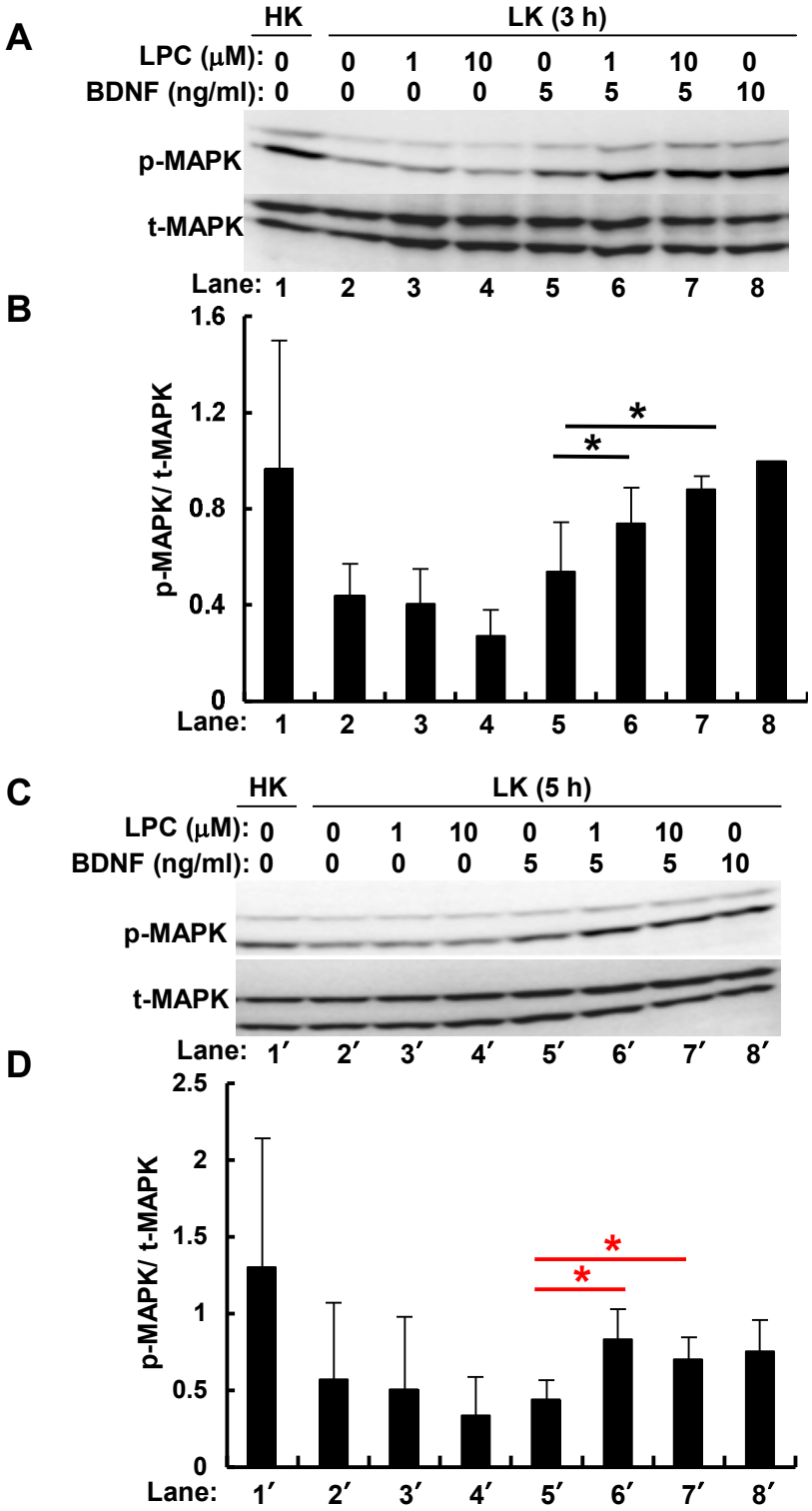

Figure 2-7 LPC significantly enhances BDNF-induced MAPK phosphorylation in CGNs. CGNs cultured for 5 days *in vitro* 24-well plate were serum-starved in HK (DMEM containing 25 mM potassium) or LK (DMEM containing 5 mM potassium) for 3 h in **A** and **B**, for 5 h in **C** and **D**. Cells were treated with vehicle control (DMEM plus methanol), BDNF (5 and 10 ng/ml) or LPC (1 and 10 μM) alone, or BDNF (5 ng/ml) together with LPC for 10 min. **A** and **C**, phosphorylated and total MAPK (p-MAPK and t-MAPK) were analyzed by Western blotting using anti-phospho-p44/42 MAPK and anti-44/42 MAPK antibodies, respectively. **B** and **D**, the amounts of p-MAPK and t-MAPK were quantified and the relative ratio of p-MAPK vs t-MAPK in each condition was calculated. Data are means ± SD of five independent experiments. *, $p<0.05$ by Student's *t*-test in **B**, by one-way ANOVA in **D**.

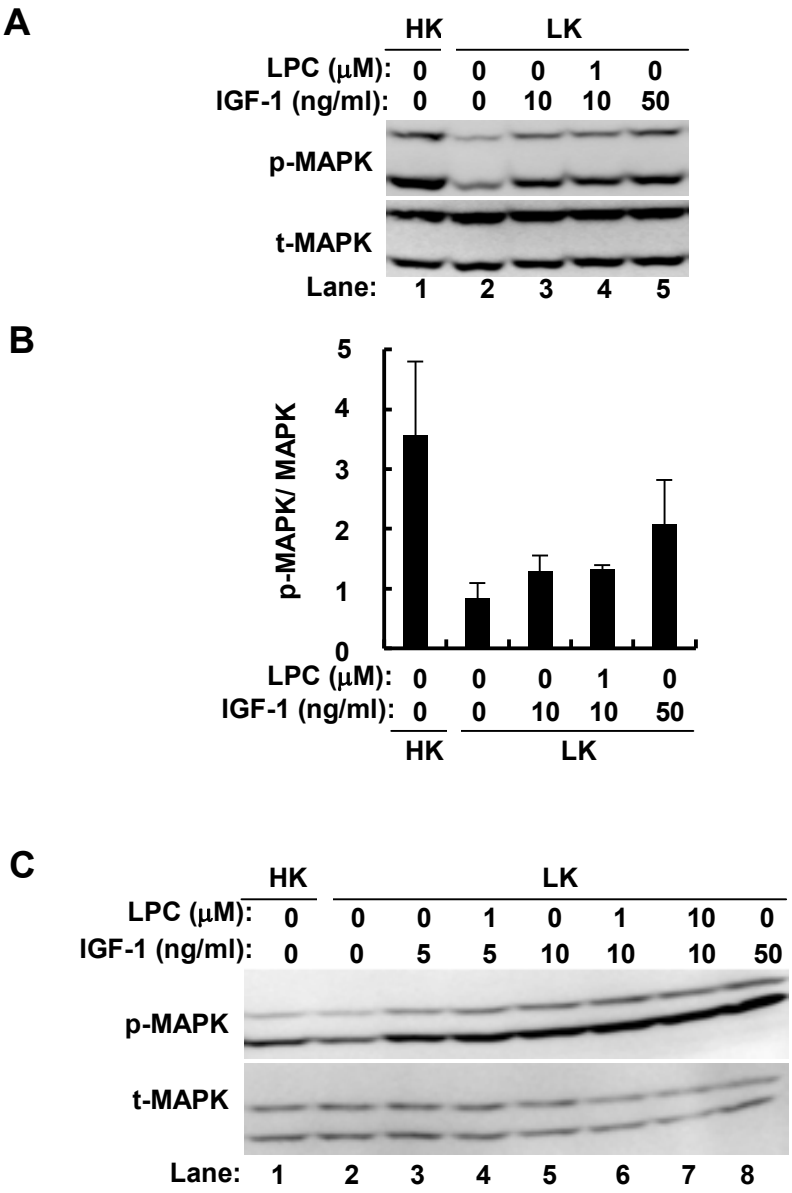

Figure 2-8 LPC does not affect IGF-1-induced MAPK phosphorylation in CGNs. CGNs cultured for 5 days *in vitro* were serum-starved in HK (DMEM containing 25 mM potassium) or LK (DMEM containing 5 mM potassium) for 3 h. Cells were treated with vehicle control (DMEM plus methanol), IGF-1 (5, 10, and 50 ng/ml) or LPC (1 and 10 μM) alone, or IGF-1 (5 and 10 ng/ml) together with LPC for 10 min as indicated. **A** and **C,** phosphorylated and total MAPK (p-MAPK and t-MAPK) were analyzed by Western blotting using anti-phospho-p44/42 MAPK and anti-44/42 MAPK antibodies, respectively. **B**, the amounts of p-MAPK and t-MAPK were quantified and the relative ratio of p-MAPK vs t-MAPK in each condition was calculated. Data are means ± SD of three independent experiments. Result in **C** is the the representative of two independent experiments which gave similar results.

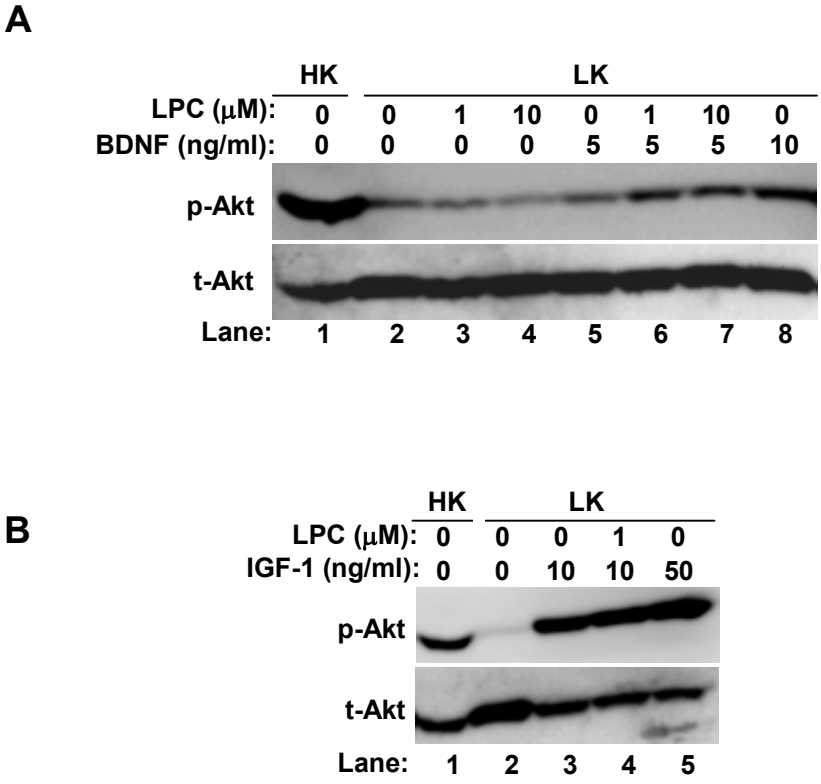

Figure 2-9 LPC promotes BDNF-induced, but not IGF-1-induced, Akt phosphorylation in CGNs. CGNs cultured for 5 days *in vitro* were serum-starved in HK (DMEM containing 25 mM potassium) or LK (DMEM containing 5 mM potassium) for 3 h. **A,** cells were treated with vehicle control (DMEM plus methanol), BDNF (5 and 10 ng/ml) or LPC (1 and 10 μM) alone, or BDNF (5 ng/ml) together with LPC for 10 min. **B,** cells were treated with vehicle control (DMEM plus methanol), or IGF-1 (10 and 50 ng/ml) alone, or IGF-1 (10 ng/ml) together with LPC (1 μM) for 10 min. **A** and **B**, phosphorylated Akt (p-Akt) and total Akt (t-Akt) were analyzed by Western blotting using anti-phospho-Akt (Ser473) and anti-Akt antibodies, respectively. The images shown are the representatives of five independent experiments which gave similar results.

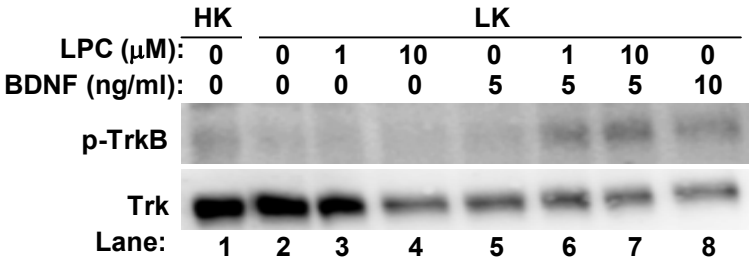

Figure 2-10 LPC potentiates BDNF-induced TrkB phosphorylation in CGNs. CGNs cultured for 5 days *in vitro* were serum-starved in HK (DMEM containing 25 mM potassium) or LK (DMEM containing 5 mM potassium) for 3 h. Cells were treated with vehicle control (DMEM plus methanol), BDNF (5 and 10 ng/ml) or LPC (1 and 10 μM) alone, or BDNF (5 ng/ml) together with LPC for 10 min. Phosphorylated TrkB (p-TrkB) was analyzed by Western blotting using anti-phospho-TrkA (Tyr490) antibody. Total Trk was analyzed using anti-Trk primary antibody. One representative result from two independent experiments which gave similar results is shown.

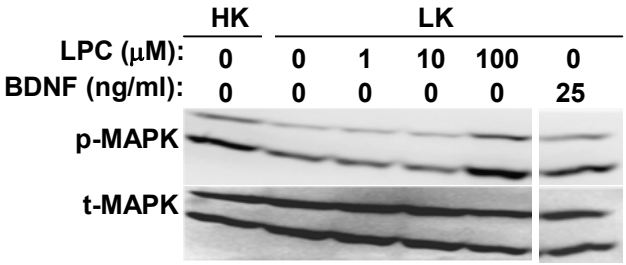

Figure 2-11 LPC added at high concentration induces MAPK phosphorylation in the absence of BDNF in CGNs. CGNs cultured for 5 days *in vitro* (24-well plate) were serum-starved in HK (DMEM containing 25 mM potassium or LK (DMEM containing 5 mM potassium) for 3 h. Cells were treated with vehicle control (DMEM plus methanol), LPC (1, 10, and 100 μM) alone, or BDNF (25 ng/ml) alone for 10 min. Phosphorylated and total MAPK (p-MAPK and t-MAPK) were analyzed by Western blotting using anti-phospho-p44/42 MAPK and anti-44/42 MAPK antibodies, respectively. One representative result from two independent experiments which gave similar results is shown.

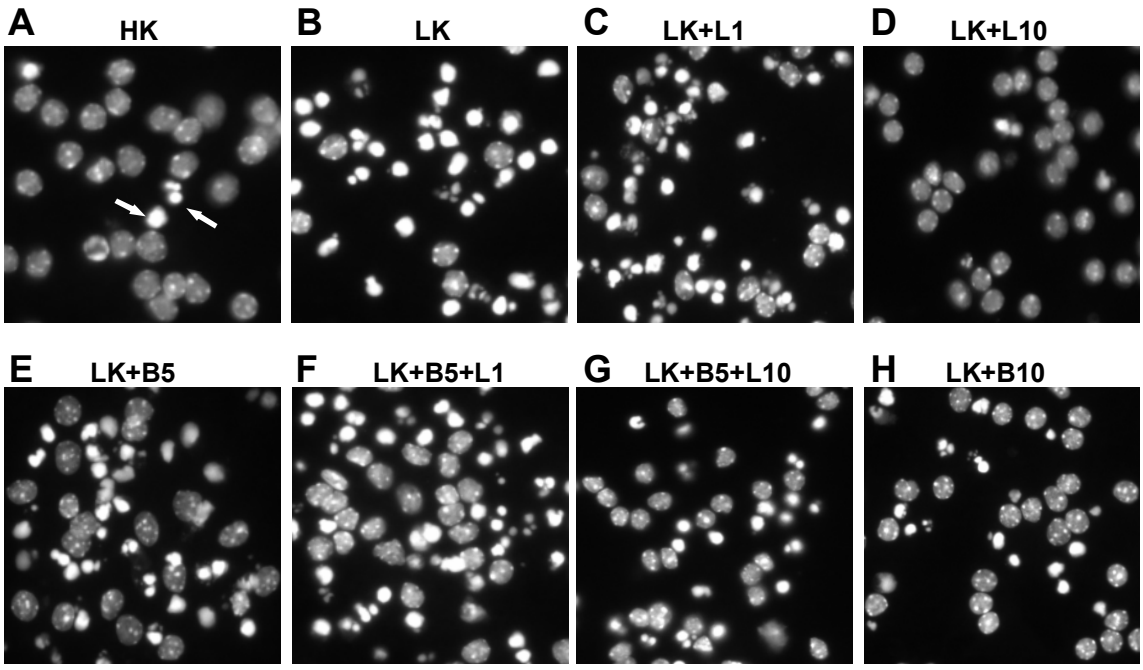

L1, LPC 1 μM; L10, LPC 10 μM; B5, BDNF 5 ng/ml; B10, BDNF 10 ng/ml.

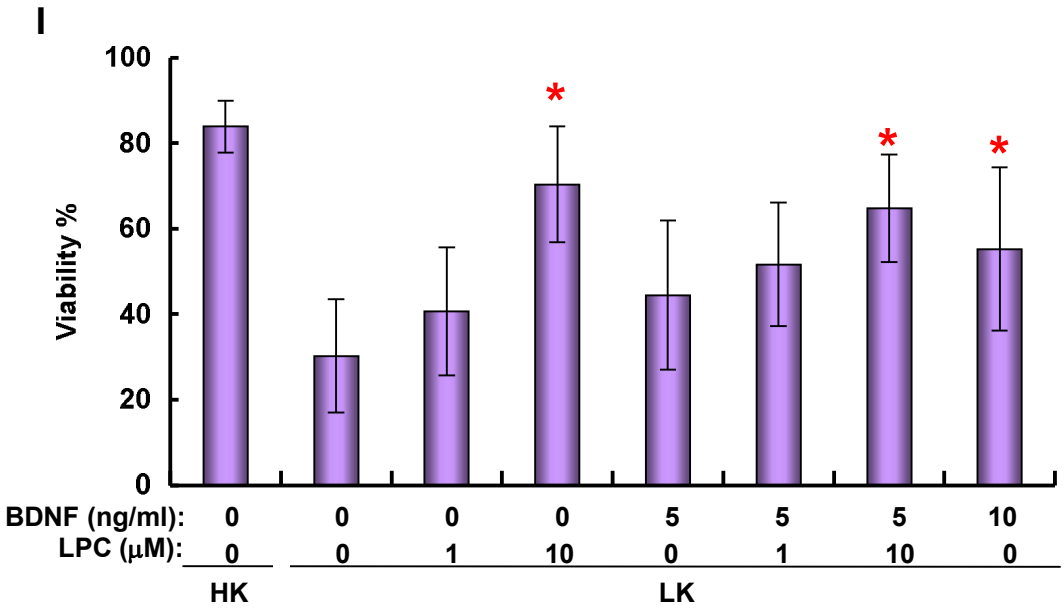

Figure 2-12 LPC at 10 μM alone is sufficient to protect CGNs from LK-induced apoptosis. CGNs cultured for 5 days *in vitro* (on coverslips coated with 0.2 % PEI in 24-well plate) were incubated in HK (DMEM containing 25 mM potassium), or LK (DMEM containing 5 mM potassium) supplemented with vehicle control (DMEM plus methanol), LPC (1 and 10 μM), BDNF (5 and 10 ng/ml), BDNF (5 ng/ml) together with LPC for 24 h. Cells were then fixed with 4% paraformaldehyde and stained with Hoechst 33258 (1 μg/ml). Morphology of nuclei was observed by fluorescent microscopy. **A-H,** Representative images from nine independent experiments which gave similar results are shown. Arrows in **A** indicate nuclei of apoptotic cells. **I,** apoptotic cells were counted and the percentage of viable cells was calculated. Data are means ± SD of nine independent experiments. *, $p<0.05$ by one-way ANOVA, compared with LK.

Chapter 3. Analyses on the mechanism whereby lysophosphatidylcholine potentiates NGF-induced TrkA signal

3.1 Introduction

Results in Chapters 1 and 2 have shown that LPC promotes both NGF- and BDNF-induced signals through enhancing the activation of their receptors TrkA and TrkB, respectively. The finding in Chapter 1 that TrkA (Fig. 1-9), but not EGF receptor (EGFR) (Fig. 1-17), was responsive to the effect of LPC on MAPK phosphorylation suggests that LPC plays a specific role on the neurotrophin-induced activation of TrkA, and possibly TrkB. To further understand the underlying mechanism of action of LPC, I next aimed to determine the domain(s) of TrkA involved in the effect of LPC on NGF-induced MAPK phosphorylation. This was done by examining the phosphorylation of MAPK in TrkA-, EGFR-, or TrkA/EGFR chimera-transfected cells. TrkA/EGFR chimeras were constructed by swapping the extracellular, transmembrane, and intracellular domains between TrkA and EGFR.

As described, $sPLA_2$ was previously found to show neurotrophin-like effect in PC12 cells and in CGNs through the release of LPC (52,53,55,56). Since LPC enhances NGF- and BDNF-induced MAPK phosphorylation, whether or not $sPLA_2$ has similar effect on NGF-induced MAPK phosphorylation was also tested in PC12 cells.

Accumulating evidence suggests the involvement of GPCRs such as G2A and GPR4 in the biological actions of LPC. For example, G2A was shown to mediate the chemoattractive effect of LPC in murine T hybridoma DO11.10 cells (40), migration of

phagocytes to apoptotic "find me" signals triggered by LPC in human monocytes (88), and the increase in transforming growth factor-β1 expression by LPC in regulatory T cells (89). On the other hand, G2A was also found to be a proton-sensing GPCR which was antagonized by LPC (90). Also, GPR4 was reported to mediate LPC-induced barrier dysfunction in endothelial cells (91). Our previous observation that G2A mediates the neuritogenic action of LPC in PC12 cells (55) suggests that G2A might regulate the enhancement of NGF-TrkA- and BDNF-TrkB-induced MAPK and Akt phosphorylation by LPC. In this Chapter, whether or not G2A and GPR4 modulate the effect of LPC on NGF-induced MAPK phosphorylation was tested by overexpressing G2A or GPR4 in PC12 cells, and co-transfecting G2A or GPR4 with TrkA to CHO-K1 cells.

In an alternative mode of action, LPC might act directly on TrkA without requiring the involvement of GPCRs. It is widely accepted that NGF induces dimerization and autophosphorylation of TrkA, thereby stimulating the downstream signaling events. However, recent studies have shown that the majority of TrkA preforms dimers in the endoplasmic reticulum before reaching to the cell surface, and dimerization is not regulated by NGF. NGF activates the preformed, yet inactive, TrkA dimer on the cell surface (57). To examine if LPC plays any role in the dimerization state of TrkA, I performed crosslinking experiment using the divalent crosslinker bis[sulfosuccinimidyl] suberate in TrkA-transfected PC12 cells.

3.2 Objective

One objective of the study in this Chapter is to identify the domain(s) of TrkA essential for the effect of LPC on NGF-induced MAPK phosphorylation. Another is to further understand the molecular mechanism of how LPC potentiates NGF-induced signals.

3.3 Results

3.3.1 Analyses of TrkA and EGFR exogenously expressed in CHO-K1, PC12, and HEK293 cells

3.3.1.1 Construction of the plasmids for expression of TrkA and EGFR fused with EGFP

Results in Chapters 1 and 2 showed that LPC promotes NGF- and BDNF-induced signals through enhancing the activation of their receptors, TrkA and TrkB, respectively. To test whether or not this phenomenon can be reproduced in the cells exogenously expressing TrkA, I transfected TrkA to CHO-K1 cells that do not express functional TrkA. To this end, a plasmid to exogenously express TrkA was constructed. Briefly, a cDNA fragment encoding the full-length mouse TrkA (GeneBank accession No. NM_001033124.1), 799 amino acids-long (Fig. 3-1 A), was amplified by PCR. The resultant PCR product was cloned into the *Eco*R I site of EGFP-N1 expression vector; in this construct, the intracellular, C-terminal end of TrkA was fused with EGFP (TrkA-EGFP-N1; Fig. 3-1 B).

In a similar way, the plasmid for expression of EGFR was also constructed. A cDNA fragment encoding the full-length rat EGFR (GeneBank accession No. M37394.2), 1209 amino acids-long (Fig. 3-1 C), was amplified by PCR, and was introduced into the *Xho* I site of EGFP-N1 expression vector; in this construct, the intracellular, C-terminal end of EGFR was fused with EGFP (EGFR-EGFP-N1; Fig. 3-1 D).

TrkA-EGFP-N1 and EGFR-EGFP-N1 were transiently transfected to CHO-K1 cells, respectively, and their expression was detected by Western blotting using anti-GFP

antibody (Fig. 3-1 E). The sizes of endogenous TrkA and EGFR are 140 and 175 kDa, respectively, and the expected sizes of TrkA and EGFR fused with EGFP (30 kDa) are 170 and 205 kDa, respectively. The result shown in Fig. 3-1 E demonstrates that both fusion proteins were successfully expressed with their expected sizes.

3.3.1.2 Phosphorylation of TrkA and EGFR in transfected CHO-K1 cells

Next, to test if the exogenously-expressed TrkA and EGFR in CHO-K1 cells behave as the endogenous receptors in PC12 cells, CHO-K1 cells untransfected or transiently transfected with TrkA-EGFP-N1 or EGFR-EGFP-N1 were analyzed for receptor phosphorylation. When the wild type, untransfected CHO-K1 cells were analyzed for phosphorylated TrkA using anti-phospho-TrkA antibody, no band was detected as expected (Fig. 3-2 A, top, lanes 1-5). However, when the same samples were probed with the anti-TrkA antibody that recognizes total TrkA (t-TrkA), a band with the size of ~170 kDa was detected (Fig. 3-2 A, middle, lanes 1-5). I speculated that this band is not endogenous TrkA, but due to non-specific reaction of the anti-TrkA antibody, since (1) the size was nearly equal to that of the band detected by anti-TrkA and anti-GFP antibodies in the TrkA-EGFP-transfected cells (Fig. 3-2 A, middle and bottom, lanes 6-9); (2) no phosphorylation product was detected upon stimulation as described above. In the case of EGFR, neither phosphorylated nor total EGFR was detected in the untransfected cells (Fig. 3-2 B, top and middle, lanes 1-4).

In TrkA-transfected cells, TrkA was highly autophosphorylated (Fig. 3-2 A, top, lane 6), which was not significantly increased by NGF and/or LPC (Fig. 3-2 A, top, lanes 7-9). In EGFR-transfected cells, autophosphorylation of EGFR was also observed (Fig. 3-2 B, top, lane 5), but unlike TrkA, phosphorylation of EGFR was greatly

increased by its ligand EGF (Fig. 3-2 B, top, lane 7). LPC alone did not enhance the phosphorylation of EGFR (Fig. 3-2 B, top, lane 6). Also, the addition of LPC together with EGF did not further elevate EGF-induced EGFR phosphorylation (Fig. 3-2 B, top, lane 8). Thus, although the response of EGFR was consistent with that seen in PC12 cells (Fig. 1-17), autophosphorylation of TrkA was very high upon its overexpression, and it was not significantly promoted by NGF and/or LPC, requiring further analysis. Expression of TrkA and EGFR was also confirmed using anti-GFP antibody (Fig. 3-2 A bottom, lanes 6-9, and B bottom, lanes 5-8).

3.3.1.3 Phosphorylation of TrkA in TrkA-transfected PC12 and HEK293 cells

Since the exogenously-expressed TrkA in CHO-K1 cells did not behave as endogenous TrkA in PC12 cells upon NGF and/or LPC treatments, I transfected TrkA-EGFP-N1 to PC12 cells and tried to test the effect of NGF and/or LPC on TrkA phosphorylation. When the phosphorylation status of TrkA was tested, similar result was observed as was seen in CHO-K1 cells: transfected TrkA-EGFP was spontaneously phosphorylated without NGF and LPC stimuli (Fig. 3-3 A, lane 3). Since the amount of endogenous TrkA is low even in PC12 cells, phosphorylated endogenous TrkA upon NGF and LPC treatments was not detected in the cells cultured in 24-well plates in this experiment. Although a slight increase in TrkA phosphorylation was seen upon NGF treatment (Fig. 3-3 A, lane 4) compared to that without treatment (Fig. 3-3 A, lane 3), it was not reproduced in the repeated experiments (data not shown). In addition, no enhancement of TrkA phosphorylation was detected by further addition of LPC (Fig. 3-3 A, lane 5).

In a recent study, only a slight autophosphorylaton of TrkA occurred when TrkA

was transiently transfected to HEK293 cells, and it was robustly increased by NGF treatment (92). Thus, HEK293 cells were used to express TrkA-EGFP, and the phosphorylation status of TrkA upon various stimuli was tested. In transfected cells, TrkA autophosphorylation still occurred (Fig. 3-3 B, upper, lane 2), and it was not further increased by LPC, NGF, or NGF plus LPC treatments in my experimental condition (Fig. 3-3 B, upper, lanes 3-5). Expression of TrkA was detected by anti-TrkA antibody (Fig. 3-3 B, bottom, lanes 2-5). A very weak band at the same size with endogenous TrkA, 140 kDa, was detected by anti-TrkA antibody in the wild type HEK293 cells (Fig. 3-3 B, bottom, lanes 1 and 6-9), but they were not phosphorylated upon NGF and/or LPC stimuli (Fig. 3-3 B, upper, lanes 7-9).

3.3.1.4 Construction of the plasmid for expression of TrkA without the tag and its expression in CHO-K1 and HEK293 cells

The effect of NGF and/or LPC on the phosphorylation of transfected TrkA was not seen in CHO-K1, PC12, and HEK293 cells (Figs. 3-2 and 3-3). To examine the possibility that this might be due to EGFP fused at C-terminus of TrkA, a new plasmid was constructed for expression of TrkA without the tag (TrkA-pME18S; Fig. 3-4 A). However, autophosphorylated TrkA was observed again in transfected CHO-K1 cells (Fig. 3-4 B, upper, lane 2). Although an increase in TrkA phosphorylation upon LPC or NGF treatment was detected (Fig. 3-4 B, upper, lanes 3 and 4), this was not reproduced (data not shown). Also, no significant enhancement of TrkA phosphorylation by co-addition of NGF and LPC was observed (Fig. 3-4 B, upper, lane 5).

TrkA-pME18S was also transfected to HEK293 cells. Similarly, TrkA was spontaneously phosphorylated (Fig. 3-4 C, upper, lane 2), which was not affected by the

addition of LPC, NGF, or NGF plus LPC treatments (Fig. 3-4 C, upper, lanes 3-5).

3.3.1.5 Establishment of a CHO-K1 cell line that stably expresses TrkA-EGFP and the phosphorylation analysis

Spontaneous phosphorylation of transfected TrkA was not further enhanced by NGF and LPC in the above attempts. This may be because the expression of TrkA was transient in those experiments. Therefore, a CHO-K1 cell line stably expressing TrkA-EGFP was established (CHO-K1-TrkA). The procedures for the selection of CHO-K1-TrkA stable cell line are shown in Fig. 3-5. Briefly, TrkA-EGFP-N1 was transfected to CHO-K1 cells, and the expression of TrkA-EGFP was confirmed in Fig. 3-6 A. Transfected cells were diluted and seeded in 10-cm dishes, and screened for stable cell lines by Geneticin (G418; 1000 μg/ml) selection until visible clones developed (about for 2 weeks). Then, developed clones were taken and seeded into the wells of 24-well plates, and cells from a single clone in each well were tested for the expression of TrkA-EGFP. Cells in a single well were found to express TrkA-EGFP (Fig. 3-6 B). The cells from this well were expanded, diluted, and subjected to the second selection. All the thirteen clones selected in the second selection stably expressed TrkA-EGFP (Fig. 3-6 C). From these thirteen clones, clone 7 in Fig. 3-6 C was selected, maintained in G418-free regular culture medium for about 3 weeks, and used as the CHO-K1-TrkA stable cell line for the experiment in Fig. 3-7 where phosphorylation of TrkA upon NGF and/or LPC treatments was examined. Nevertheless, phosphorylated TrkA was detected in untreated cells (Fig. 3-7 A, lane 1) and it was not affected by the stimulations of NGF and/or LPC (Fig. 3-7 A, lanes 2-4).

3.3.1.6 Phosphorylation of TrkA in CHO-K1 cells co-expressing TrkA and p75

Even in the CHO-K1 cells stably expressing TrkA, phosphorylation of TrkA was not elevated by its ligand NGF or NGF plus LPC treatment. It was reported that p75 interacts with TrkA and enhances the binding specificity to NGF (5). To test if the co-expression of p75 affects the response of TrkA, CHO-K1 cells were co-transfected with TrkA and p75 at different ratios as shown in Fig. 3-8, and treated with vehicle control or NGF. The plasmid for expression of p75 was previously constructed by inserting mouse cDNA for p75 at the *Eco*R I site of pME18S vector (p75-pME18S). A slight increase in TrkA phosphorylation was seen upon NGF treatment in the cells co-transfected with TrkA and p75 at a ratio of 5:1 (Fig. 3-8, lane 5) compared to untreated cells (Fig. 3-8, lane 2). Co-expressing p75 with TrkA might help TrkA to respond to NGF in a more physiologically-relevant way, but I did not go further to use this system.

3.3.2 LPC potentiates NGF-induced MAPK phosphorylation through the extracellular domain of TrkA

3.3.2.1 LPC enhances NGF-induced, but not EGF-induced, MAPK phosphorylation in TrkA-transfected CHO-K1 cells.

Since NGF and/or LPC failed to further increase the spontaneous phosphorylation of TrkA in both transiently and stably TrkA-transfected cells, I wondered if NGF and/or LPC are able to trigger the downstream signal, MAPK phosphorylation. Thus, I tested the effect of NGF, EGF, and/or LPC on MAPK phosphorylation in transiently transfected cells.

First, I tested the effect of NGF, EGF, and/or LPC on MAPK phosphorylation in the wild type or EGFP-N1 vector-transfected CHO-K1 cells (Fig. 3-9). MAPK was phosphorylated by none of these treatments in the wild type and vector-transfected CHO-K1 cells.

Next, TrkA-EGFP and EGFR-EGFP were transfected to CHO-K1 cells, respectively, and MAPK phosphorylation upon various stimuli was examined. In TrkA-transfected cells, the addition of NGF (50 ng/ml) weakly induced MAPK phosphorylation (Figs. 3-10 A and B, lane 3), and when LPC (1 μM) was added together, MAPK phosphorylation was significantly increased (Fig. 3-10 A and B, lane 4). In EGFR-transfected cells, EGF (25 ng/ml) induced MAPK phosphorylation (Fig. 3-10 C and D, lane 3), but this was not affected by LPC (Fig. 3-10 C and D, lane 4). These results are in a good agreement with those observed in PC12 cells, indicating that both transfected TrkA-EGFP and EGFR-EGFP behaved as endogenously-expressed receptors on the downstream signals. Therefore, I decided to use this system in the following experiments.

3.3.2.2 Construction and expression of TrkA/EGFR chimeric receptors

Next, using TrkA and EGFR as templates, TrkA/EGFR chimeric receptors C1, C2, C3, and C4 were constructed by swapping the extracellular (ED), transmembrane (TMD), and intracellular (ID) domains between TrkA and EGFR. For example, C1 contains extracellular and transmembrane domains of TrkA and the intracellular domain of EGFR (TrkA ED+TMD/EGFR ID). TrkA/EGFR chimeric cDNA products were generated using overlapping two-step PCR as shown in Fig. 3-11 (C1 is shown as an example). Resultant chimeric cDNA products were inserted into EGFP-N1 vector at

Xho I site. Schematic structures of each receptor and the plasmid map are shown in Figs. 3-12 A and B. Expression of TrkA/EGFR chimeric receptors in CHO-K1 cells was confirmed by Western blotting using anti-GFP antibody (Fig. 3-12 C). Chimeric receptors fused with EGFP appeared at around 175 kDa; the expression level of C1 and C3 was relatively lower compared to C2 and C4.

3.3.2.3 LPC enhances NGF-induced MAPK phosphorylation in C1- and C3-transfected CHO-K1 cells

TrkA/EGFR chimeric receptors C1 and C3 were transiently transfected to CHO-K1 cells, respectively, and the effect of NGF, EGF, and LPC on MAPK phosphorylation was analyzed. In C1 (TrkA ED/EGFR TMD+ID chimera)-transfected cells, NGF (50 ng/ml) slightly increased MAPK phosphorylation, and this was augmented by LPC (1 μM; Figs. 3-13 A and B, lanes 3 and 4), as was seen in the TrkA-transfected cells (Fig. 3-10 A and B). Similar result was obtained in C3 (TrkA ED+TMD/EGFR ID chimera)-transfected cells (Fig. 3-13 C and D, lanes 3 and 4). In both cases, LPC alone did not induce MAPK phosphorylation (Fig. 3-13 A-D, lane 2). EGF (25 ng/m) and EGF plus LPC treatments did not trigger MAPK phosphorylation, because C1 and C3 do not have the extracellular domain of EGFR (Fig. 3-13 A-D, lanes 5 and 6). These results indicate that the extracellular domain (ED) of TrkA is sufficient and critical to mediate the effect of LPC in enhancing NGF-induced MAPK phosphorylation.

3.3.2.4 LPC does not affect EGF-induced MAPK phosphorylation in C2- and C4-transfected CHO-K1 cells

In Fig. 3-14 A–D, C2 (EGFR ED/TrkA TMD+ID chimera)- or C4 (EGFR ED+TMD/TrkA ID chimera)-transfected cells were tested if they respond to NGF or EGF. Result shows that both responded to EGF (Figs. 3-14 A-D, lane 5), but not to NGF (Figs. 3-14 A-D, lane 3), since these cells express ED of EGFR, not TrkA. MAPK was strongly phosphorylated upon EGF treatment in both C2- and C4-transfected cells (Fig. 3-14 A-D, lane 5), but no significant enhancement was observed by the addition of LPC together with EGF (Fig. 3-14 A-D, lane 6). Since these cells express either transmembrane (TMD) or transmembrane plus intracellular domains (TMD+ID) of TrkA, the result presented here indicates that TMD and ID of TrkA are not responsible for the enhancement of ligand-induced MAPK phosphorylation by LPC.

3.3.3 Effect of LPC at different concentrations on NGF-induced TrkA and MAPK phosphorylation in PC12 cells.

In the previous study, neurotrophin-like activity of LPC in PC12 cells was observed at 100 μM in the serum-containing medium (55). In this study, however, the potentiation by LPC on NGF-induced MAPK and TrkA phosphorylation was observed at 1 μM (Figs. 1-3 and 1-9). To test if the neurotrophin-like activity of LPC at higher concentration was caused by the activation of TrkA even in the absence of NGF, I next examined TrkA phosphorylation in PC12 cells treated with LPC alone at different concentrations (1, 10, and 100 μM). The result in Fig. 3-15 demonstrates that LPC added alone at 1, 10, and 100 μM does not induce phosphorylation of TrkA (Fig. 3-15, lanes 2, 6, and 7). It should be noted that LPC at 100 μM showed some damage to cells

in the serum-free medium. Consistent with the data in Fig. 1-3 and 1-9, LPC added at 1 μM significantly enhanced NGF-induced TrkA and MAPK phosphorylation (Fig. 3-15, lane 4). Interestingly, LPC added alone at 10 and 100 μM induced phosphorylation of MAPK without inducing phosphorylation of TrkA (Fig. 3-15 lanes 6 and 7), indicating that LPC at higher concentrations might induce the activation of MAPK through an additional pathway independent of NGF-TrkA pathway in PC12 cells.

3.3.4 $sPLA_2$ enhances NGF-induced MAPK phosphorylation at a comparable level to LPC

It was previously demonstrated that $sPLA_2$ displays neurotrophin-like activities, and those effects of $sPLA_2$ were essentially attributable to the generation of LPC (55). Here, I tested if $sPLA_2$ potentiates NGF-induced MAPK phosphorylation like LPC. Exogenously-added p15, a fungal group XIV $sPLA_2$, enhanced NGF-induced MAPK phosphorylation at a similar level to LPC (Fig. 3-16). This suggests that LPC generated locally by $sPLA_2$-mediated hydrolysis of plasma membrane phosphatidylcholine acts in potentiating NGF-TrkA signaling pathway *in situ*.

3.3.5 Analyses on the possible mechanisms of action of LPC on NGF-TrkA signals

3.3.5.1 Effect of LPC on NGF-induced MAPK phosphorylation when it was added at different time points

The previous study in our laboratory demonstrated that the effect of LPC on neurite outgrowth was mediated by a GPCR, G2A, in PC12 cells (55). It was also reported that the chemotaxis of immune cells to LPC requires G2A (40). To examine if

any second messenger, possibly generated at the downstream of G2A, regulates the effect of LPC on NGF-induced MAPK phosphorylation, LPC was applied to cells at different time points relative to NGF addition as indicated in Figs. 3-17 and 3-18. The concept for this experiment is that if there is any second messenger generated by LPC treatment and this hypothetical messenger augments NGF-induced MAPK phosphorylation, then it is expected that longer pretreatment with LPC would result in the accumulation of the second messenger and further enhancement of NGF-induced signal. The result shows that when NGF and LPC were added separately at the same time, the enhancement of MAPK phosphorylation by LPC was the highest (Fig. 3-18 A and B, lane 2). The addition of premixed LPC and NGF, the experimental method with which other experiments were done, also significantly induced MAPK phosphorylation, albeit to a relatively lower level (Fig. 3-18 B, lane 3). When LPC was added 10, 30, and 60 min before NGF addition, the degree of enhancement of NGF-induced MAPK phosphorylation gradually decreased (Fig. 3-18 B, lanes 5-7). Meanwhile, when LPC was added 5 min after NGF, it failed to induce significant increase in NGF-induced MAPK phosphorylation (Fig. 3-18 B, lane 4). Although not conclusive, this result implies that it is unlikely that second messenger generation is involved in the effect of LPC on NGF-induced MAPK phosphorylation. This result also indicates that the action of LPC on NGF-induced MAPK phosphorylation might occur during the early stage of NGF-TrkA mediated signaling, since when LPC was added 5 min after NGF addition, the enhancement of MAPK phosphorylation was decreased.

3.3.5.2 G2A and GPR4 do not regulate the effect of LPC on NGF-induced MAPK phosphorylation

To test if G2A and GPR4 mediate the effect of LPC on NGF-induced MAPK phosphorylation, plasmids for the expression of G2A or GPR4 were constructed. A cDNA fragment encoding the full-length mouse G2A was amplified by PCR using the cDNA library prepared from PC12 cells as a template. The resultant PCR product was cloned into EGFP-N1 vector between *Hin*d III and *Eco*R I sites. In this construct, C-terminus of G2A was fused with EGFP (G2A-EGFP-N1). The plasmid for the expression of GPR4 was prepared previously; the amplified PCR product of full-length mouse GPR4 was cloned into EGFP-N1 vector between *Hin*d III and *Eco*R I sites (Fig. 3-19 A).

G2A and GPR4 were transfected to PC12 cells, and MAPK phosphorylation was analyzed by Western blotting. The result shows that the overexpression of G2A or GPR4 did not affect the potentiation by LPC on NGF-induced MAPK phosphorylation (Fig. 3-19 B). Similar result was observed in CHO-K1 cells co-transfected with TrkA and G2A or GPR4 (Fig. 3-19 C). Expression of G2A and GPR4 was confirmed by isolating total RNA after transfection and PCR analysis (Fig. 3-19 D). These results suggest that the effect of LPC on NGF-induced MAPK phosphorylation is not mediated by G2A and GPR4.

3.3.5.3 Effect of LPC on the formation of TrkA dimer in TrkA-transfected PC12 cells

As described in the Introduction, it has been reported that TrkA dimers form inside the cells before NGF binding; NGF does not modulate the formation of TrkA

dimer, but activates these preformed TrkA dimer on the cell surface. Whether or not LPC regulates the formation of TrkA dimer was examined using divalent crosslinker bis[sulfosuccinimidyl] suberate (BS^3) in PC12 cells transfected with TrkA-EGFP-N1. First, no TrkA dimer was detected before crosslinking by BS^3: Partially glycosylated endogenous TrkA monomer was detected at around 110 kDa in the wild type and TrkA-transfected PC12 cells (Fig. 3-20, lanes 1 and 2). In TrkA-transfected cells, both partially and fully glycosylated TrkA-EGFP monomer were also detected at 140 and 170 kDa, respectively. (Fig. 3-20, lanes 2-5). After crosslinking, preformed dimer of partially glycosylated endogenous TrkA was detected at around 220 kDa (Fig. 3-20, lane 3), although the band was very faint. The intensity of this band was not affected by NGF and/or LPC treatments (Fig. 3-20, lanes 4 and 5). Preformed dimers of partially or fully glycosylated TrkA-EGFP were detected in untreated TrkA-transfected PC12 cells (Fig. 3-20, lane 3) at 280 and 340 kDa, respectively, and again these were not affected by the addition of NGF (Fig. 3-20, lane 4). This is consistent with the report that TrkA preforms dimers, which is not regulated by NGF. In the cells treated with NGF together with LPC, the same level of TrkA dimers were observed after crosslinking (Fig. 3-20, lane 5), suggesting that LPC has no effect on the formation of TrkA dimer.

3.4 Discussion

Spontaneous phosphorylation of TrkA occurred in all cases tested in the present study when TrkA was overexpressed, and it was not further enhanced by its ligand NGF, as well as NGF plus LPC treatment. Hence, the effect of LPC on NGF-induced TrkA phosphorylation was not examined in transfected cells. The precise reason for autophosphorylation is not clear, but it is likely due to the unique property of Trk receptors. It was reported that Trk receptors are much easier to undergo autophosphorylation following overexpression in the absence of neurotrophins, which made it difficult to study the mechanism associated with NGF-TrkA signal in transfected cells (93). Even so, the downstream signal of TrkA activation, MAPK phosphorylation, was responsive to NGF and LPC stimuli in TrkA-transfected cells. Autophosphorylation of EGFR was also observed following transfection, but unlike TrkA, its phosphorylation was further increased by the ligand EGF.

Studies using TrkA/EGFR chimeric receptors expressed in CHO-K1 cells showed that the extracellular domain, not the transmembrane and intracellular domains, of TrkA is responsible for the effect of LPC on NGF signals. The extracellular immunoglobulin-like subdomains (Ig-like subdomains shown in Fig. 1-1) of TrkA, D4 and D5, were reported to be important for NGF binding. When D4 and D5 were removed from TrkA, NGF binding was abolished (94). Subsequent studies showed that D5, located near the transmembrane region, is critical and sufficient for NGF binding (95,96). Also, the mutation of proline 203 to alanine in the Ig-like subdomain of TrkA caused the spontaneous activation of the receptor. These findings suggested that Ig-like subdomain contributes to the ligand binding and ligand-induced activation of receptor. Modulating the structure of Ig-like subdomain may induce spontaneous activation of

TrkA (97,98). LPC is an amphiphlic molecule that should distribute into both membrane and soluble compartments. Since the potentiation by LPC of the phosphorylation of TrkA was observed only in the presence of NGF, not by LPC alone, it might be speculated that LPC evokes allosteric changes in the membrane-proximal D5 subdomain, thereby modulating the affinity and/or stability of TrkA-NGF complex.

In contrast to other lysophospholipids including LPA, LPE, and LPS, the biological actions of which are mostly mediated by specific GPCRs and are observed at submicromolar or micromolar concentrations, most studies wherein the effects of LPC were examined used LPC at or higher than 10 μM (99). For example, the chemotactic effect of LPC to phagocytes and the potentiation by LPC in the suppressive function of human naturally occurring regulatory T cells were observed when LPC was used at 10 μM (88,89). The results in this study showing that the effect of LPC was observed at 1 μM (or less) of LPC, along with the previous observation that G2A mediates the neuritogenic action of LPC in PC12 cells (55), suggest that G2A might regulate the enhancement of NGF-TrkA- and BDNF-TrkB-induced MAPK and Akt phosphorylation. However, neither overexpression of G2A (or GPR4) in PC12 cells nor co-transfection of G2A (or GPR4) with TrkA in CHO-K1 cells affected the ability of LPC to promote NGF-induced MAPK phosphorylation. This result still leaves a possibility, if any, that the effect of LPC on NGF-induced MAPK phosphorylation is mediated by different GPCR(s). In addition to G2A and GPR4, orphan GPCR, GPR11, was also found to be involved in the induction of insulin secretion from pancreatic β-cells by LPC (100). Close association of receptor tyrosine kinases, including Trk receptors, and GPCRs has been reported in some cellular systems. For example, a G_i-coupled receptor, β2-adrenergic receptor (β2AR), transactivates EGFR through a multi-receptor complex

containing both β2AR and EGFR (101). Also, G_s-coupled receptor, adenosine 2A receptor, induces the activation of TrkA and Akt, but not MAPK, survival signaling pathway in PC12 cells (102). Trk activation is also associated with GPCRs including PAC1 receptors (103) and endocannabinoid receptors (93). Therefore, the involvement of GPCRs other than G2A or GPR4 in the effect of LPC on NGF-TrkA and BDNF-TrkB signals still needs to be investigated.

As an alternative mechanism, LPC might stimulate the formation of TrkA dimer as mentioned in the Introduction. However, the result shows that LPC does not seem to play a role on TrkA dimer formation, implying that a different pathway is involved in the effect of LPC on NGF-induced MAPK phosphorylation. Examining the effect of LPC on the binding affinity of NGF and TrkA dimer might be of interest in the future study.

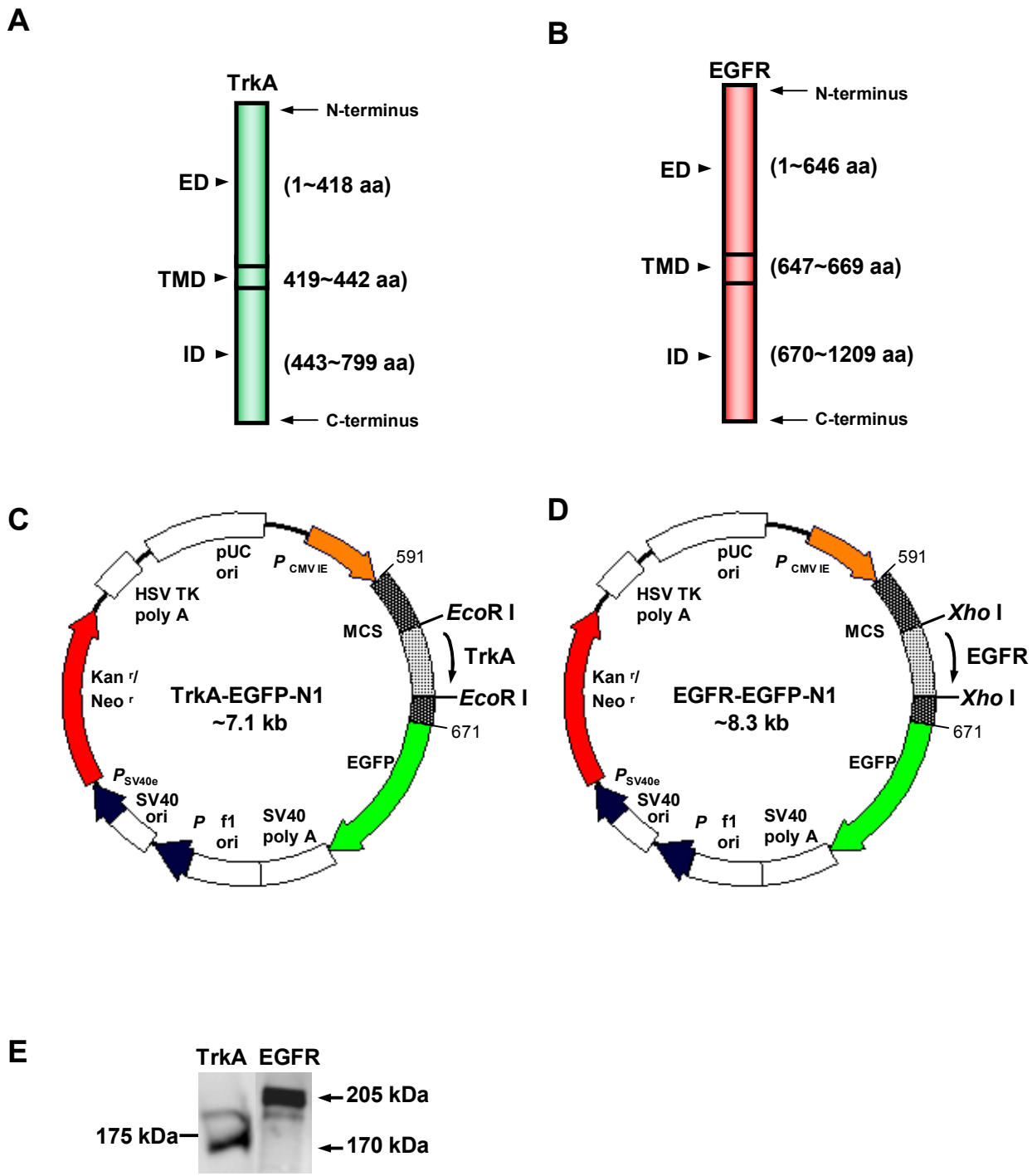

Figure 3-1 A and B, schemes showing the extracellular (ED), transmembrane (TMD), and intracellular domains (ID) of TrkA and EGFR. *C* and *D*, the plasmids map for expression of TrkA and EGFR. *E*, expression of TrkA and EGFR was confirmed by Western blotting using anti-GFP antibody.

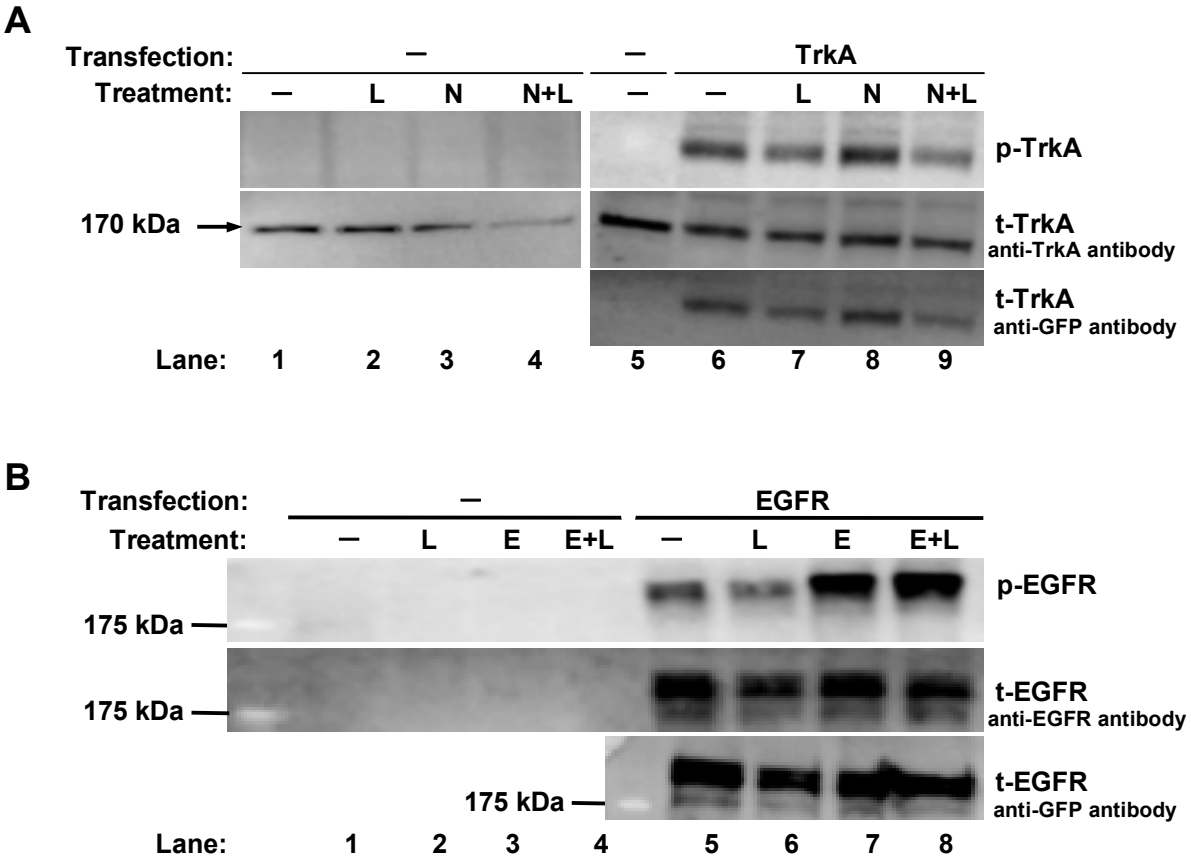

Figure 3-2 Phosphorylation of TrkA and EGFR upon NGF and EGF stimuli in the presence or absence of LPC in wild type CHO-K1 and TrkA or EGFR transfected-CHO-K1 cells. CHO-K1 cells cultured in 24-well plate were untransfected (—) or transiently transfected with TrkA-EGFP-N1 (TrkA, 0.8 μg/well) or EGFR-EGFP-N1 (EGFR, 0.8 μg/well) by Lipofectamine 2000 (1.5 μl/well) for 18-24 h. Then, cells were serum-starved for 1.5 h, and stimulated with vehicle control (DMEM plus methanol), LPC (L, 1 μM), NGF (N, 50 ng/ml), NGF and LPC together (N+L), EGF(E, 25 ng/ml), or EGF and LPC together (E+L) for 5 min. **A and B, top and middle panels**, phosphorylated and total TrkA (p-TrkA or t-TrkA) and EGFR (p-EGFR or t-EGFR) were analyzed by Western blotting. **A and B, bottom panel**, expression of TrkA and EGFR was detected using anti-GFP antibody.

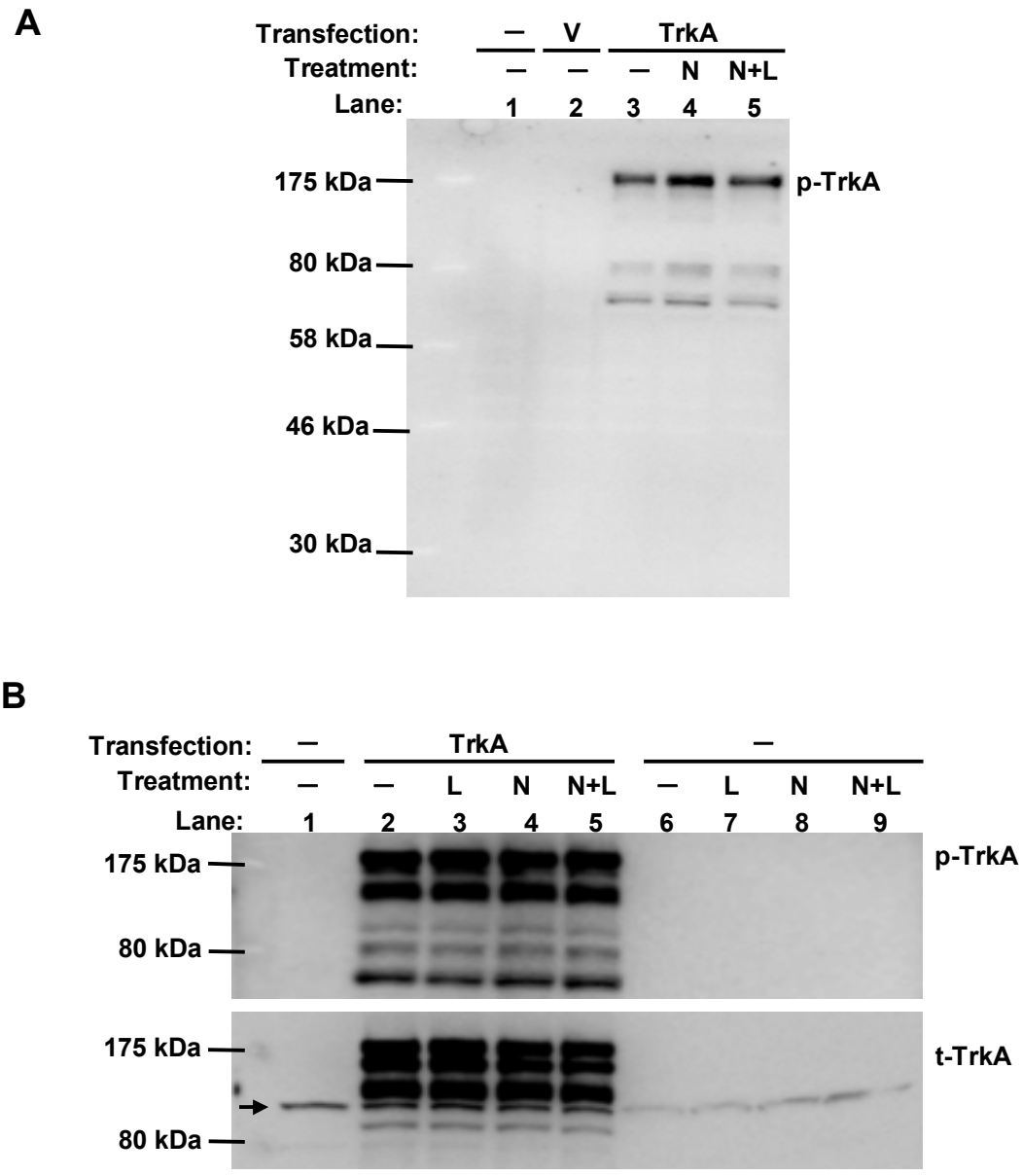

Figure 3-3 Phosphorylation of TrkA in TrkA-transfected PC12 and HEK293 cells. PC12 (**A**) or HEK293 cells (**B**) cultured in 24-well plate were untransfected (—), transiently transfected with TrkA-EGFP-N1(TrkA, 0.5 μg/well), or EGFP-N1 vector (V) by Lipofectamine 2000 (1.5 μl/well) for 18-24 h. Cells were then serum-starved for 1.5 h, and treated with vehicle control (—, DMEM plus methanol), LPC (L, 1 μM), NGF (N, 50 ng/ml), or NGF and LPC together (N+L) for 3 min. Phosphorylated and total TrkA (p-TrkA and t-TrkA) were analyzed using anti-phospho-TrkA (Tyr490) and anti-TrkA antibodies. **A**, the result shown is the reprensentative of two independent experiments. **B**, the result shown is the representative of two independent experiments which gave similar results. Arrow indicates the band (140 kDa) detected by anti-TrkA antibody in wild type HEK293 cells.

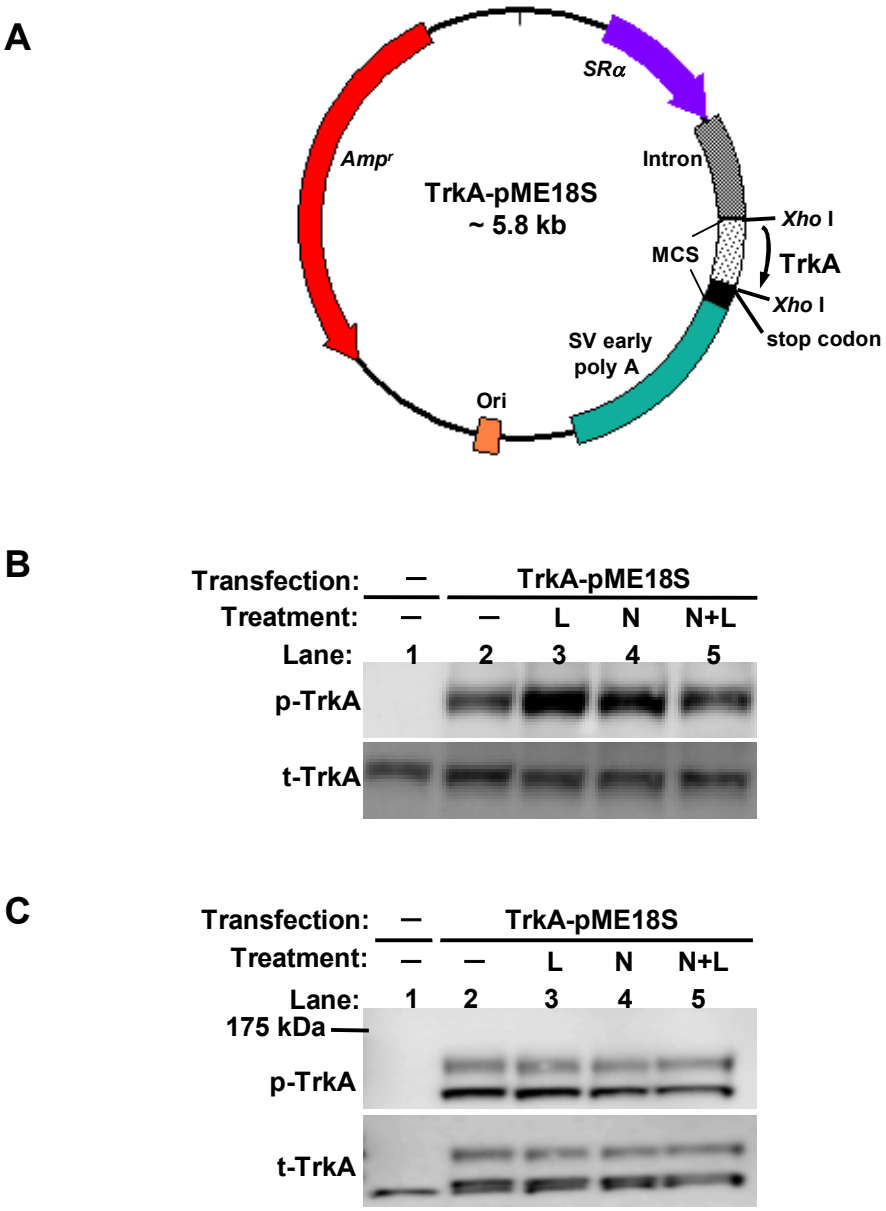

Figure 3-4 Construction of the plasmid for expression of TrkA without tag and its phosphorylation in CHO-K1 and HEK293 cells. **A**, the map of plasmid map for expression of TrkA without tag in pME18S vector (TrkA-pME18S. CHO-K1 (**B**) or HEK293 (**C**) cells cultured in 24-well plate were untransfected (—) or transfected with TrkA-pME18S (0.8 μg/well) by Lipofectamine 2000 (1.5 μl/well) for 18-24 h. Cells were then treated with vehicle control (—, DMEM plus methanol), LPC (L, 1 μM) or NGF (N, 50 ng/ml) alone, or NGF and LPC together (N+L) for 5 min. Phosphorylated TrkA (p-TrkA) and total TrkA (t-TrkA) were analyzed by Western blotting using anti-phospho-TrkA (Tyr490) and anti-TrkA antibodies, respectively. **B** and **C**, the result shown is the representative of two independent experiments.

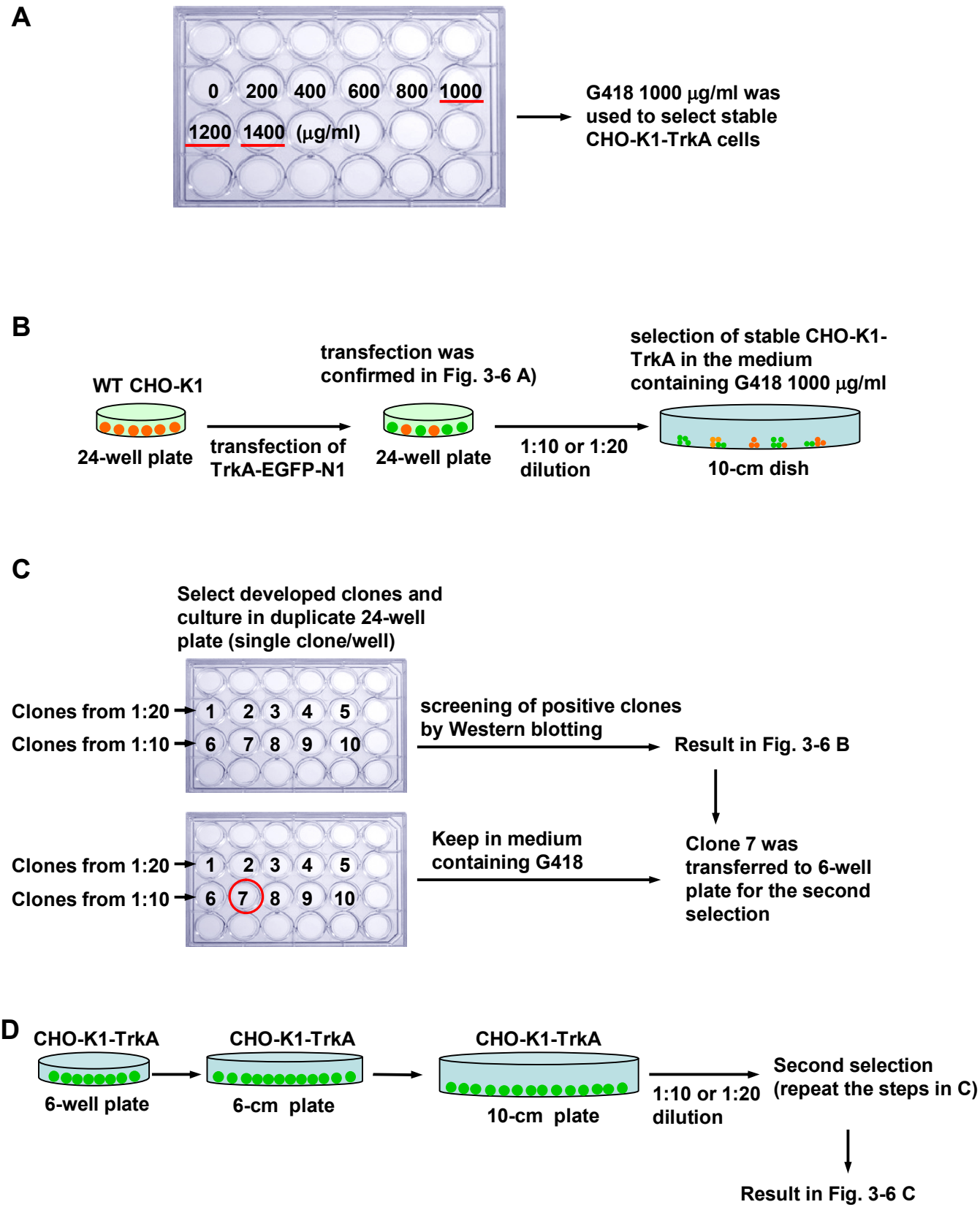

Figure 3-5 Scheme showing the experimental procedures for the selection of CHO-K1-TrkA stable cell line using G418

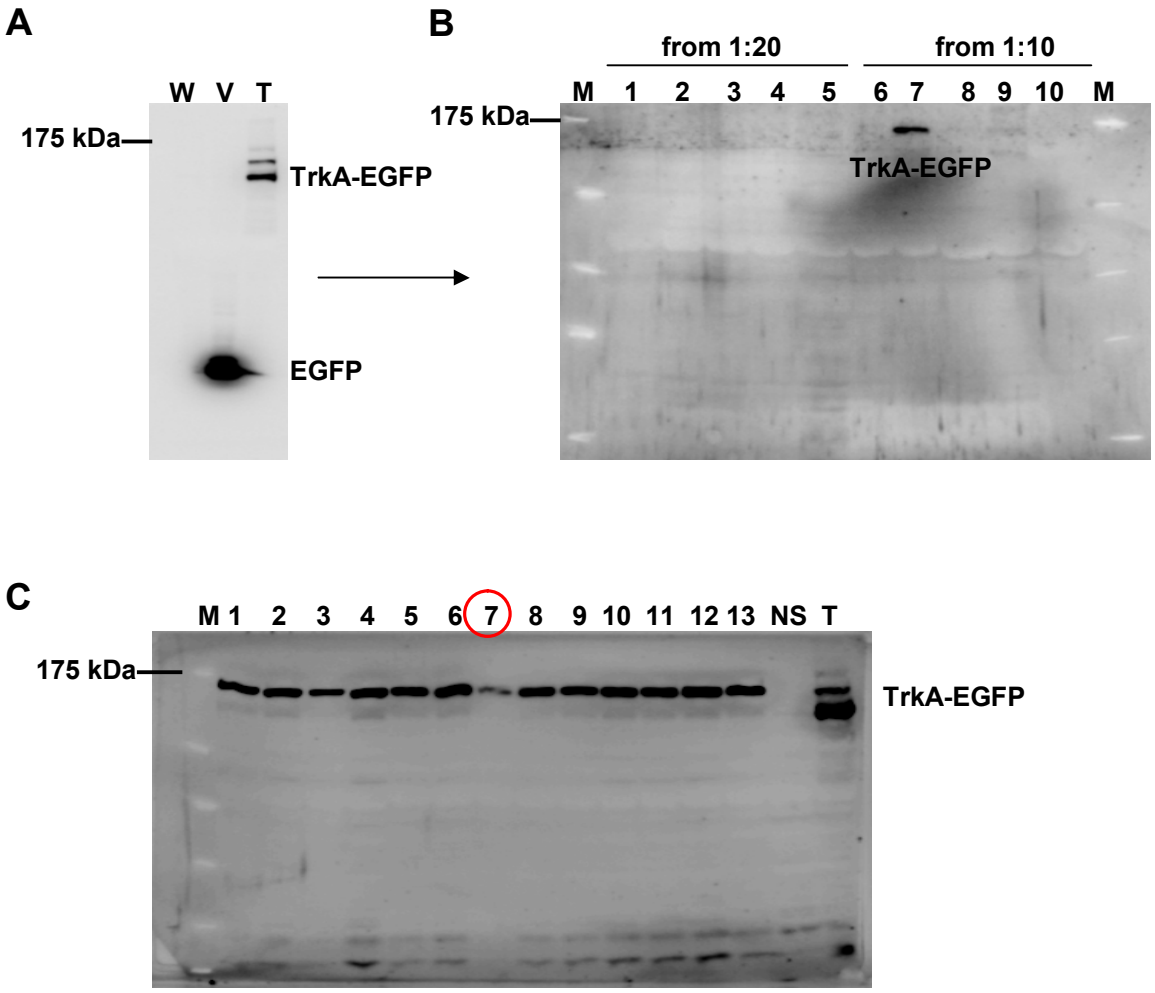

Figure 3-6 Selection of stable CHO-K1-TrkA cell line using G418

A, TrkA-EGFP-N1 was transfected in CHO-K1 cells, and expression of TrkA-EGFP was confirmed by Western blotting. **B**, screening of CHO-K1 cells stably expressing TrkA-EGFP from the first selection by Western blotting. **C**, screening for CHO-K1 cells stably expressing TrkA-EGFP from the second selection by Western blotting. Expression of TrkA-EGFP was detecd by anti-GFP antibody. M, marker; V, EGFP-N1 vector transfection; T, transient transfection of TrkA-EGFP-N1; NS, no sample.

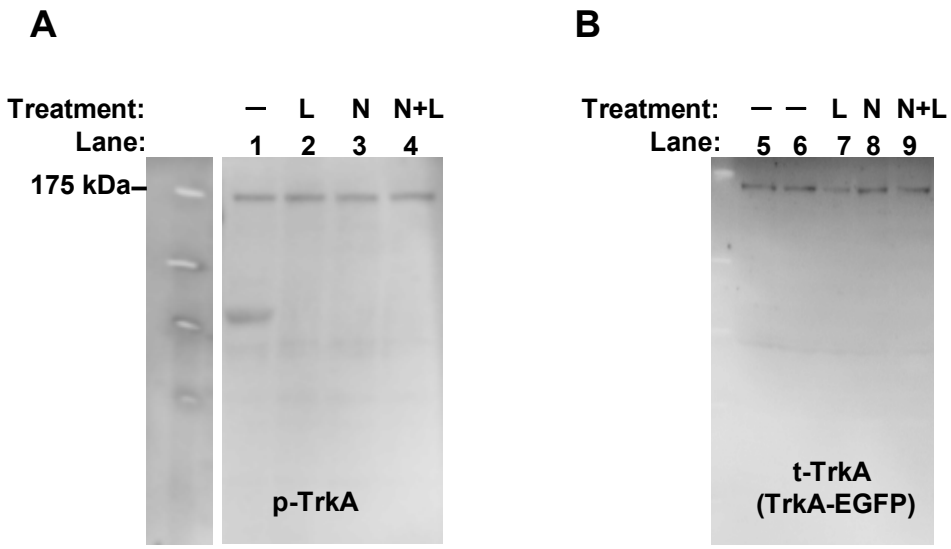

Figure 3-7 Phosphorylation of TrkA in CHO-K1-TrkA cells. CHO-K1-TrkA cells (stably expressing TrkA) were serum-starved for 26 h, and then treated with vehicle control (—, DMEM plus methanol), LPC (L, 1 μM) or NGF (N, 50 ng/ml) alone, or NGF and LPC together (N+L) for 5 min. **A**, phosphorylated TrkA (p-TrkA) was analyzed by Western blotting using anti-phospho-TrkA (Tyr490) antibody. **B**, expression of TrkA-EGFP was detected by anti-GFP antibody.

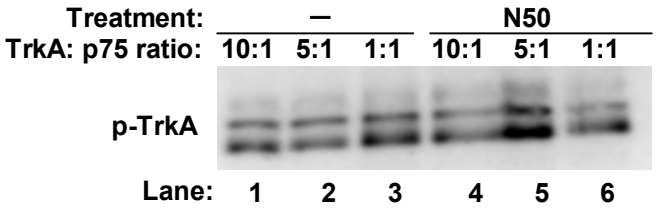

Figure 3-8 Phosphorylation of TrkA in CHO-K1 cells co-expressing TrkA and p75. CHO-K1 cells cultured in 24-well plate were transiently transfected with TrkA-EGFP-N1 (TrkA, 0.5 μg/well) or TrkA-EGFP-N1 (0.5 μg/well) and p75-pME18S (0.05, 0.1, and 0.5 μg/well) together by Lipofectamine 2000 (1.5 μl/well) for 24 h. Cells were then serum-starved for 1.5 h, and treated with vehicle control (—, DMEM plus methanol) or NGF (N, 50 ng/ml) for 5 min. Phosphorylated TrkA (p-TrkA) was analyzed by Western blotting using anti-phospho-TrkA (Tyr490) antibody.

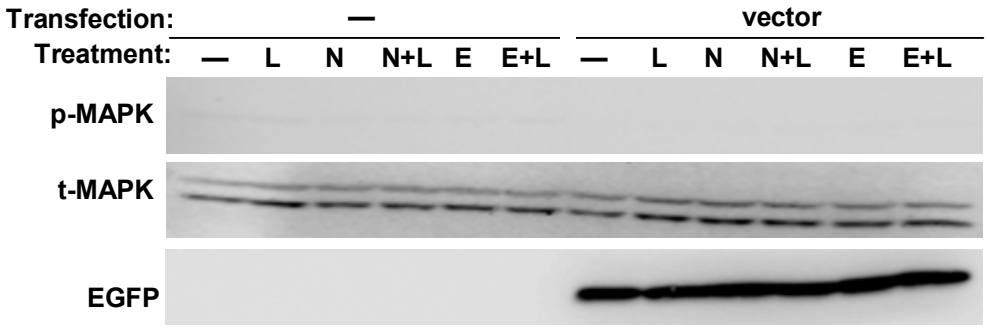

Figure 3-9 NGF, EGF and/or LPC do not induce MAPK phosphorylation in the wild type and vector-transfected CHO-K1 cells. CHO-K1 cells cultured in 24-well plate were untransfected (－) or transiently transfected with EGFP-N1 vector (vector, 0.8 μg/well) by Lipofectamine 2000 (1.5 μl/well) for 18-24 h. Then, cells were serum-starved for 1.5 h, and stimulated with vehicle control (－, DMEM plus methanol), LPC (L, 1 μM), NGF (N, 50 ng/ml), NGF and LPC together (N+L), EGF (E, 25 ng/ml), or EGF and LPC together (E+L) for 5 min. Phosphorylated MAPK (p-MAPK) and total MAPK (t-MAPK) were analyzed using phospho-p44/42 (Thr202/Tyr204) MAP Kinase and p44/42 MAP Kinase antibodies, respectively (upper and middle panels). Expression of EGFP was detected by Western blotting using anti-GFP antibody (bottom panel). The result shown is the representative of three independent experiments which gave similar results.

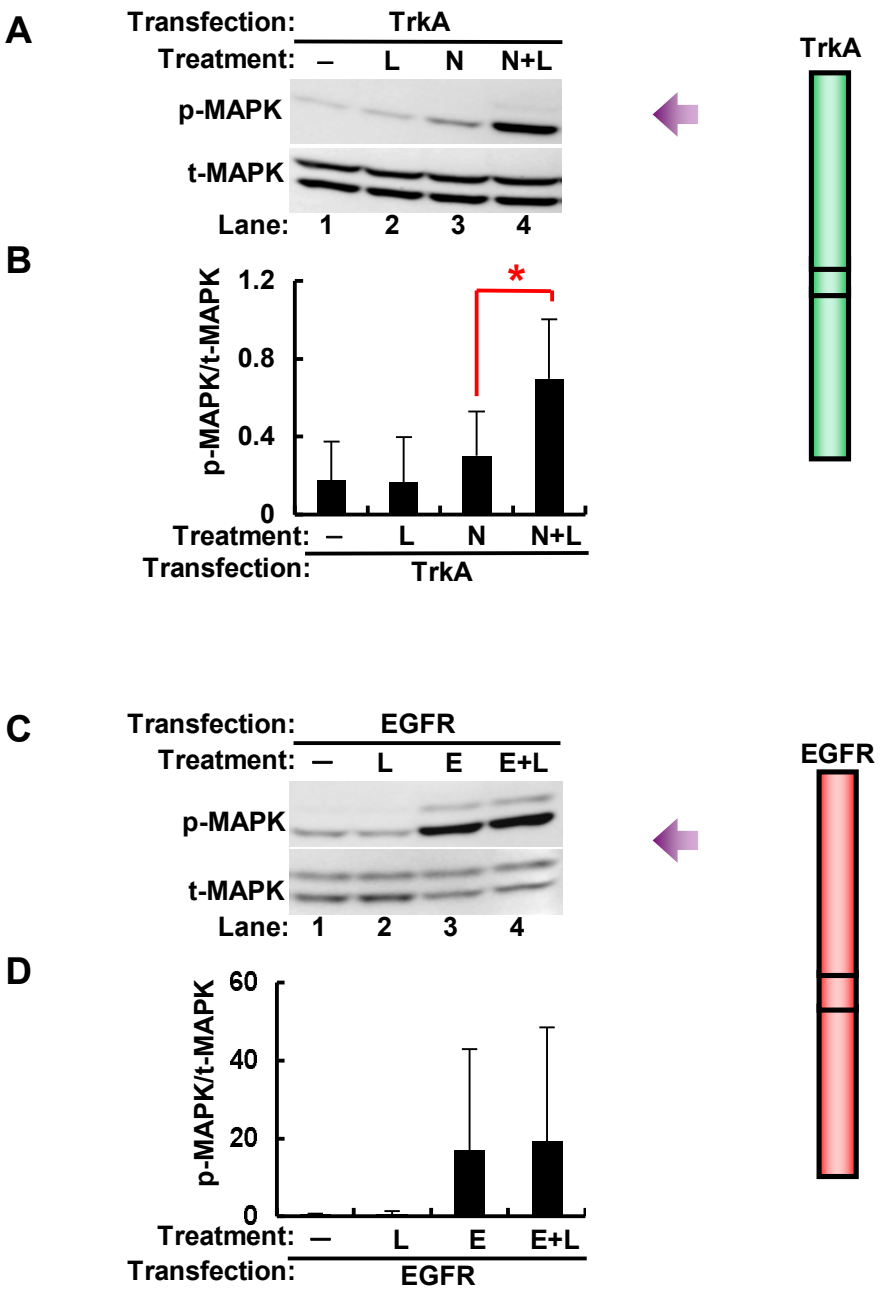

Figure 3-10 LPC enhances NGF-induced, but not EGF-induced, MAPK phosphorylation in TrkA- or EGFR-transfected CHO-K1 cells. CHO-K1 cells cultured in 24-well plate were transiently transfected with TrkA-EGFP-N1 (TrkA, 0.8 μg/well) in **A** and **B**, or EGFR-EGFP-N1 (EGFR, 0.8 μg/well) in **C** and **D** by Lipofectamine 2000 (1.5 μl/well) for 18-24 h. Cells were then serum-starved for 1.5 h, and treated with vehicle control (−, DMEM plus methanol), LPC (L, 1 μM), NGF (N, 50 ng/ml), NGF and LPC together (N+L), EGF (E, 25 ng/ml), or EGF and LPC together (E+L) for 5 min. In **A** and **C**, phosphorylated MAPK (p-MAPK) and total MAPK (t-MAPK) were analyzed by Western blotting using phospho-p44/42 (Thr202/Tyr204) MAP Kinase and p44/42 MAP Kinase primary antibodies, respectively. In **B** and **D**, the amounts of p-MAPK and t-MAPK were quantified and the relative ratio of p-MAPK vs t-MAPK in each condition was calculated. Data are means ± SD of three independent experiments.
*, $p<0.05$ by one-way ANOVA.

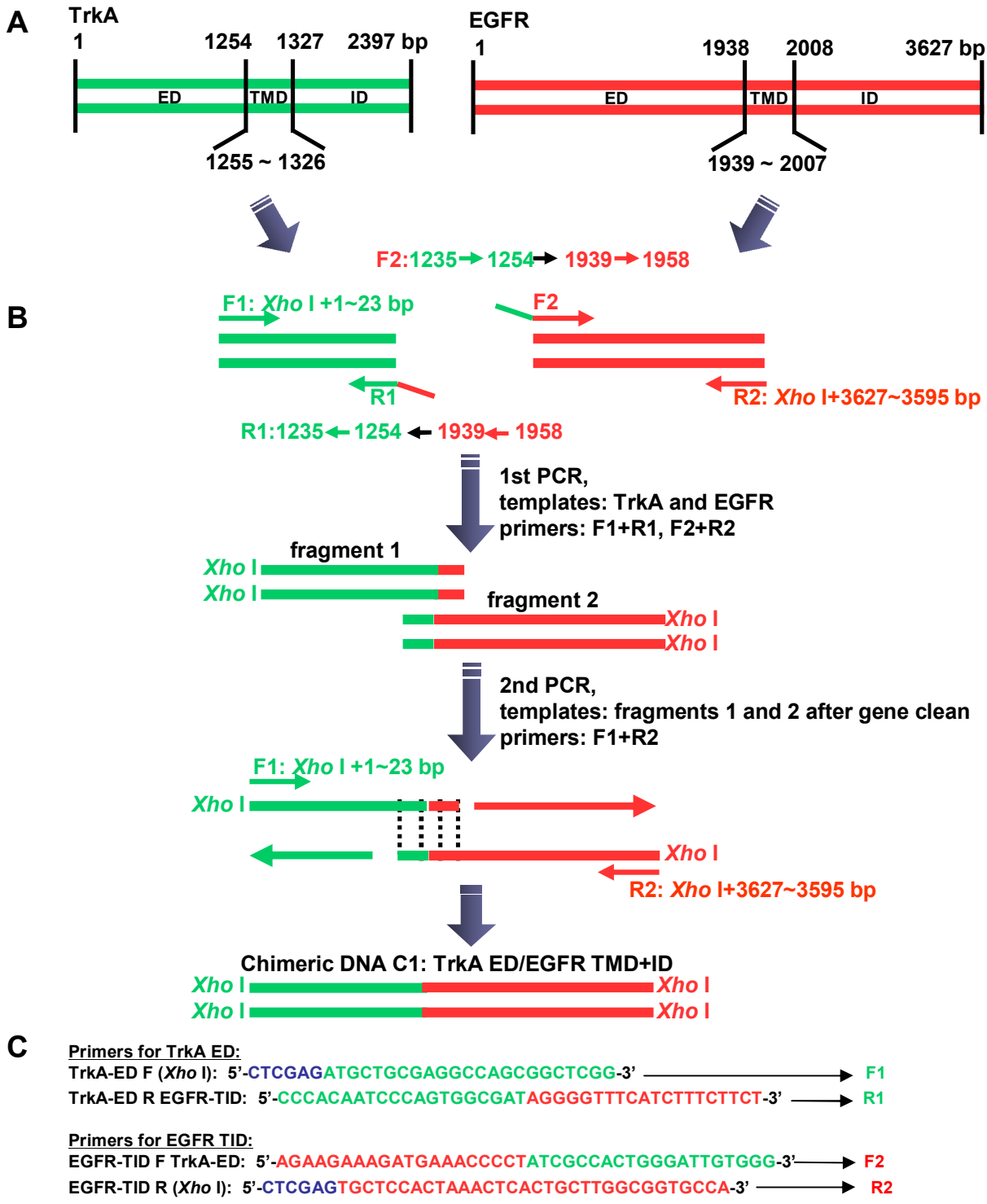

Figure 3-11 Scheme showing the strategy of overlapping PCR to create chimeric cDNA product C1 as an example. **A**, extracellular (ED), transmembrane domain (TMD), and intracellular domains (ID) of TrkA and EGFR. **B**, In the 1st PCR, primers F1 and R1 were used to amplify ED of TrkA. R1, at its 3'-end, has additional sequence (in red) corresponding to the TMD sequence of EGFR. Like wise, F2 and R2 were used for amplifying TMD+ID of EGFR. F2, at its 5'-end, has additional sequence corresponding to TrkA ED (in red). In the 2nd PCR, TrkA ED and EGFR TMD+ID was joined by amplification using primers F1 and R2. **C**, nucleotide sequence of primers are shown. Nucleotides in blue are the *Xho* I sites.

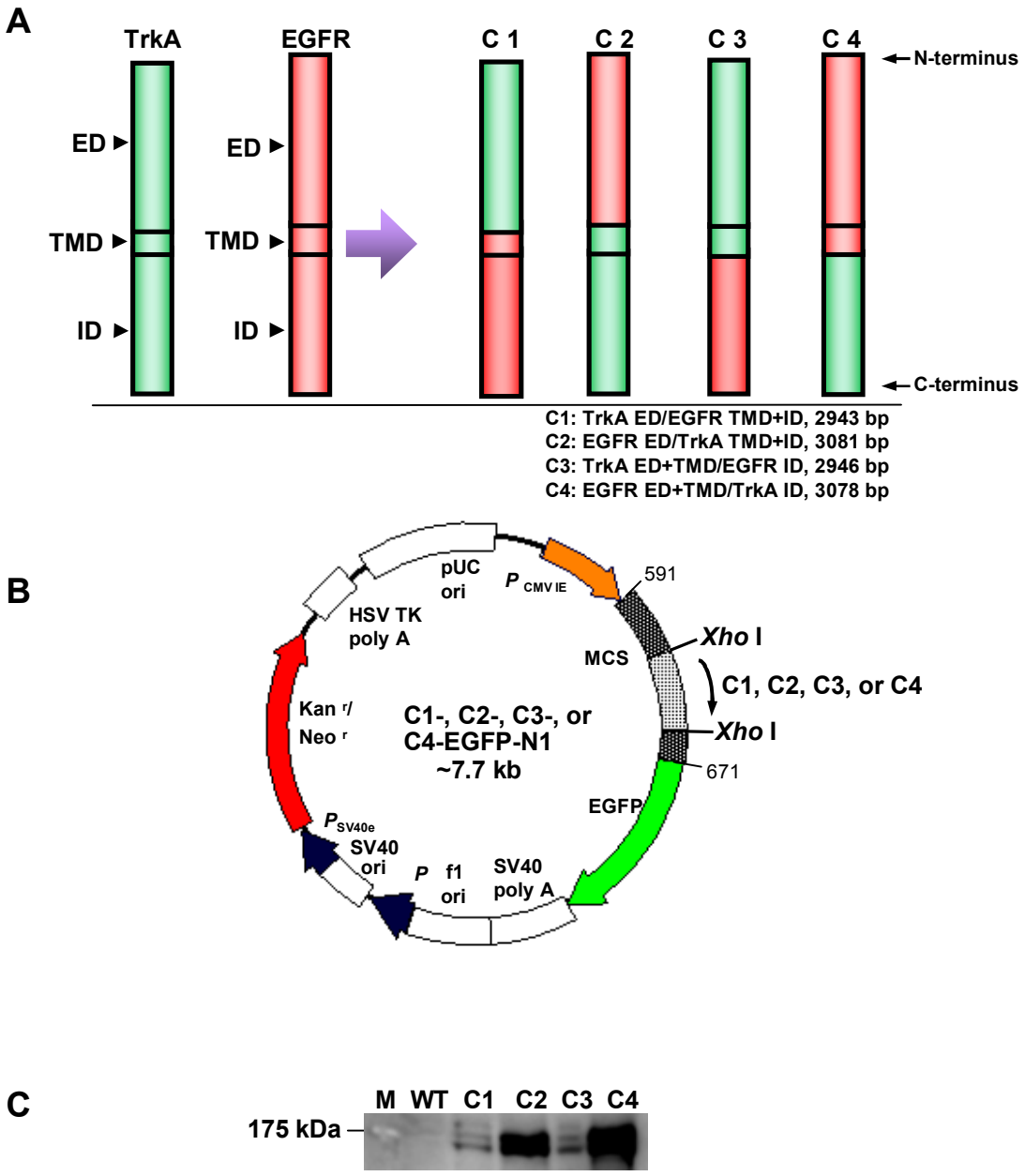

Figure 3-12 Construction of TrkA/EGFR chimeric receptors and their expression in CHO-K1 cells. **A**, schematic representation of TrkA, EGFR, and TrkA/EGFR chimeric cDNA products C1, C2, C3, and C4. **B**, the plasmid map for the expression of TrkA/EGFR chimeric receptors, C1, C2, C3, and C4. Each of chimeric cDNA product was introduced into expression vector EGFP-N1, at *Xho* I site. C-terminus of these receptors was fused with EGFP. **C**, CHO-K1 cells were untransfected (WT) or transiently transfected with C1, C2, C3, or C4 (0.8 μg/well) by Lipofectamine 2000 (1.5 μl/well) for 24 h. Expression of cheimeric receptors C1, C2, C3, and C4 was detected by Western blotting using anti-GFP antibody. M, protein marker.

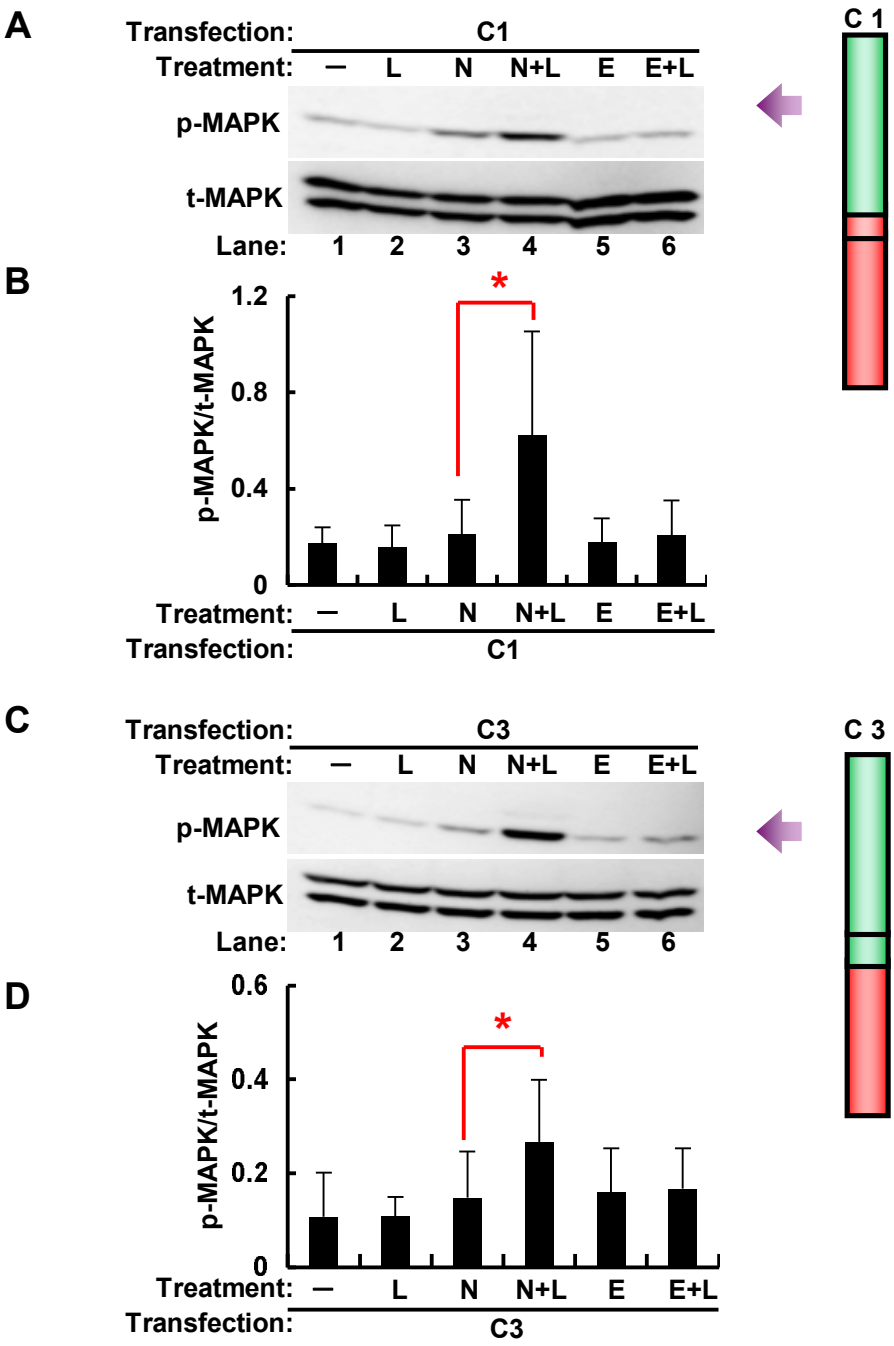

Figure 3-13 LPC enhances NGF-induced MAPK phosphorylation in C1- and C3-transfected CHO-K1 cells. CHO-K1 cells cultured in 24-well plate were transiently transfected with C1-EGFP-N1 (C1, 0.8 μg/well) in **A** and **B**, or C3-EGFP-N1 (C3, 0.8 μg/well) in **C** and **D**, by Lipofectamine 2000 (1.5 μl/well) for 18-24 h. Cells were then serum-starved for 1.5 h, and treated with vehicle control (—, DMEM plus methanol), LPC (L, 1 μM), NGF (N, 50 ng/ml), NGF and LPC together (N+L), EGF (E, 25 ng/ml), or EGF and LPC together (E+L) for 5 min. In **A** and **C**, phosphorylated MAPK (p-MAPK) and total MAPK (t-MAPK) were analyzed by Western blotting using phospho-p44/42 (Thr202/Tyr204) MAP Kinase and p44/42 MAP Kinase primary antibodies, respectively. In **B** and **D**, the amounts of p-MAPK and t-MAPK were quantified and the relative ratio of p-MAPK vs t-MAPK in each condition was calculated. Data are means ± SD of three independent experiments. *, $p<0.05$ by one-way ANOVA.

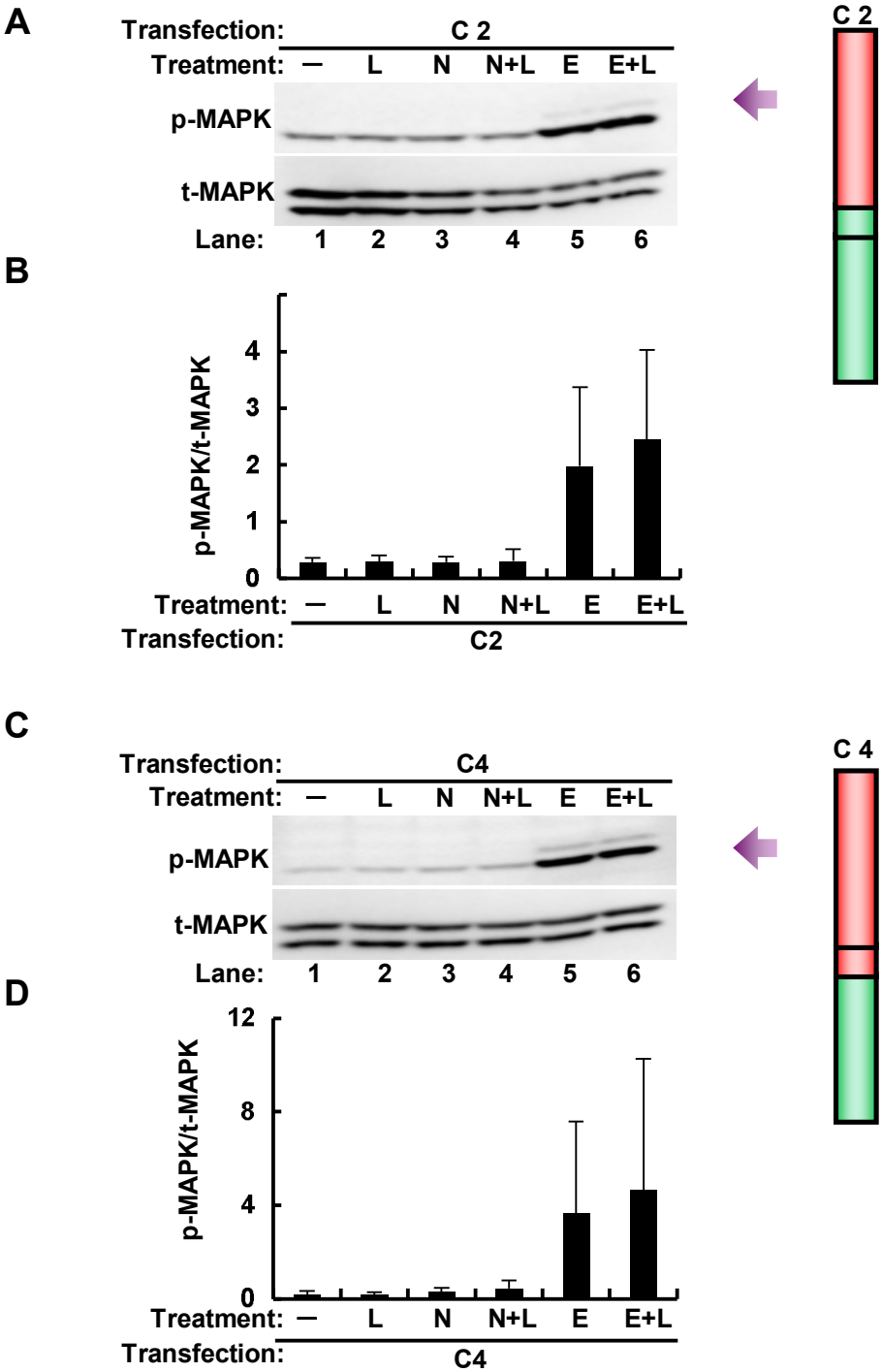

Figure 3-14 LPC does not affect EGF-induced MAPK phosphorylation in C2- and C4-transfected CHO-K1 cells. CHO-K1 cells were transiently transfected with C2-EGFP-N1 (C2, 0.8 μg/ml) in **A** and **B**, C4-EGFP-N1 (C4, 0.8 μg/ml) in **C** and **D**, respectively. Cells were serum-starved for 1.5 h, and treated with vehicle control (—, DMEM plus methanol), LPC (L, 1 μM), NGF (N, 50 ng/ml), NGF and LPC together (N+L), EGF (E, 25 ng/ml), or EGF and LPC together (E+L) for 5 min. In **A** and **C**, phosphorylated MAPK (p-MAPK) and total MAPK (t-MAPK) were analyzed by Western blotting using phospho-p44/42 (Thr202/Tyr204) MAP Kinase and p44/42 MAP Kinase primary antibodies, respectively. In **B** and **D**, the amounts of p-MAPK and t-MAPK were quantified and the relative ratio of p-MAPK vs t-MAPK in each condition was calculated. Data are means ± SD of three independent experiments.

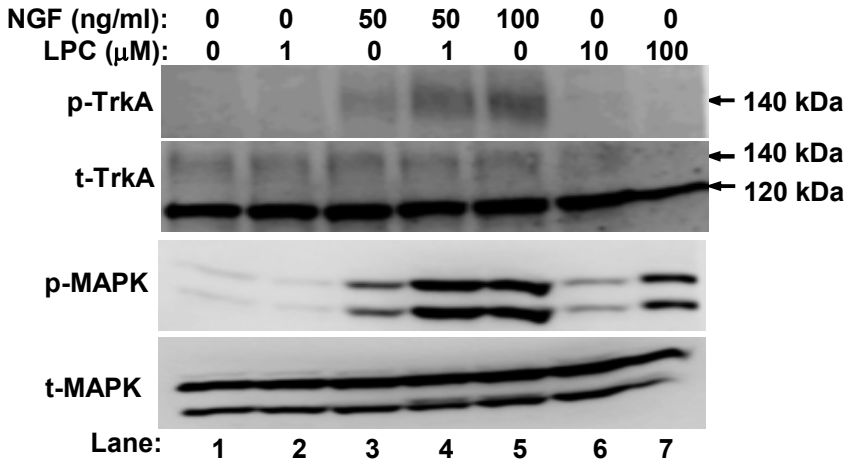

Figure 3-15 Effect of LPC at different concentrations on NGF-induced TrkA and MAPK phosphorylation in PC12 cells. PC12 cells cultured in 6-well plate were serum-starved for 1.5 h, and treated with vehicle control (DMEM plus methanol), NGF (50 and 100 ng/ml) or LPC (1, 10, and 100 μM) alone, or NGF (50 ng/ml) and LPC (1 μM) together, for 5 min. In upper panels, phosphorylated TrkA (p-TrkA) and total TrkA (t-TrkA) were analyzed using anti-phospho-TrkA (Tyr490) and anti-TrkA antibodies, respectively. In the bottom panels, phosphorylated MAPK (p-MAPK) and total MAPK (t-MAPK) were analyzed by Western blotting using phospho-p44/42 (Thr202/Tyr204) MAP Kinase and p44/42 MAP Kinase antibodies, respectively. The image shown is the representative of three independent experiments which essentially gave similar results.

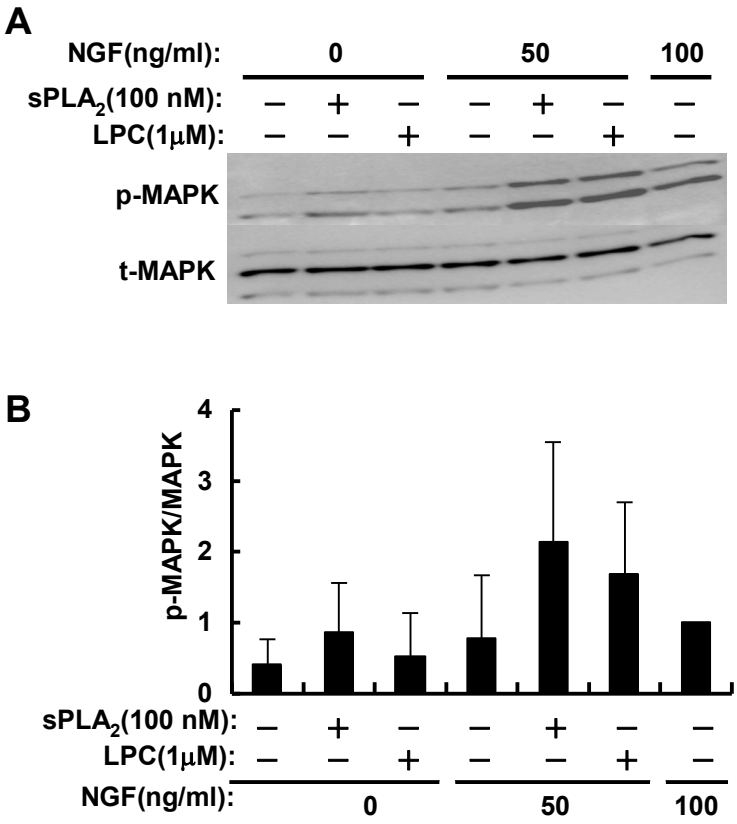

Figure 3-16 $sPLA_2$ enhances NGF-induced MAPK phosphorylation at similar level to LPC. PC12 cells cultured in 24-well plate were serum-starved for 1.5 h, and treated with vehicle control (－, DMEM plus methanol), LPC (1 μM), $sPLA_2$ (100 nM), NGF (50 ng/ml), or NGF together with LPC or $sPLA_2$ for 2 min. **A**, phosphorylated MAPK (p-MAPK) and total MAPK (t-MAPK) were analyzed by Western blotting using phospho-p44/42 (Thr202/Tyr204) MAP Kinase and p44/42 MAP Kinase antibodies, respectively. **B**, the amounts of p-MAPK and total MAPK were quantified and the relative ratio of p-MAPK vs total MAPK was calculated by setting the value for NGF (100 ng/ml) at 1. Data are means ± SD of four independent experiments.

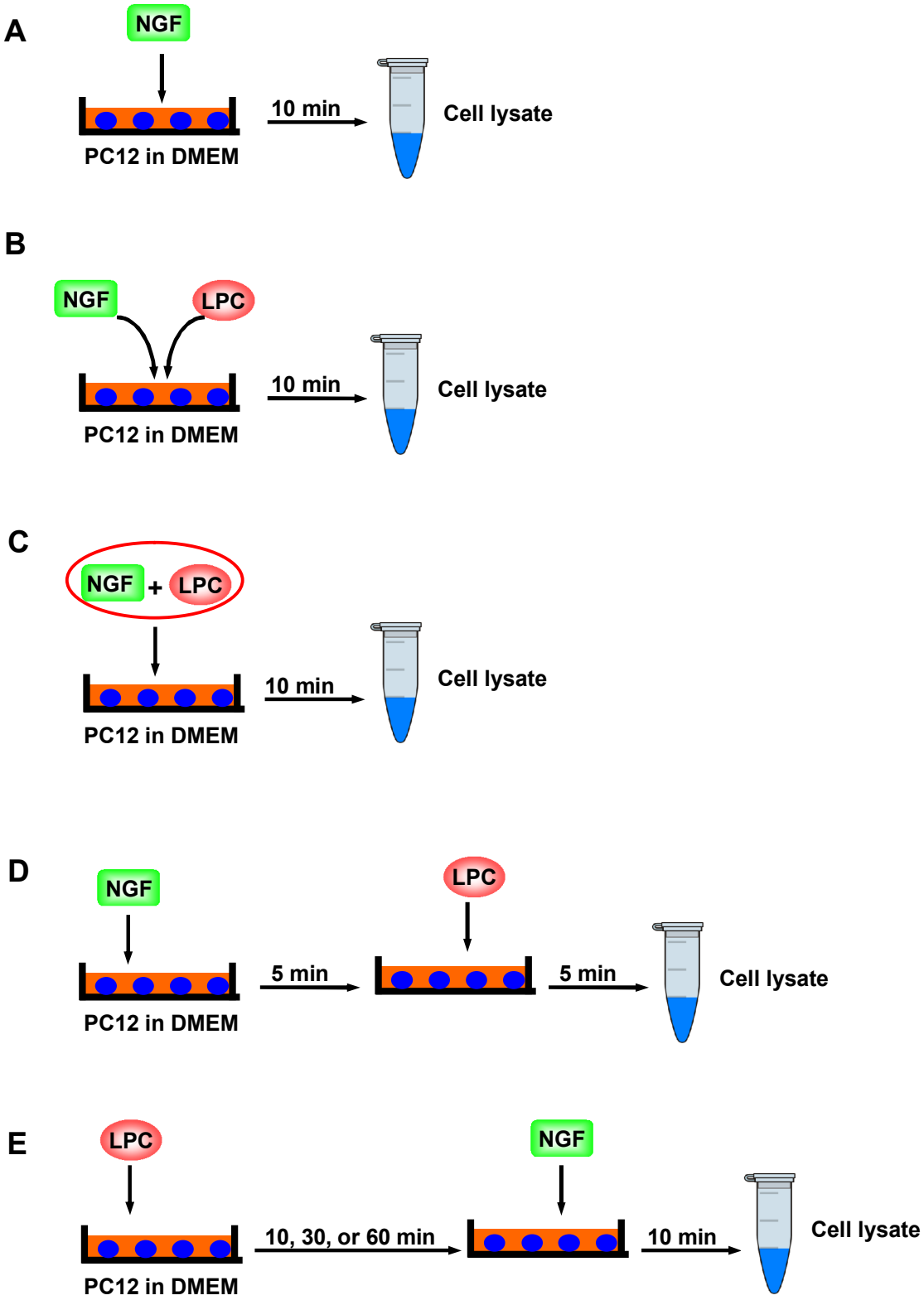

Figure 3-17 Scheme describing the experimental strategy for testing the effect of LPC on NGF-induced MAPK phosphorylation by applying LPC at different time points. Schemes in **A-D** and **E** show the experimental designs of Figure 3-18, **lanes 1-4**, and **5-7**, respectively.

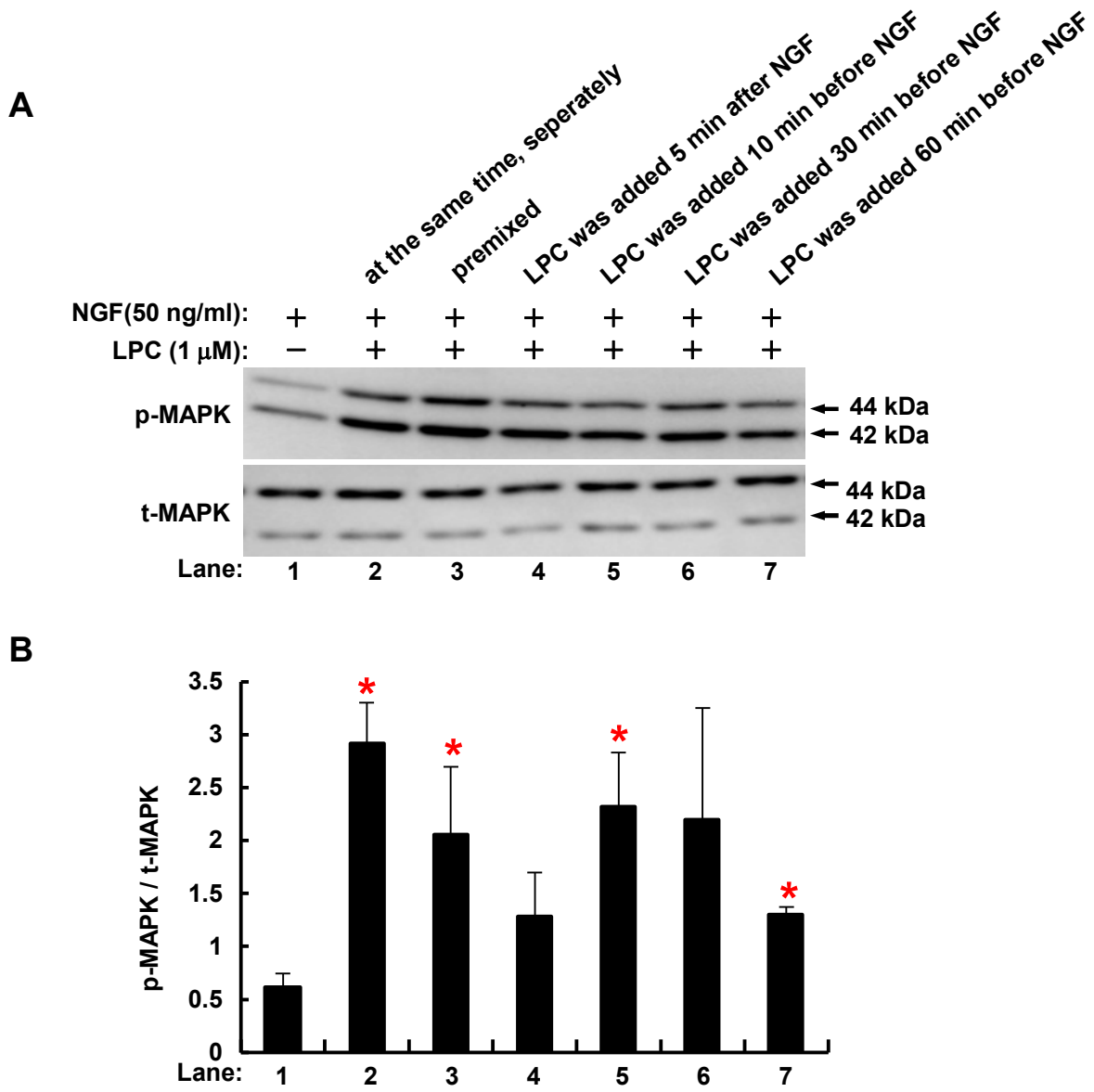

Figure 3-18 The potentiation of LPC on NGF-induced MAPK phosphorylation when it was added at different time points. PC12 cells cultured in 24-well plate were serum-starved for 1.5 h, and treated with NGF (50 ng/ml, in **lane 1**) or NGF together with LPC (1 μM). NGF and LPC were added at the same time, independently (**lane 2**), or premixed and then added (**lane 3**). In **lane 4**, LPC was added 5 min after NGF addition. In **lanes 5**, **6**, **and 7**, LPC was added 10, 30, or 60 min before NGF addition. Cells were treated with NGF for 10 min in all cases. **A**, phosphorylated MAPK (p-MAPK) and total MAPK (t-MAPK) were analyzed by Western blotting using phospho-p44/42 (Thr202/Tyr204) MAP Kinase and p44/42 MAP Kinase primary antibodies, respectively. **B**, the amounts of p-MAPK and t-MAPK were quantified and the relative ratio of p-MAPK vs t-MAPK in each condition was calculated. Data are means ± SD of three independent experiments. *, $p<0.05$ by one-way ANOVA, compared with **lane 1**, respectively.

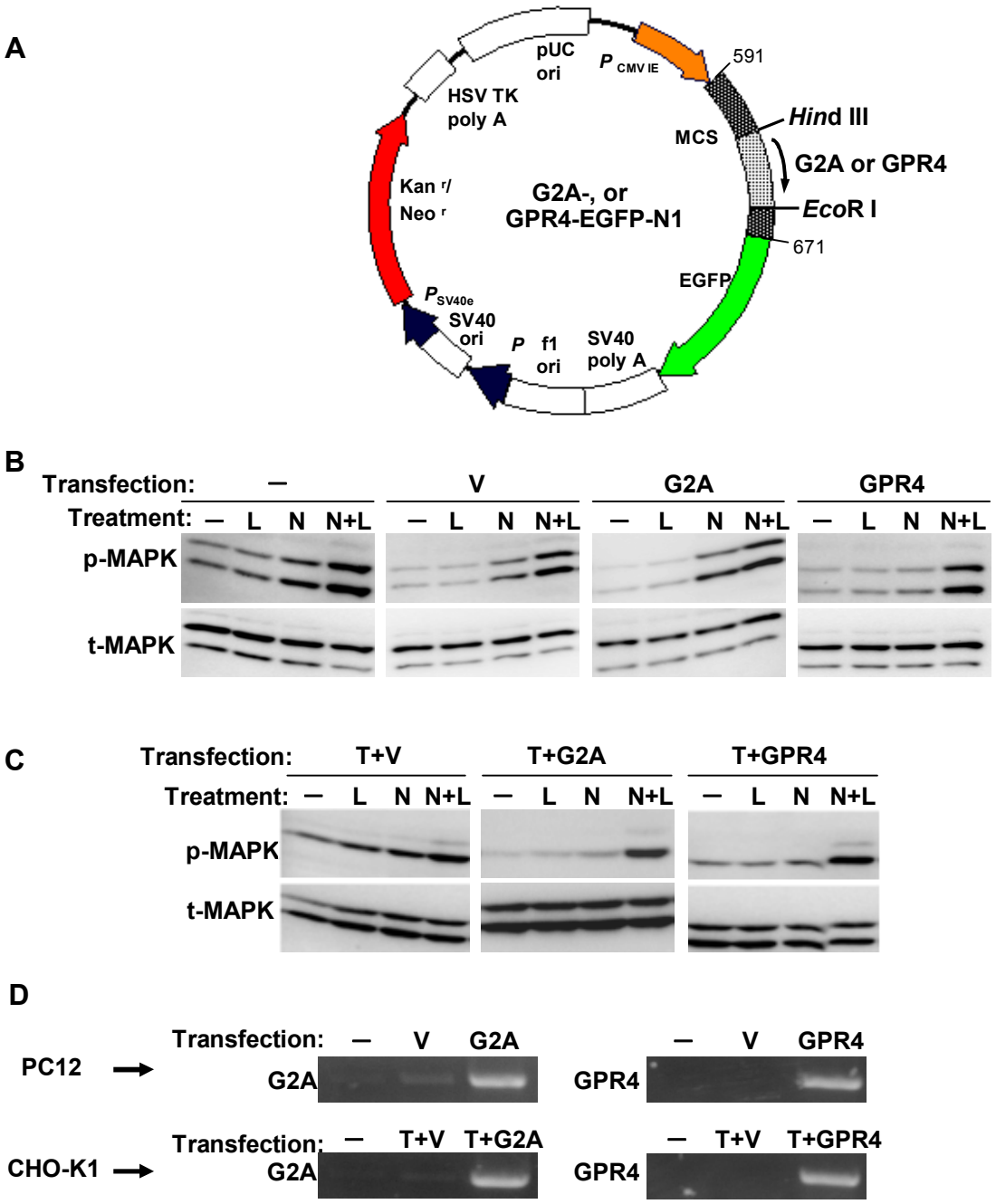

Figure 3-19 Effect of GPR4 and G2A overexpression on the potentiation of LPC on NGF-induced MAPK phosphorylation in PC12 cells and CHO-k1 cells co-transfected with TrkA. **A**, the map of plasmid used for the expression of G2A or GPR4. **B**, PC12 cells cultured in 24-well plate were untransfected (—) or transfected with EGFP-N1 (v), G2A-EGFP-N1 (G2A) or GPR4-EGFP (GPR4, 0.8 μg/well), by Lipofectamine 2000 (1.5 μl/well) overnight. **C**, CHO-K1 cells cultured in 24-well plate were co-transfected EGFP-N1, G2A-EGFP-N1, or GPR4-EGFP-N1 (0.8 μg/well), with TrkA-EGFP-N1 (T, 0.8 μg/well), by Lipofectamine 2000 (1.5 μl/well) overnight. Cells were then serum-starved for 1.5 h, and treated with vehicle control (—, DMEM plus methanol), LPC (L, 1μM), NGF (N, 50 ng/ml) alone, or together (N+L) for 10 min. **A-C**, phosphorylated MAPK (p-MAPK) and total MAPK (t-MAPK) were analyzed by Western blotting using phospho-p44/42 (Thr202/Tyr204) MAP Kinase and p44/42 MAP Kinase primary antibodies, respectively. Result shown is the representative of three independent experiments. **D**, Expression of G2A and GPR4 in PC12 and CHO-K1 cells was analyzed by isolating total RNA and PCR analysis.

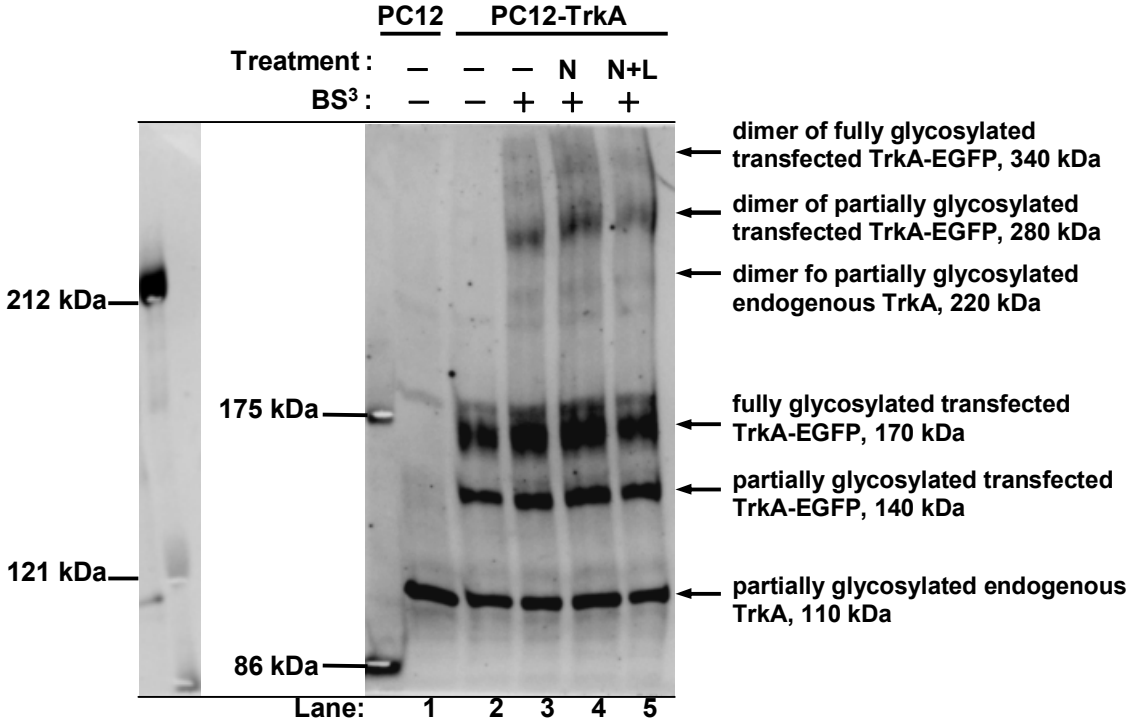

Figure 3-20 LPC does not affect the formation of TrkA dimer in PC12 cells. PC12 cells cultured in 6-cm dishes were untransfected (PC12) or transfected with TrkA-EGFP-N1(2 μg/well; PC12-TrkA) using Lipofectamine 2000 (8 μl/well) overnight. Cells were serum-starved for 3 h, and incubated in DMEM containing 0.45 M sucrose for 20 min. Cells were treated with vehicle control (－, DMEM plus methanol), NGF (50 ng/ml; N50), or NGF plus LPC (1 μM; N+L) for 5 min. Cells were then untreated (－) or treated with BS^3 (+) at the final concentration of 1 mM. Monomer and dimer of TrkA were detected by Western blotting using anti-TrkA antibody.

Conclusion

LPC has been found to display various biological activities as described in the General introduction, including the neurotrophin-like effects found in the previous studies in our laboratory. However, the molecular mechanisms involved in these biological actions and neurotrophin-like activity of LPC have not been fully elucidated. This study departed from the observation of neurite outgrowth-promoting and survival-supporting effects of LPC and $sPLA_2$ in PC12 cells and in CGNs in our laboratory. I have demonstrated the potentiating effect of LPC on NGF-induced (Chapter 1) and BDNF-induced (Chapter 2) differentiating and cell survival signals, further characterized the mode of action of LPC, and analyzed the possibilities associated with the mechanism (Chapter 3).

Results in Chapter 1 have shown that LPC promotes NGF-induced MAPK and Akt signaling cascades which are known to be essential for the differentiation and survival, as the consequence of enhanced activation of the receptor TrkA in PC12 cells. Although other growth factors, such as EGF, bFGF, and IGF-1 were also capable of inducing MAPK phosphorylation, it was not regulated by LPC in PC12 cells. In Chapter 2, LPC exhibited similar effect on BDNF-TrkB signal in CGNs. LPC potentiated BDNF-induced activation of the receptor TrkB, and the phosphorylation of downstream signals, MAPK and Akt, which are critical for the survival of CGNs. In contrast, LPC did not affect IGF-1-induced MAPK and Akt signals in CGNs. Findings in Chapters 1 and 2 implicated the existence of a specific role of LPC on Trk receptors, TrkA and TrkB, and their downstream signals, which might contribute to the neurotrophin-like effect of LPC in PC12 cells and in CGNs. In addition, $sPLA_2$ showed an effect similar to LPC on NGF-induced MAPK phosphorylation in PC12 cells. Furthermore, studies using TrkA/EGFR chimeras demonstrated that the extracellular domain, but not the transmembrane and intracellular domains, of TrkA is responsible for the effect of LPC. Based on these findings, I propose a model (Fig. 4-1) describing the functional role of $sPLA_2$ and LPC on NGF-induced signals: $sPLA_2$ hydrolyzes phosphatidylcholine in the plasma membrane to release LPC; LPC then

enhances NGF-induced MAPK and Akt signaling cascades via promoting the activation of TrkA through its extracellular domain.

In Fig. 1-4, LPA, LPE, and LPS showed some enhancement of NGF-induced MAPK phosphorylation, but the level was lower than that by LPC in PC12. This is in agreement with the previous findings that only LPC, but not LPA, LPE, nor LPS, displayed neurotrophin-like activity (52,56). These facts and observations have implied the existence of transmembrane signal transduction pathway(s) specific to LPC.

To see if the enhancement of NGF- and BDNF-induced MAPK and Akt signals by LPC demonstrated in this study contributes to the neurotrophin-like effect of LPC in PC12 cells and in CGNs found in the previous study, I performed the neurite outgrowth assay in PC12 cells and apoptosis assay in CGNs. In PC12 cells, increased NGF-induced MAPK phosphorylation by LPC (1 μM) did not lead to a significant increase in NGF-triggered neurite outgrowth. This is likely because the enhancement of NGF-induced MAPK phosphorylation by LPC is transient; nevertheless, the enhancement of NGF-induced MAPK phosphorylation lasted for as long as 30 min, and it is known that a sustained activation of MAPK phosphorylation is required for the complete differentiation of PC12 cells. Increased number of cells representing the initial stage of morphological differentiation was observed by co-treatment of LPC with NGF, suggesting that enhanced NGF-TrkA signals contributed at least in part to the differentiation of PC12 cells. Since neurite outgrowth assay was performed in the serum-free medium in this study, the effect of LPC on NGF-induced differentiation of PC12 cells in the medium containing reduced amount of serum still needs to be tested.

In the previous study, the neurotrophin-like effect of LPC was observed at higher concentration (100 μM) of LPC alone, which was mediated by G2A in PC12 cells (55). In this study, LPC added alone at 10 or 100 μM was able to induce phosphorylation of MAPK without activating TrkA. On the other hand, the potentiation of LPC (1 μM) on NGF-induced MAPK and Akt signals was not affected by the overexpression of G2A or GPR4 in PC12 cells. These findings indicate that neurotrophin-like effect of LPC observed at different concentrations in PC12 cells

might involve distinct signaling pathways: LPC at low concentration potentiates the differentiation of PC12 cells through enhancing NGF-TrkA-induced MAPK phosphorylation, which is not mediated by G2A and GPR4, whereas LPC at high concentrations might involve NGF-TrkA-independent MAPK phosphorylation, which is regulated by G2A.

In CGNs, although LPC (1 μM) also potentiated BDNF-induced MAPK and Akt signals, it did not enhance the survival effect of BDNF. On the other hand, unlike in PC12 cells, LPC added alone at 10 μM sufficiently rescued CGNs from LK-induced apoptotic death without triggering the phosphorylation of TrkB and downstream components. It implies that an additional pathway rather than TrkB-mediated signal is involved in the neurotrophin-like effect of LPC in CGNs. Whether or not a specific receptor for LPC mediates the neurotrophin-like effect of LPC in CGNs might be of interest in the future study.

Although LPC does not act through enhancing/stabilizing the formation of TrkA dimer that occurs intracellularly, which is, in fact, compatible with our finding that LPC acts on the extracellular domain of TrkA. Taken together, these results suggest a mechanism whereby LPC acts directly on NGF, TrkA, or on the membrane component, thereby enhancing/stabilizing binding of NGF to TrkA. Examining if LPC modulates the binding affinity of NGF to TrkA, and/or analyzing the localization of TrkA might provide more important insight into the mechanism by which LPC displays neurotrophin-like activity.

It was previously found that when PC12 cells were treated with $sPLA_2$, LPC was released into the culture medium due to its hydrolytic activity. Release of LPC was also detected in the medium of PC12 cells treated with the culture supernatant of COS1 cells expressing $sPLA_2$-X, but not $sPLA_2$-IB and $sPLA_2$-IIA (55). Another study has shown that the amount of LPC in extracted phospholipids from PC12 cells that had been infected with the adenovirus containing $sPLA_2$-X, but not $sPLA_2$-IIA and V for three days, was greatly increased compared to that from the control cells; around 15~20% of total PC was found to be converted to LPC (104). Furthermore, the expression of $sPLA_2$s including $sPLA_2$-X in the skin is known to be increased during

inflammation caused by UV irradiation. Recombinant $sPLA_2$-X promoted the tyrosinase activity and dendricity in human melanocytes that play important roles in the protection of skin from UV damage, which was mainly dependent on the release LPC (105). Thus it is conceivable that LPC is locally generated in vivo and associated with some of the biological actions of $sPLA_2$.

Furthermore, intravenously injected LPC (200 nM/kg) was found to protect neurons in the brain in an in vivo model of global ischemia in mice. In this model, 0.1% of intravenously injected LPC passed through the blood-brain barrier and entered the brain, 55% of which was in unmetabolized form. In addition, in an in vitro model of high glutamate-induced excitotoxicity of primarily cultured CGNs, LPC also significantly prevented the neuronal death (106). These findings indicate that LPC is neuroprotective in the physiological conditions and might be a therapeutic candidate for preventing neuronal death, although the exact working concentration of LPC is unclear at present. In-depth understanding of the action of LPC might provide important evidences for the development of a new therapeutic method for neurodegenerative diseases.

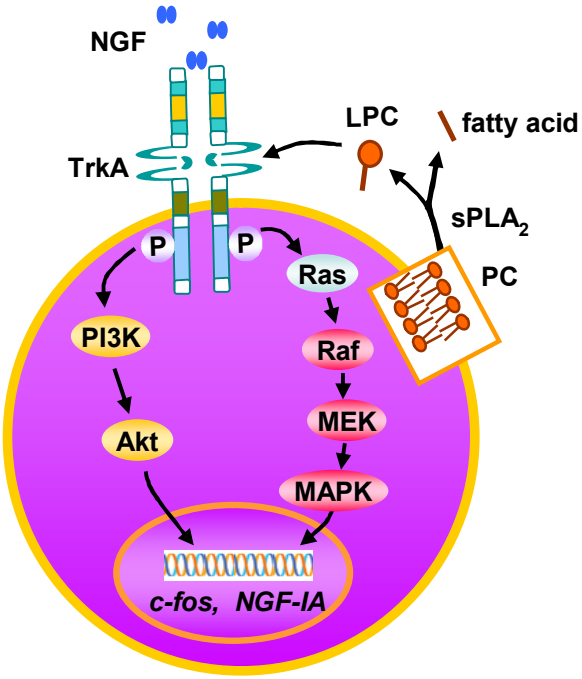

Figure 4-1 Hypothetical model describing the possible role of LPC in NGF-induced signals. LPC generated by the hydrolysis of phosphatidylcholine (PC) by $sPLA_2$ enhances NGF-induced MAPK and Akt signals through the extracellular domain of TrkA in PC12 cells.

Materials and Methods

1. Materials

1.1 Lysophospholipids

LPC used in this study is 1-palmitoyl-*sn*-glycero-3-phosphocholine (C16:0; Cat. No. 855675P). Other lysophospholipids used are: 1-lauroyl-2-hydroxy-*sn*-glycero-3-phosphocholine (C12:0; 855475P), 1-myristoyl-2-hydroxy-*sn*-glycero-3-phosphocholine (C14:0; 855575P), 1-stearoyl-2-hydroxy-*sn*-glycero-3-phosphocholine (C18:0; 855775P), 1-oleoyl-2-hydroxy-*sn*-glycero-3-phosphocholine (C:18:1; 845875P), lysophosphatidic acid (LPA; C16:0; 857123P), lysophosphatidylethanolamine (LPE; C16:0; 856705P), and lysophosphatidylserine (LPS; C18:1; 858143P). All these lysophospholipids were purchased from Avanti Polar Lipids. LPC, LPA, and LPS were dissolved in methanol. LPE was dissolved in DMSO.

1.2 Growth factors

Nerve growth factor (NGF; NGF-301), epidermal growth factor (EGF; EGF-201), and brain-derived growth factor (BDNF; PT45002) were from Toyobo. Recombinant human insulin-like growth factor-1 (IGF-1; GPT-10011L) was obtained from Pepro Tech. These growth factors were dissolved in DMEM.

1.3 Antibodies

Primary antibodies used are: phospho-p44/42 (Thr202/Tyr204) MAP kinase antibody, #9101; p44/42 MAP kinase antibody, #9102; phospho-Akt (Ser473) antibody,

#9271; Akt antibody, #9272; phospho-TrkA (Tyr490) antibody, #9141; TrkA antibody, #2505; phospho-EGF receptor (Tyr1173) antibody, #4407; EGF receptor antibody, #2232; phospho-MEK1/2 (Ser217/221) antibody, #9121; and MEK1/2 antibody, #9122. All these primary antibodies were purchased from Cell Signaling Technology and used at 1:1000 dilution in TBS. The secondary antibody, horseradish peroxidase-linked anti-rabbit-IgG (#7074; Cell Signaling Technology), was used at 1:2000 dilution in TTBS.

For the detection of EGFP fusion proteins, living colors® A.v. monoclonal antibody (JL-8), #632380 from Clontech was used at 1:5000 dilution in TBS as primary antibody (it is described in the figures as anti-GFP-antibody), and peroxidase-labeled anti-mouse IgG (H+L), #PI-2000 from Vector was used at 1:500 dilution in TBS as secondary antibody.

For the detection of phosphorylated and total TrkB, phospho-TrkA (Tyr490; #9141) antibody and Trk antibody were used (1:1000 dilution in TBS, Cell Signaling Technology) as primary antibodies, and horseradish peroxidase-linked anti-rabbit-IgG (#7074; Cell Signaling Technology), was used at 1:2000 dilution in TTBS as secondary antibody. Since TrkB has the phosphorylation site analogous to TrkA tyrosine 490, phosphorylated TrkB at this site was detected using phospho-TrkA (Tyr490) antibody.

2. Methods

2.1 Cell culture

2.1.1 Rat pheochromocytoma PC12

Rat pheochromocytoma PC12 cells were maintained in 10 ml of Dulbecco's modified Eagle's medium (DMEM, Invitrogen) supplemented with 5% fetal calf serum

and 5% horse serum (DMEM (5% FCS/5%HS)) in 10-cm tissue culture dish, at 37°C in a humidified and CO_2-controlled (10%) incubator. Cells were kept with regular transfer of once in two or three days. PBS containing 1 mM EDTA (PBS /EDTA) was used to detach cells during transfer.

PC12 cells were inoculated on collagen type 1 (rat tail)-coated 24-well culture plates at a density of 1×10^5 cells/well in 0.5 ml/well DMEM (5%HS/5%FCS), in 6-well plates at a density of 4×10^5 cells/well in 2 ml/well DMEM (5%HS/5%FCS), or in 6-cm dishes at a density of 1×10^6 cells/dish in 4 ml/dish DMEM (5%HS/5%FCS), and incubated for 24 h or longer until >80% confluent. Before cells were subjected to various treatments as specified in the text, culture medium was removed by aspiration. Then, cells were washed twice with DMEM carefully (do not detach cells), added DMEM 0.5 ml/well for 24-well plates, 2 ml/well for 6-well plates and 6-cm dishes, and incubated for 1.5 h (serum-starvation). After 1.5 h serum-starvation, cells were subjected to various treatments by applying vehicle control or various treatments as specified in the text. Vehicle control for various stimuli was prepared by mixing the same amount of DMEM and methanol.

2.1.2 CHO-K1 cells

Chinese hamster ovary K1 (CHO-K1) cells were maintained in 7 ml DMEM supplemented with 10% fetal calf serum (DMEM/10% FCS) in falcon tissue culture flask (50-ml). Cells were kept with regular transfer of three times a week at 37°C in a humidified and CO_2-controlled (10%) incubator. During transfer, 0.25% trypsin (around 0.5 ml every time) was used to detach cells. For the experiment using CHO-K1 cells cultured in 24-well or 6-well plates, collagen-coating of plates is not needed.

2.1.3 HEK293 cells

HEK293 cells were maintained in 10 ml DMEM supplemented with 10% fetal calf serum (DMEM/10% FCS) in 10-cm tissue culture dish. Cells were kept with regular transfer of twice a week at 37°C in a humidified and CO_2-controlled (10%) incubator. During transfer, 0.25% trypsin (around 0.5 ml every time) was used to detach cells. For the experiment using HEK293 cells, collagen-coating of plates is not needed.

2.1.4 Cerebellar granule neurons

Cerebellar granule neurons (CGNs) were obtained by dissociating the cerebella of mice on postnatal day 7 (P7), and were cultured in DMEM (10% FCS) containing 25 mM KCl, in 0.2 % polyethylenimine-coated 24-well plates. Cells were maintained at 37°C in 10% CO_2 in humidified incubator. After 24 h, culture medium was changed to DMEM (10% FCS) containing 25 mM KCl and 10 μM cytosine arabinoside, and cultured for 48 h to remove proliferating cells. After 48 h, the medium was changed to DMEM (10% FCS) containing 25 mM KCl, and incubated for another 48 h. Five days after the culture was prepared; cells were subjected to various treatments.

2.2. Western blotting analysis

After serum-starvation and treatments by various stimuli, medium was removed by aspiration, and PC12, CHO-K1 or HEK293 cells were lysed in 1×SDS sample buffer at 50 μl/well for 24-well plates, 100 μl/well for 6-well plates, and 300 μl/well for 6-cm dishes, and boiled for 3 min. In each experiment, equal volume (usually 18 μl) of cell lysate was subjected to electrophoresis on 10% acrylamide gel. Proteins were transferred onto polyvinylidene fluoride (PVDF) microporous membrane (Millipore) for

45 min at 125 mA using a semi-dry blotter. The membrane was blocked with 5% skim milk for 1 h with gentle shaking, and washed with distilled water. Then, the membrane was incubated overnight at 4°C with the primary antibodies as described. The membrane was washed with TTBS for five times (use 5 ml of TTBS and shake for 5 min every time), and incubated with the secondary antibody for 2 h at room temperature with gentle shaking. After washing with TTBS for three times, immunoreactive bands were visualized using the SuperSignal®WestPico Lumino/Enhancer (Pierce #1856136) and SuperSignal®WestPico Stable Peroxide (#1856135) solution. When the bands are weak, Western Lightning® Ultra solutions from PerkinElmer, Inc. was used to get clear bands. Imaging was then carried out using FUJI Image Reader. The amount of proteins was quantified by FUJI FILM Multi Gauge software.

2.3 Total RNA isolation and cDNA synthesis

Total RNA (10 μg) was extracted using TRI reagent from PC12 cells cultured in 6-cm dishes after the treatments, 5 μg of which was subjected to DNase treatment using RQ[1] RNase-Free DNase (Promega). Then, 0.6 μg of RNA was reverse transcribed to cDNA in a volume of 20μl reaction using random primer and PrimeScript reverse transcriptase. Details for the isolation of total RNA and cDNA synthesis can be seen in the protocol.

In the experiment for checking the expression of G2A and GPR4 after transfection in PC12 cells, 6 μg of total RNA isolated from each dish was subjected to DNase treatment using RQ[1] RNase-Free DNase (Promega). Then, 0.9 μg of RNA was reverse transcribed to cDNA in a volume of 20 μl reaction using random primer and PrimeScript reverse transcriptase. In the experiment for checking the expression of G2A

and GPR4 after co-transfection with TrkA-EGFP-N1 in CHO-K1 cells, 10 μg of total RNA isolated from each dish was subjected to DNase treatment using RQ[1] RNase-Free DNase (Promega). Then, 2.3 μg of RNA was reverse transcribed to cDNA in a volume of 20 μl reaction using random primer and PrimeScript reverse transcriptase.

2.4 Semi-quantitative and quantitative real time PCR

After the reverse transcription reaction, 1 μl of reaction mixture was proceeded to PCR reaction using rTAQ (95°C for 5 min; 35 cycles of 94°C for 30 s, 52.5°C for 30 s (for *GAPDH*; 54.3°C for 30 s for c-*fos*; 50°C for 30 s for *NGF-IA*), and 72°C for 30 s (for *GAPDH*; 72°C for 40 s for c-*fos*; 72°C for 1 min for *NGF1A*); 72°C for 5 min) using specific primer pairs:

GAPDH: 5'-GACCACAGTCCATGCCATCACT-3'

and 5'-TCCACCACCCTGTTGCTGTAG-3';

c-*fos* :5'-AGAATCCGAAGGGAAAGGAA-3'

and 5'-ATGATGCCGGAAACAAGAAG-3'; and

NGF-IA : 5'-CCACAACAACAGGGAGACCT-3'

and 5'-GGGATGGG TAGGAAGAGAGG-3'.

PCR products were subjected to electrophoresis on 2% agarose gel to confirm that each primer pair amplified a single product of predicted size, and to determine the relative expression level of c-*fos*, *NGF-IA*, and *GAPDH* in response to different treatments.

Also, transcript levels of c-*fos*, *NGF-IA*, and *GAPDH* were measured by quantitative real-time PCR using LightCycler® FastStart DNA Master SYBR Green I kit (Roche). The reaction was performed in a volume of 20 μl according to the

manufacturer's instructions. In each reaction, 2 μl of cDNA from each sample was added. For each primer pair, PCR efficiency was determined by standard curve and the transcript levels of c-*fos* and *NGF-IA* were normalized against *GAPDH*. Quantitative real-time PCR experiments were independently performed three times and each experiment was done in triplicate.

Expression of G2A and GPR4 was tested by semi-quantitative PCR after the reverse transcription reaction. 1 μl of cDNA was proceeded to PCR reaction, and subjected to electrophoresis on 2% agarose gel.

Primers used are:

G2A S1:5'-GGTGACTGCTTACATCTTCTTCTGC-3',

G2A as1:5'-CTGTGTGGATTCTGGACACTTCTTG-3',

GPR4 s1:5'-ATATCAGCATCGCCTTCCTGTGCTG-3', and

GPR4 as1:5'-CAGCCACACAATTGAGGCTGGTGAA-3'.

PCR reaction for testing the expression of G2A or GPR4:

Buffer 10X	2 μl
dNTPs	2 μl
Primer F	2 μl
Primer R	2 μl
rTAQ	0.1 μl
D.W.	11.9μl
Total	20 μl

PCR reaction: 94°C for 5 min; 30 cycles of 94°C for 30 s, 55°C for 30 s,72°C for 50 s; 72°C for 5 min.

2.5 Neurite outgrowth assay in PC12 cells

PC12 cells were incubated at the density of 5×10^3 cells/well in 0.5 ml/well DMEM (5%HS/5%FCS) in collagen-coated 24-well plates for 24 h. Cells were then washed with serum-free DMEM (0.5 ml/well) twice and incubated in DMEM (0.5 ml/well) medium containing vehicle control or NGF and/or LPC for 48 h. After 48 h, Cells were fixed with 4% paraformaldehyde by adding 0.5 ml/well and keep for 30 min at room temperature. Paraformaldehyde was collected after using. Cells were washed once with PBS (0.5 ml/well) and stained with CBB (250 μl/well) for 15 sec. Then, cells were washed with PBS (0.5 ml/well) twice, and added PBS (0.5 ml/well). Finally, cells were observed under phase-contrast microscopy and photos were taken from different area, and cells having neurites longer than the cell diameter was considered as positive and counted. In each well, at least 5 of pictures were taken randomly, and total of 100 cells were counted. The percentage of differentiating cells (positive) to total cells was calculated.

2.6 Plasmids

To construct the plasmid TrkA-EGFP-N1 for the expression of mouse TrkA fused with EGFP, a cDNA fragment encoding the full-length TrkA, 799 amino acid-long, was amplified by PCR using oligonucleotides
5’-GGAATTCATGCTGCGAGGCCAGCGGCA-3’ and
5’-GGA ATTCTGCCCAGAACGTCCAGGTAAC-3’. The resulting PCR product was digested with *Eco*R I, and was cloned into *Eco*R I site of EGFP-N1 expression vector.

To construct the plasmid EGFR-EGFP-N1 for the expression of rat EGFR fused with EGFP, a cDNA fragment encoding the full-length EGFR, 1209 amino acid-long,

was amplified by PCR using oligonucleotides

5'-CTCGAGATGCGACCCTCAGGGACTGCGAGAACCAAGC-3'

and 5'-CTCGAGTGCTCCACTAAACTCACTGCTTGGCGGTGCCA-3'. This cDNA fragment was digested with *Xho* I, and cloned into the expression vector EGFP-N1 at *Xho* I site (EGFR-EGFP-N1).

TrkA/EGFR chimeric receptors were constructed by swapping each domain between TrkA and EGFR. cDNA fragments encoding the extracellular domain (ED), extracellular and transmembrane domains (ED+TMD), transmembrane and intracellular domains (TMD+ID), and intracellular domain (ID) of both TrkA and EGFR were amplified by PCR, using TrkA-EGFP-N1 and EGFR-EGFP-N1 as templates, respectively. Resultant fragments were fused by overlapping PCR strategy to create chimeric cDNAs. Chimeric receptor 1 (C1) is composed of ED of TrkA and TMD+ID of EGFR. C2 contains ED of EGFR and TMD+ID of TrkA. C3 contains ED+TMD of TrkA and ID of EGFR. C4 contains ED+TMD of EGFR and ID of TrkA. Chimeric cDNAs for C1, C2, C3, and C4 was digested with *Xho* I and introduced into EGFP-N1 vector at *Xho* I site. Primers used are:

TrkA ED, **F1**: 5'-ctcgagATGCTGCGAGGCCAGCGGCTCGG-3', and

R1: 5'-cccacaatcccagtggcgatAGGGGTTTCATCTTTCTTCT-3';

EGFR TMD+ID, **F2**: 5'-AGAAGAAAGATGAAACCCCTatcgccactgggattgtggg-3', and

R2: 5'-ctcgagtgctccactaaactcactgcttggcggtgcca-3';

For producing C1 (TrkA ED/EGFR TMD+ID), gene clean products of TrkA ED and EGFR TMD+ID were used as templates, and primers F1 and R2 were used.

EGFR ED, **F3**: 5'-ctcgagatgcgaccctcagggactgcgagaaccaagc-3', and

R3: 5'-ACAGCCACAGAGACCCCAAAggatgggatctttggccctt-3';

TrkA TMD+ID, **F4**: 5'-aagggccaaagatcccatccTTTGGGGTCTCTGTGGCTGT-3', and

R4: 5'-ctcgagGCCCAGAACGTCCAGGTAACTGGGTGGC-3'.

For producing C2 (EGFR ED/TrkA TMD+ID), gene clean products of EGFR ED and TrkA TMD+ID were used as templates, and primers F3 and R4 were used.

TrkA ED+TMD, **F1**: 5'-ctcgagATGCTGCGAGGCCAGCGGCTCGG-3', and

R5: 5'-aagctgacgtcgacgGAGCACAAGAAGGAGGG-3';

EGFR ID, **F5**: 5'-CCCTCCTTCTTGTGCTCcgaaggcgtcacattgtccg-3', and

R2: 5'-ctcgagtgctccactaaactcactgcttggcggtgcca-3';

For producing C3 (TrkA ED+TMD/EGFR ID), gene clean products of TrkA ED+TMD and EGFR ID were used as templates, and primers F1 and R2 were used.

EGFR ED+TMD, **F3**: 5'-ctcgagatgcgaccctcagggactgcgagaaccaagc-3', and

R6: 5'-CTCCTCTGTCCACATTTGTTCATGAAGaggccgatcccaa-3';

TrkA ID, **F6**: 5'-ttgggatcggcctCTTCATGAACAAATGTGGACAGAGGAG-3', and

R4: 5'-ctcgagGCCCAGAACGTCCAGGTAACTGGGTGGC-3'.

For producing C4 (EGFR ED+TMD/TrkA ID), gene clean products of EGFR ED and TMD/TrkA ID were used as templates, and primers F3 and R4 were used. C-terminus of all these receptors was fused with N-terminal region of EGFP. The sequence of these plasmids has been checked. These plasmids were amplified in *E.coli*, and isolated using QIAGEN DNA extraction midi kit.

Note: some primers shown above are the same.

PCR reaction of the amplification of TrkA, EGFR and chimeric cDNA:

Buffer 10X	5 μl
dNTPs	4 μl
Primer F	2.5 μl
Primer R	2.5 μl
Pyrobest	0.25 μl
D.W.	34.75 μl
Total	50 μl

PCR reaction: 98°C for 10 sec; 30 cycles of 98°C for 10 s, TM (depends on primers)°C for 30 s,72°C for 1 min/kb (depends on the length);16°C after finished.

2.7 DNA transfection

PC12, CHO-K1, or HEK293 cells seeded in 24-well plate (>80% confluent) were transiently transfected with various plasmids (0.8 μg/well), for 18-24 h by Lipofectamine^{TM}2000 (1.5 μl/well, Invitrogen), according to manufacturer's instruction. In the experiment for testing expression of G2A and GPR4, PC12 cells cultured in 6-cm dishes were transfected with G2A-EGFP-N1 or GPR4-EGFP-N1 (5 μg/dish) using Lipofectamine 12 μl/dish. CHO-K1 cells were co-transfected with TrkA-EGFP-N1 (5 μg/dish) and G2A-EGFP-N1 (or GPR4-EGFP-N1, 5 μg/dish) using Lipofectamine 20 μl/dish.

2.8 Establishment of CHO-K1-TrkA stable cell line

First, the best concentration of G418 for CHO-K1 cells was determined. To do this, CHO-K1 cells were cultured at the density of 1×10^4 cells/well in 0.5 ml/well in 24-well plate in DMEM (10%FCS) containing different concentrations of G418, 200,

400, 600,800, 1000, 1200, and 1400 μg/ml in each well. Cells were kept in a good condition by changing medium once in 3 days or more when it was needed. After 9 days, cells in wells containing G418, 1000, 1200, and 1400 μg/ml all died. Therefore, 1000 μg/ml was confirmed to be a best selecting concentration for CHO-K1 cells.

Next, CHO-K1 cells were cultured at the density of 1×10^4 cells/well in 0.5 ml/well in duplicate 24-well plates in DMEM (10%FCS, 0.5 ml/well) for 24 h. Plasmid TrkA-EGFP-N1 (0.8 μg/well) was transfected into CHO-K1 cells using Lipofectamine 2000 (1.5 μl/well) overnight. The expression of transfected TrkA was confirmed by Western blotting using anti-GFP antibody using the cells in one 24-well plate. 24 h after transfection, cells in another 24-well plate, were collected and plated in 10-cm dishes at 1:10 or 1:20 dilution in selection medium 10 ml/dish (DMEM 10% FCS containing G418 1000 μg/ml). Cells were kept in selection medium untill visible clones developed changing medium once in 3 days or more. After 2 weeks, 15 clones were picked up using oxford-cup method and inoculated in duplicate 24-well plates in the same selection medium (0.5 ml/well). When cells in each well were almost fully confluent, medium was removed, and the cells in one 24-well plate were lysed with 1×SDS sample buffer (50 μl/well), and screened for positive clones that stably express TrkA, by Western blotting using anti-GFP antibody. The culture of positive clone was expanded by tranfering cells to 6-well plate, 6-cm dish, and 10-cm dish, gradually, and kept in selection medium. Every time when cells were transfered, expression of TrkA was detected and confirmed by Western blotting using anti-GFP antibody. Most of cells from this clone were froze at -80°C first, and stored in liquid nitrogen.

Some amount of cells from the positive clone from first selection was also inoculated at the density of 1×10^4 cells/well in 0.5 ml/well selection medium, and

subjected to second selection to get a single clone by repeating the steps described above. A positive clone (clone 7) was selected from the second selection and cultured in normal DMEM (10% FCS) for around 3 weeks. After 3 weeks, these cells still stably express TrkA, which was confirmed by Western blotting. Thus, these cells were used as stable CHO-K1-TrkA cells.

2.9 Apoptosis assay in CGNs

CGNs were cultured on coverslips coated with 0.2% polyethylenimine in 24-well plates for 5 days. Culture medium was removed by aspiration, and cells were incubated in HK (DMEM containing 25 mM potassium), or LK (DMEM containing 5 mM potassium) supplemented with vehicle control (DMEM plus methanol), BDNF and/or LPC for 24 h. The medium was removed, and cells were fixed with 4% paraformaldehyde (0.5 ml/well) for 30 min at room temperature. Used paraformaldehyde was collected. Cells were washed twice with PBS (0.5 ml/well), and stained with Hoechst 33258 (1 μg/ml, 0.5 ml/well) for 15 min at room temperature avoiding direct light. Cells were washed again with PBS twice. Coverslips were carefully taken from 24-well plate and fixed on slide glass using 5 μl/each 50% glycerol. Morphology of nuclei was observed by fluorescent microscopy, with 40X magnification. For each sample, at least 5 of images were taken, and cells were counted as apoptotic if their nuclei were condensed or fragmented. Generally, more than 200 cells in total from each well were counted for each condition in each independent experiment. The viability of cells was calculated by dividing the number of live cells by the total number of live and apoptotic cells.

2.10 Detection of TrkA dimer by chemical cross-linker bis[sulfosuccinimidyl]

suberate (BS^3)

The same amount of PC12 cells were cultured in collagen-coated 6-cm dishes in 4 ml/well DMEM (5%HS/5%FCS), and incubated for until >80% confluent. Cells were untransfected or transfected with TrkA-EGFP-N1 (2 μg/well, diluted in 0.4 ml/well DMEM), using Lipofectamine 2000 (8 μl/well diluted in 0.4 ml/well DMEM) overnight. Cells were washed with DMEM twice (2 ml/well), and serum-starved in DMEM (2 ml/well) for 3 h. Then, DMEM was removed, added DMEM containing 0.45 M sucrose (2 ml/well), and incubated for 20 min at 37°C. Cells were untreated or treated with NGF 50 ng/ml and/or LPC 1 μM for 5 min in DMEM containing 0.45 M sucrose. Cells were then washed with PBS containing 0.45 M sucrose for three times (2 ml/well), and treated with BS^3 (1 mM, 2 ml/well) for 30 min at 37°C, avoiding light. Reaction was stopped by adding Tris-HCl (80 mM, 2 ml/well), and incubating for 15 min at room temperature. Cells were then washed with ice-cold PBS containing 0.45 M sucrose twice. Finally, cells were lysed with 1% NP40 containing 1× protease inhibitor and 1× phosphatase inhibitor (100 μl/well), incubate on ice for 30 min, and collect the lysis in tubes. Centrifuge these samples at 10,000 rpm, 4°C for 10 min, get supernatant (~120 μl) into new tubes, add 4 × SDS (~40 μl), and boil for 3 min. The equal amount of these samples was subjected to Western blotting analysis on 5.5% acrylamide gel.

3. Statistical analysis

The results shown are from at least three independent experiments. Data are expressed as the means±standard deviations (SD). Data were analyzed for statistical significance using one-way ANOVA. Differences were considered significant at $p<0.05$ as indicated.

Recipes for solutions:

PBS (phosphate-buffered-saline)**:**

NaCl	8 g
KCl	0.2 g
$Na_2HPO_4.12H_2O$	2.9 g
KH_2PO4	0.2 g
Fill with D.W.	to 1000 ml, and autoclave at 121°C for 15 min.

EDTA 0.5 M, pH 8.0:

Add 18.62 g of EDTA to 80 ml of distilled water and stir vigorously. Adjust the pH to 8.0 with NaOH. The salt will not dissolve until the pH is adjusted to pH 8.0. Fill up to 100 ml with distilled water (D.W.), and autoclave at 121°C for 15 min.

PBS containing EDTA (1 mM) for cells:

PBS	500 ml
Add EDTA 0.5 M pH8.0	1 ml, mix in clean bench, and autoclave at 121°C for 15 min. Store at room temperature.

Collagen for coating the plates for PC12 cells:

Collagen (rat type I tail, 4.1 mg/ml	2.4 ml (5 mg)
Acidic acid	240 µl
D.W.	in 200 ml. Autoclave at 121°C for 15 min.

G418:

Add 137.7 mg G418 carefully in 4 ml PBS in 15-ml falcon tube, shake by hand to dissolve. Filter the solution using 0.2 µm filter in the clean bench. The concentration of this solution is 25 mg/ml. It is ready for use. Store at -4°C.

1 mM BS^3:

The powder of BS^3 in tubes (products are in small PCR 8-tubes, not good to store for long time) was dissolved in PBS containing 0.45 M sucrose, according to manufacturer's instruction. The solution of BS^3 should be prepared just before using and should avoid light.

1% NP40 containing 1× protease inhibitor and 1 × phosphatase inhibitor:

D.W.	0.656 ml
10% NP40	0.1 ml
7 × protease inhibitor	0.144 ml
10 × phosphatase inhibitor	0.1 ml
total	1 ml

Phosphatase inhibitor cocktail (EDTA free, 07575-51) was from nacalai tesque. This is a 100 × stock solution. The protease inhibitor cocktail (EDTA free, 11836170001) complete mini was from Roche. To make 7 × protease inhibitor solutions, 1 tablet of this protease inhibitor was dissolve in 1.5 ml D.W. Nonidet p-40 (NP40, 25223-04) was from nacalai tesque. 1 ml of original NP40 solution was diluted in 9 ml of distilled water to make 10% NP40. Prepare this solution just prior to use.

4% paraformaldehyde:

Weigh 0.4 g paraformaldehyde and add in 10 ml PBS in a 15-ml falcon tube, close and seal the cap tightly, shake vigorously, and boil for 10 min. Cool down at room temperature. It is active within 24 h. Thus, it is better to prepare this solution prior to use. After using, it should be collected in the waste bottle for paraformaldehyde.

KRHG buffer:

Contents:120 mM NaCl, 4.8 mM KCl, 1.26 mM $CaCl_2$, 1.18 mM KH_2PO_4, 1.22 mM $MgSO_4$ 25.2 mM $NaHCO_3$, 25 mM Hepes-NaOH, pH 7.4. Store at -4°C.

10×TBS:

Tris	24.2 g
NaCl	87.7 g

Dissolve in 900 ml DW, adjust pH to 7.5, and fill with D.W. up to 1000 ml.

TBS can be prepared by diluting 10×TBS ten times in D.W.

10×TTBS:

Tris	24.2 g
NaCl	87.7 g
Tween 20	10 ml

Dissolve in 900 ml DW, adjust pH to 7.5, and fill with D.W. up to 1000 ml.

TTBS can be prepared by diluting 10×TTBS ten times in D.W.

4×SDS (sodium dodecyl sulfate) sample buffer:

1 M Tris-HCl (pH 6.8)	5 ml (0.2 M)
SDS (sodium dodecyl sulfate)	2 g (8%)
Glycerol	10 ml (40%)
2-mercaptoethanol	5 ml (20%)
BPB (bromophenol blue)	little (0.05%)
D.W.	5 ml
Total	25 ml

1×SDS sample buffer:

4×SDS sample buffer	10 ml
D.W.	30 ml
Total	40 ml

1 M Tris-HCl pH 6.8:

Tris	6.057 g
D.W.	45 ml

Adjust pH to 6.8, fill with D.W. up to 50 ml.

10% acrylamide gel (for 4 pages):

Separation gel:	
30% acrylamide	10 ml
2 x Tris-SDS (pH 8.8)	15 ml
D.W.	5 ml
10% APS	0.3 ml
TEMED	30 µl
Stacking gel:	
30% acrylamide	2 ml
2 x Tris-SDS (pH 6.8)	6 ml
D.W.	4 ml
10% APS	100 µl
TEMED	10 µl

5.5% acrylamide gel (for 4 pages):

Separation gel:	
30% acrilamide	5.5 ml

2 x Tris-SDS (pH 8.8)	15 ml
D.W.	9.5 ml
10% APS	0.3 ml
TEMED	30 μl

Stacking gel is the same.

5% Skim Milk:

Dissolve 5 g of Skim Milk in 100 ml TBS. Store at -20°C.

1.125 M Sucrose:

Dissolve 46.2 g sucrose in 120 ml DW, and autoclave at 121°C for 15 min.
Store at room temperature.

DMEM containing 0.45 M sucrose:

DMEM	6 ml
1.125 M sucrose	4 ml
Total	10 ml

PBS containing 0.45 M sucrose:

PBS	30 ml
1.125 M sucrose	20 ml
Total	50 ml

Store at room temperature.

80 mM Tris-HCl containing 0.45 M sucrose:

133.3 mM Tris-HCl pH 7.5	12 ml
1.125 M sucrose	8 ml
Total	20 ml

Store at room temperature.

Protocol: Total RNA isolation and cDNA synthesis from PC12 cells in 6-cm dishes

Coat 6-cm dish with 2 ml of collagen solution.
Inoculate 1×10^6 cells/dish in 4 ml/dish of DMEM (5%FCS/5%HS) medium for overnight or longer until >80% confluent.

Wash cells twice with serum-free DMEM (2 ml each), and Incubate cells in 2 ml of DMEM for 1.5 h.

During this 1.5 h, prepare stimulation solutions:

		NGF	LPC
Sample 1: 200 μl DMEM	22 μl MeOH	0	0
Sample 2: 200 μl DMEM	22 μl LPC (100 μM)	0	1
Sample 3: 200 μl NGF (500 ng/ml)	22 μl MeOH	50	0
Sample 4: 200 μl NGF (500 ng/ml)	22 μl LPC (100 μM)	50	1
Sample 5: 200 μl NGF (1,000 ng/ml)	22 μl MeOH	100	0
	Final concentration:	(ng/ml)	(μM)

Working solution:
NGF (1,000 ng/ml): 500 μl of DMEM + 5.5 μl of NGF (100 μg/ml)
NGF (500 ng/ml): 250 μl of DMEM + 250 μl of NGF (1,000 ng/ml)
LPC (100 μM): 90 μl of MeOH + 10 μl of LPC (1 mM)

After 1.5 h, stimulate cells for 30 min by adding the above solutions at 37° C in incubator.

Remove medium in dishes by aspiration.
Wash twice with ice cold KRHG, 3 ml each.
Add TRI reagent, 500 μl/dish, collect all cells by scratching using a plastic tube (prepared for this), and take lysis in new 1.5-ml tubes (prepared only for RNA). Mix the lysis by carefully pippeting 5 times using syringe (1 ml).
Add 50 μl of 1-bromo-3-chloropropane in each tube, and shake vigorously for 15 sec.
Leave 2-15 min at room temperature.
Centrifuge at 12,000g for 15 min at 2-8° C (RNA is contained in the upper clear layer).

Transfer supernatant to new tubes.
Add isopropanol, 250 μl in each tube, mix by hand, and leave for 5-10 min at room temperature.
Centrifuge at 12,000g for 10 min at 2-8° C (RNA is precipitated).

Carefully remove supernatant.
Add 70% ethanol, 500 μl in each tube, and vortex.
Centrifuge at 7,500g for 5 min at 2-8° C.
Remove supernatant by aspiration.
Dry for 5-10 min in the air.
Dissolve the palates in 20-40 μl (depends on the amount of RNA) DEPC water.

Measure A260 at 50-times dilution (2 μl/100 μl)
Calculate the concentration of RNA (RNA is 38 μg per A260; use the calculation sheet).
Usually, the total amount of RNA is 6-8 μg per 6-cm dish.

DNase treatment
+6 μl (or >6 μl, 5 ~ 10 μg of total RNA)
+1 μl DNase buffer (Promega, 400 mM Tris-HCl, pH 8.0; 100 mM MgSO4; 10 mM CaCl2)
+3 μl of DNase (Promega)
37° C for 1 h.

+90 μl (or <90 μl) of DEPC water
+100 μl of RNase free phenol, shake by hands
Centrifuge at 10,000 rpm for 5 min at 25°C

Get upper layer (~70 μl, collected in new tubes)
+100 μl of chloroform, shake by hands
Centrifuge at 10,000 rpm for 5 min at 25°C.
PS: set the machines at 4°C.

Get upper layer (collected in new tubes)
+260 μl of ethanol precipitation solution (24 ml ethanol and 1 ml 3 M sodium acetate), shake by hands. Then, keep at -80°C for 20 min
PS: switch the water bath at 65°C/ 30°C/ 42°C.

Centrifuge at 12,000 rpm for 10 min at 4°C
Remove supernatant, add 800 μl of 70% ethanol.
Centrifuge again at 12,000 rpm for 10 min at 4°C.
Remove supernatant and let it dry for 5 min at room temperature.
Around 20 μl of DEPC-treated water was added to dissolve the pellet.

Calculate the concentration of RNA again by measuring A_{260}, as indicated above.

Reverse transcription:

Then, same amount of RNA was reverse transcribed.

+1-5 μg of total RNA (2-3 μl)

+4 μl of dNTP (2.5 mM each)

+1 μl of random primer (250 ng/ml)

Total volume of 10 μl

65° C, 5 min

Cool on ice

+4 μl 5x Buffer

+0.5 μl RNase inhibitor (20 units)

+0.5 μl PrimeScript reverse transcriptase (100-200 units)

+5 μl DEPC water

Total volume of 20 μl

30° C, 10 min

42° C, 1 h

70° C, 15 min

Now, cDNA was synthesized. Store at -20° C, or proceed to PCR.

Note: "+" indicates "add".

Appendixes

Abbreviation list

AA	arachidonic acid
BDNF	brain-derived neurotrophic factor
BS^3	Bissulfosuccinimidyl suberate
bFGF	basic fibroblast growth factor
CGNs	cerebellar granule neurons
$cPLA_2$	cytosolic PLA_2
Ca^{2+}/CaM	Ca^{2+}/calmodulin-dependent kinase
COX-2	cyclooxygenase type 2
CREB	cAMP response element-binding protein
CNS	central nervous system
DMEM	Dulbecco's modified Eagle's medium
DMSO	Dimethyl sulfoxide
EGF	epidermal growth factor
EGFR	EGF receptor
GPCR	G protein-coupled receptors
HAEC	human aortic endothelial cells
HSPG	heparan sulfate proteoglycans
IGF-1	insulin-like growth factor-1
JNK	c-Jun N-terminal kinase
LPA	lysophosphatidic acid
LPA_1	LPA receptor 1
LPC	lysophosphatidylcholine
LPE	lysophosphatidylethanolamine
LPS	lysophosphatidylserine
LDL	low density lipoprotein
MAPK	mitogen-activated protein kinase
MEK	mitogen-activated protein kinase kinase
NGF	nerve growth factor
NT-3	neurotrophin-3
NT-4	neurotrophin-4
Ox-LDL	oxidized low-density lipoproteins
PA	phosphatidic acid
PC	phosphatidylcholine
PE	phosphatidylethanolamine
PS	phosphatidylserine
PI-3K	phosphatidylinositol 3-kinase
PLA_2	phospholipase A_2
PLC-γ1	phospholipase C-γ1
PNS	peripheral nervous system
PMNs	polymorphonuclear leukocytes
RT-PCR	reverse transcription-polymerase chain reaction

ROS	reactive oxygen species
S1P	sphingosine 1-phosphate
SH2	Src homology domain 2
$sPLA_2$	secretory PLA_2
Trk	tropomyosin-related kinase
BSA	bovine serum albumin
cDNA	complementary cDNA
CBB	coomassie brilliant blue
DNA	deoxyribonucleic acid
EDTA	ethylenediaminetetraacetic acid
SDS	sodium dodecyl sulfate
TTBS	Tris-buffered saline containing 0.01% Tween 20.
TBS	Tris-buffered saline
^oC	degree Celsius
kDa	kilo Dalton
kb	kilo base
μg	micro gram
h	hour
min	minutes
sec	second
ml	milliliter
μl	micro liter
μM	micro mole
mRNA	messenger RNA
PBS	phosphate buffered saline
PCR	polymerase chain reaction
RNA	ribonucleic acid
RT-PCR	reverse transcription-polymerase chain reaction
SDS	sodium dodecyl sulfate
Tris	tris(hydroxymethyl)aminomethane

References

1. Levi-Montalcini, R. (1987) The nerve growth factor 35 years later. *Science* **237**, 1154-1162
2. Barde, Y. A., Edgar, D., and Thoenen, H. (1982) Purification of a new neurotrophic factor from mammalian brain. *EMBO J.* **1**, 549-553
3. Maisonpierre, P. C., Belluscio, L., Squinto, S., Ip, N. Y., Furth, M. E., Lindsay, R. M., and Yancopoulos, G. D. (1990) Neurotrophin-3: a neurotrophic factor related to NGF and BDNF. *Science* **247**, 1446-1451
4. Ip, N. Y., Ibáñez, C. F., Nye, S. H., McClain, J., Jones, P. F., Gies, D. R., Belluscio, L., Le Beau, M. M., Espinosa, R., and Squinto, S. P. (1992) Mammalian neurotrophin-4: structure, chromosomal localization, tissue distribution, and receptor specificity. *Proc. Natl. Acad. Sci. U. S. A.* **89**, 3060-3064
5. Wiesmann, C., and de Vos, A. M. (2001) Nerve growth factor: structure and function.*Cell Mol. Life Sci.* **58**, 748-759
6. Sofroniew, M. V., Howe, C. L., and Mobley, W. C. (2001) Nerve growth factor signaling, neuroprotection, and neural repair. *Annu. Rev. Neurosci.* **24**, 1217-1281
7. Huang, E. J., and Reichardt, L. F. (2003) Trk receptors: Roles in neuronal signal transduction. *Annu. Rev. Biochem.* **72**, 609-642
8. Segal, R. A. (2003) Selectivity in neurotrophin signaling: theme and variations. *Annu. Rev. Neurosci.* **26**, 299-330
9. Pardon, M. C. (2010) Role of neurotrophic factors in behavioral processes: implications for the treatment of psychiatric and neurodegenerative disorders. *Vitam. Horm.* **82**, 185-200
10. Lemmon, M. A., and Schlessinger, J. (2010) Cell signaling by receptor tyrosine kinases. *Cell* **141**, 1117-1134
11. McDonald, N. Q., Lapatto, R., Murray-Rust, J., Gunning, J., Wlodawer, A., and Blundell, T. L. (1991) New protein fold revealed by a 2.3-A resolution crystal structure of nerve growth. *Nature* **354**, 411-414
12. Arakawa, T., Haniu, M., Narhi, L. O., Miller, J. A., Talvenheimo, J., Philo, J. S., Chute, H. T., Matheson, C., Carnahan, J., Louis, J. C., and et al. (1994) Formation of heterodimers from three neurotrophins, nerve growth factor. *J. Biol. Chem.* **269**, 27833-27839
13. Reichardt, L. F. (2006) Neurotrophin-regulated signalling pathways. *Philos. Trans. R. Soc. Lond. B. Biol. Sci.* **361**, 1545-1564
14. Chowdary, P. D., Che, D. L., and Cui, B. (2012) Neurotrophin signaling via long-distance axonal transport. *Annu. Rev. Phys. Chem.* **63**, 571-594
15. Allen, S. J., Watson, J. J., and Dawbarn, D. (2011) The neurotrophins and their role in Alzheimer's disease. *Curr. Neuropharmacol.* **9**, 559-573
16. Ichim, G., Tauszig-Delamasure, S., and Mehlen, P. (2012) Neurotrophins and cell death. *Exp. Cell Res.* **318**, 1221-1228
17. Zuccato, C., and Cattaneo, E. (2009) Brain-derived neurotrophic factor in

neurodegenerative diseases. *Nat*. *Rev*. *Neurol*. **5**(6):311-22

18. Scarpi, D., Cirelli, D., Matrone, C., Castronovo, G., Rosini, P., Occhiato, E. G., Romano, F., Bartali, L., Clemente, A. M., Bottegoni, G., Cavalli, A., De Chiara, G., Bonini, P., Calissano, P., Palamara, A. T., Garaci, E., Torcia, M. G., Guarna, A., and Cozzolino, F. (2012) Low molecular weight, non-peptidic agonists of TrkA receptor with NGF-mimetic. *Cell Death*. *Dis*. **3**, e389
19. Burke, J. E., and Dennis, E. A. (2009) Phospholipase A2 structure/function, mechanism, and signaling. *J*. *Lipid Res*. **50** Suppl., S237-242
20. Kudo, I., and Murakami, M. (2002) Phospholipase A(2) enzymes. *Prostaglandins & Other Lipid Mediat*. **68**-9, 3-58
21. Murakami, M., Taketomi, Y., Girard, C., Yamamoto, K., and Lambeau, G. (2010) Emerging roles of secreted phospholipase A2 enzymes: Lessons from transgenic and knockout mice. *Biochimie*. **92**, 561-582
22. Schmitz, G., and Ruebsaamen, K. (2010) Metabolism and atherogenic disease association of lysophosphatidylcholine. *Atherosclerosis* **208**(1):10-8.
23. Boggs, K. P., Rock, C. O., and Jackowski, S. (1995) Lysophosphatidylcholine and 1-O-octadecyl-2-O-methyl-rac-glycero-3-phosphocholine. *J*. *Biol*. *Chem*. **270**, 7757-7764
24. Rousset, X., Vaisman, B., Amar, M., Sethi, A. A., and Remaley, A. T. (2009) Lecithin: cholesterol acyltransferase - from biochemistry to role in cardiovascular disease. *Curr*. *Opin*. *Endocrinol*. *Diabetes Obes*. **16**, 163-171
25. Sekas, G., Patton, G. M., Lincoln, E. C., and Robins, S. J. (1985) Origin of plasma lysophosphatidylcholine: evidence for direct hepatic secretion. *J*. *Lab*. *Clin*. *Med*. **105**, 190-194
26. Ojala, P. J., Hirvonen, T. E., Hermansson, M., Somerharju, P., and Parkkinen, J. (2007) Acyl chain-dependent effect of lysophosphatidylcholine on human neutrophils. *J*. *Leukoc*. *Biol*. **82**, 1501-1509
27. Croset, M., Brossard, N., Polette, A., and Lagarde, M. (2000) Characterization of plasma unsaturated lysophosphatidylcholines in human and rat. *Biochem*. *J*. **345** Pt1, 61-67
28. Sevastou, I., Kaffe, E., Mouratis, M. A., and Aidinis, V. (2013) Lysoglycerophospholipids in chronic inflammatory disorders: The PLA(2)/LPC and ATX/LPA axes. *Biochim*. *Biophys*. *Acta*. **1831**(1):42-60
29. Cathcart, M. K., McNally, A. K., and Chisolm, G. M. (1991) Lipoxygenase-mediated transformation of human low density lipoprotein to an oxidized and cytotoxic complex. *J*. *Lipid Res*. **32**, (1):63-70
30. Morel, D. W., DiCorleto, P. E., and Chisolm, G. M. (1984) Endothelial and smooth muscle cells alter low density lipoprotein in vitro by free radical oxidation. *Arteriosclerosis* **4**, (4): 357-364
31. Gauster, M., Rechberger, G., Sovic, A., Horl, G., Steyrer, E., Sattler, W., and Frank, S. (2005) Endothelial lipase releases saturated and unsaturated fatty acids of high density lipoprotein phosphatidylcholine. *J*. *Lipid Res*. **46**, 1517-1525
32. Secchi, A. G., Fregona, I., and D'Ermo, F. (1979) Lysophosphatidyl choline in

the aqueous humour during ocular inflammation. *Br. J. Ophthalmol*. **63**, 768-770

33. Ryborg, A. K., Gron, B., and Kragballe, K. (1995) Increased lysophosphatidylcholine content in lesional psoriatic skin. *Br. J. Dermatol*. **133**, 398-402
34. Rikitake, Y., Hirata, K., Kawashima, S., Takeuchi, S., Shimokawa, Y., Kojima, Y., Inoue, N., and Yokoyama, M. (2001) Signaling mechanism underlying COX-2 induction by lysophosphatidylcholine. *Biochem. Biophys. Res. Commun*. **281**, 1291-1297
35. Brkic, L., Riederer, M., Graier, W. F., Malli, R., and Frank, S. (2012) Acyl chain-dependent effect of lysophosphatidylcholine on cyclooxygenase (COX)-2 expression in endothelial cells. in *Atherosclerosis* **224**(2):348-54.
36. Ruiperez, V., Casas, J., Balboa, M. A., and Balsinde, J. (2007) Group V phospholipase A2-derived lysophosphatidylcholine mediates cyclooxygenase-2 induction in lipopolysaccharide-stimulated macrophages. *J. Immunol*. **179**, 631-638
37. Kume, N., Cybulsky, M. I., and Gimbrone, M. A. (1992) Lysophosphatidylcholine, a component of atherogenic lipoproteins, induces mononuclear leukocyte adhesion molecules in cultured human and rabbit arterial endothelial cells. *J. Clin. Invest*. **90**, 1138-1144
38. Lauber, K., Bohn, E., Kröber, S. M., Xiao, Y. J., Blumenthal, S. G., Lindemann, R. K., Marini, P., Wiedig, C., Zobywalski, A., Baksh, S., Xu, Y., Autenrieth, I. B., Schulze-Osthoff, K., Belka, C., Stuhler, G., and Wesselborg, S. (2003) Apoptotic cells induce migration of phagocytes via caspase-3-mediated release of a lipid attraction signal. *Cell* **113**, 717-730
39. Quinn, M. T., Parthasarathy, S., and Steinberg, D. (1988) Lysophosphatidylcholine: a chemotactic factor for human monocytes and its potential role in atherogenesis. *Proc. Natl. Acad. Sci. U. S. A*. **85**, 2805-2809
40. Radu, C. G., Yang, L. V., Riedinger, M., Au, M., and Witte, O. N. (2004) T cell chemotaxis to lysophosphatidylcholine through the G2A receptor. *Proc. Natl. Acad. Sci. U. S. A*. **101**, 245-250
41. Ogita, T., Tanaka, Y., Nakaoka, T., Matsuoka, R., Kira, Y., Nakamura, M., Shimizu, T., and Fujita, T. (1997) Lysophosphatidylcholine transduces Ca2+ signaling via the platelet-activating factor receptor in macrophages. *Am. J. Physiol*. **272**, H17-H24
42. Khan, S. Y., McLaughlin, N. J., Kelher, M. R., Eckels, P., Gamboni-Robertson, F., Banerjee, A., and Silliman, C. C. (2010) Lysophosphatidylcholines activate G2A inducing G(alphai)(-)(1)-/G(alphaq/)(1)(1). *Biochem. J*. **432**, 35-45
43. Marquardt, D. L., and Walker, L. L. (1991) Lysophosphatidylcholine induces mast cell secretion and protein kinase C. *J. Allergy Clin. Immunol*. **88**, 721-730
44. Kugiyama, K., Ohgushi, M., Sugiyama, S., Murohara, T., Fukunaga, K., Miyamoto, E., and Yasue, H. (1992) Lysophosphatidylcholine inhibits surface receptor-mediated intracellular signals. *Circ. Res*. **71**, 1422-1428

45. Bassa, B. V., Roh, D. D., Vaziri, N. D., Kirschenbaum, M. A., and Kamanna, V. S. (1999) Lysophosphatidylcholine activates mesangial cell PKC and MAP kinase by PLCgamma-1. *Am. J. Physiol.* **277**, F328-337
46. Fang, X. J., Gibson, S., Flowers, M., Furui, T., Bast, R. C., and Mills, G. B. (1997) Lysophosphatidylcholine stimulates activator protein 1 and the c-Jun N-terminal kinase activity. *J. Biol. Chem.* **272**, 13683-13689
47. Yoshida, K., Nishida, W., Hayashi, K., Ohkawa, Y., Ogawa, A., Aoki, J., Arai, H., and Sobue, K. (2003) Vascular remodeling induced by naturally occurring unsaturated lysophosphatidic. *Circulation* **108**, 1746-1752
48. Tanaka, M., Kishi, Y., Takanezawa, Y., Kakehi, Y., Aoki, J., and Arai, H. (2004) Prostatic acid phosphatase degrades lysophosphatidic acid in seminal plasma. *FEBS Lett.* **571**, 197-204
49. Makide, K., Kitamura, H., Sato, Y., Okutani, M., and Aoki, J. (2009) Emerging lysophospholipid mediators, lysophosphatidylserine. *Prostaglandins Other Lipid Mediat.* **89**, 135-139
50. Moughal, N. A., Waters, C., Sambi, B., Pyne, S., and Pyne, N. J. (2004) Nerve growth factor signaling involves interaction between the Trk A receptor and lysophosphatidate receptor 1 system: nuclear translocation of the lysophosphatidate receptor 1 and TrkA receptors in pheochromocytoma 12 cells. *Cell Signal.* **16**, 127-136
51. Moughal, N. A., Waters, C. M., Valentine, W. J., Connell, M., Richardson, J. C., Tigyi, G., Pyne, S., and Pyne, N. J. (2006) Protean agonism of the lysophosphatidic acid receptor-1 with Ki16425 reduces nerve growth factor-induced neurite outgrowth in pheochromocytoma 12 cells. *J. Neurochem.* **98**, 1920-1929
52. Nakashima, S., Ikeno, Y., Yokoyama, T., Kuwana, M., Bolchi, A., Ottonello, S., Kitamoto, K., and Arioka, M. (2003) Secretory phospholipases A(2) induce neurite outgrowth in PC12 cells. *Biochem. J.* **376**, 655-666
53. Arioka, M., Cheon, S. H., Ikeno, Y., Nakashima, S., and Kitamoto, K. (2005) A novel neurotrophic role of secretory phospholipases A2 for cerebellar granule neurons. *FEBS Lett.* **579**, 2693-2701
54. Reddy, C. V., Malinowska, K., Menhart, N., and Wang, R. (2004) Identification of TrkA on living PC12 cells by atomic force microscopy. *Biochim. Biophys. Acta.* **1667**, 15-25
55. Ikeno, Y., Konno, N., Cheon, S. H., Bolchi, A., Ottonello, S., Kitamoto, K., and Arioka, M. (2005) Secretory phospholipases A(2) induce neurite outgrowth in PC12 cells through lysophosphatidylcholine generation and activation of G2A receptor. *J. Biol. Chem.* **280**, 28044-28052
56. Ikeno, Y., Cheon, S. H., Konno, N., Nakamura, A., Kitamoto, K., and Arioka, M. (2009) Lysophosphatidylcholine Protects Cerebellar Granule Neurons From Apoptotic Cell Death. *J. Neurosci. Res.* **87**, 190-199
57. Shen, J., and Maruyama, I. N. (2011) Nerve growth factor receptor TrkA exists as a preformed, yet inactive, dimer in living cells. *FEBS Lett.* **585**, 295-299
58. Barbacid, M. (1995) Structural and functional properties of the TRK family of

neurotrophin receptors. *Ann. N. Y. Acad. Sci.* **766**, 442-458
59. Dijkmans, T. F., van Hooijdonk, L. W. A., Schouten, T. G., Kamphorst, J. T., Fitzsimons, C. P., and Vreugdenhil, E. (2009) Identification of new Nerve Growth Factor-responsive immediate-early genes. *Brain Res.* **1249**:19-33.
60. Greene, L. A., and Tischler, A. S. (1976) Establishment of a noradrenergic clonal line of rat adrenal pheochromocytoma. *Proc. Natl. Acad. Sci. U. S. A.* **73**, 2424-2428
61. Dichter, M. A., Tischler, A. S., and Greene, L. A. (1977) Nerve growth factor-induced increase in electrical excitability and acetylcholine. *Nature* **268**, 501-504
62. Fujita, K., Lazarovici, P., and Guroff, G. (1989) Regulation of the differentiation of PC12 pheochromocytoma cells. *Environ Health Perspect.* **80**, 127-142
63. Vaudry, D., Stork, P. J., Lazarovici, P., and Eiden, L. E. (2002) Signaling pathways for PC12 cell differentiation: making the right connections. *Science* **296**, 1648-1649
64. Marshall, C. J. (1995) Specificity of receptor tyrosine kinase signaling: transient versus sustained. *Cell* **80**, 179-185
65. Riederer, M., Ojala, P. J., Hrzenjak, A., Tritscher, M., Hermansson, M., Watzer, B., Schweer, H., Desoye, G., Heinemann, A., and Frank, S. (2010) Acyl chain-dependent effect of lysophosphatidylcholine on endothelial prostacyclin production. *J. Lipid Res.* **51**, 2957-2966
66. Herschman, H. R. (1991) Primary response genes induced by growth factors and tumor promoters. *Annu. Rev. Biochem.* **60**, 281-319
67. Marek, L., Levresse, V., Amura, C., Zentrich, E., Van Putten, V., Nemenoff, R. A., and Heasley, L. E. (2004) Multiple signaling conduits regulate global differentiation-specific gene expression in PC12 cells. *J. Cell Physiol.* **201**, 459-469
68. Pellegrino, M. J., and Stork, P. J. (2006) Sustained activation of extracellular signal-regulated kinase by nerve growth factor regulates c-fos protein stabilization and transactivation in PC12 cells. *J. Neurochem.* **99**, 1480-1493
69. Mullenbrock, S., Shah, J., and Cooper, G. M. (2011) Global expression analysis identified a preferentially nerve growth factor-induced transcriptional program regulated by sustained mitogen-activated protein kinase/extracellular signal-regulated kinase (ERK) and AP-1 protein activation during PC12 cell differentiation. *J. Biol. Chem.* **286**, 45131-45
70. Obermeier, A., Bradshaw, R. A., Seedorf, K., Choidas, A., Schlessinger, J., and Ullrich, A. (1995) Definition of signals for neuronal differentiation. *Ann. N. Y. Acad. Sci.* **766**, 1-17
71. Lu, X., Kambe, F., Cao, X., Yamauchi, M., and Seo, H. (2008) Insulin-like growth factor-I activation of Akt survival cascade in neuronal cells requires the presence of its cognate receptor in caveolae. Exp. Cell Res. 314, 342-351
72. Robinson, M. J., and Cobb, M. H. (1997) Mitogen-activated protein kinase pathways. *Curr. Opin. Cell. Biol.* **9**, 180-186

73. Morooka, T., and Nishida, E. (1998) Requirement of p38 mitogen-activated protein kinase for neuronal differentiation. *J. Biol. Chem.* **273**, 24285-24288
74. Tsang, M., and Dawid, I. B. (2004) Promotion and attenuation of FGF signaling through the Ras-MAPK pathway. *Sci. STKE.* **228,** pe17
75. Yamada, S., Taketomi, T., and Yoshimura, A. (2004) Model analysis of difference between EGF pathway and FGF pathway. *Biochem. Biophys. Res. Commun.* **314**, 1113-1120
76. Minichiello, L. (2009) TrkB signalling pathways in LTP and learning. *Nat. Rev. Neurosci.* **10**(12):850-60
77. Numakawa, T., Suzuki, S., Kumamaru, E., Adachi, N., Richards, M., and Kunugi, H. (2010) BDNF function and intracellular signaling in neurons. *Histol. Histopathol.* **25**, 237-258
78. Nagahara, A. H., and Tuszynski, M. H. (2011) Potential therapeutic uses of BDNF in neurological and psychiatric disorders. *Nat. Rev. Drug. Discov.* **10**(3):209-19
79. Gallo, V., Kingsbury, A., Balazs, R., and Jorgensen, O. S. (1987) The role of depolarization in the survival and differentiation of cerebellar granule cells in culture. *J. Neurosci.* **7**, 2203-2213
80. D'Mello, S. R., Galli, C., Ciotti, T., and Calissano, P. (1993) Induction of apoptosis in cerebellar granule neurons by low potassium: inhibition of death by insulin-like growth factor I and cAMP. *PProc. Natl. Acad. Sci. U. S. A.* **90**, 10989-10993
81. Kubo, T., Nonomura, T., Enokido, Y., and Hatanaka, H. (1995) Brain-derived neurotrophic factor (BDNF) can prevent apoptosis of rat cerebellar granule neurons in culture. *Brain Res. Dev. Brain Res.* **85**(2):249-58.
82. Lindholm, D., Dechant, G., Heisenberg, C. P., and Thoenen, H. (1993) Brain-derived neurotrophic factor is a survival factor for cultured rat cerebellar granule neurons and protects them against glutamate-induced neurotoxicity. *Eur. J. Neurosci.* **5**, 1455-1464
83. Dudek, H., Datta, S. R., Franke, T. F., Birnbaum, M. J., Yao, R., Cooper, G. M., Segal, R. A., Kaplan, D. R., and Greenberg, M. E. (1997) Regulation of neuronal survival by the serine-threonine protein kinase Akt. *Science* **275**, 661-665
84. Bonni, A., Brunet, A., West, A. E., Datta, S. R., Takasu, M. A., and Greenberg, M. E. (1999) Cell survival promoted by the Ras-MAPK signaling pathway by transcription-dependent and -independent mechanisms. *Science*, **286**(5443):1358-62
85. Blair, L. A., Bence-Hanulec, K. K., Mehta, S., Franke, T., Kaplan, D., and Marshall, J. (1999) Akt-dependent potentiation of L channels by insulin-like growth factor-1 is required for neuronal survival. *J. Neurosci.* **19**, 1940-1951
86. Zhong, J., Deng, J., Huang, S., Yang, X., and Lee, W. H. (2004) High K+ and IGF-1 protect cerebellar granule neurons via distinct signaling pathways. *J. Neurosci. Res.* **75**, 794-806
87. See, V., Boutillier, A. L., Bito, H., and Loeffler, J. P. (2001)

Calcium/calmodulin-dependent protein kinase type IV (CaMKIV) inhibits apoptosis. *FASEB. J.* **15**, 134-144

88. Peter, C., Waibel, M., Radu, C. G., Yang, L. V., Witte, O. N., Schulze-Osthoff, K., Wesselborg, S., and Lauber, K. (2008) Migration to apoptotic "find-me" signals is mediated via the phagocyte receptor. *J. Biol. Chem.* **283**, 5296-5305
89. Hasegawa, H., Lei, J., Matsumoto, T., Onishi, S., Suemori, K., and Yasukawa, M. (2011) Lysophosphatidylcholine enhances the suppressive function of human naturally occurring regulatory T cells through TGF-beta production. *Biochem. Biophys. Res. Commun.* **415**, 526-531
90. Murakami, N., Yokomizo, T., Okuno, T., and Shimizu, T. (2004) G2A is a proton-sensing G-protein-coupled receptor antagonized by lysophosphatidylcholine. *J. Biol. Chem.* **279**, 42484-42491
91. Qiao, J., Huang, F., Naikawadi, R. P., Kim, K. S., Said, T., and Lum, H. (2006) Lysophosphatidylcholine impairs endothelial barrier function through the G protein-coupled receptor GPR4. *Am. J. Physiol. Lung Cell Mol. Physiol.* **291**, L91-101
92. Takahashi, Y., Shimokawa, N., Esmaeili-Mahani, S., Morita, A., Masuda, H., Iwasaki, T., Tamura, J., Haglund, K., and Koibuchi, N. (2011) Ligand-induced downregulation of TrkA is partly regulated through ubiquitination. *FEBS Lett.* **585**, 1741-1747
93. Schecterson, L. C., and Bothwell, M. (2010) Neurotrophin receptors: Old friends with new partners. *Dev. Neurobiol.* **70**, 332-338
94. Perez, P., Coll, P. M., Hempstead, B. L., Martin-Zanca, D., and Chao, M. V. (1995) NGF binding to the trk tyrosine kinase receptor requires the extracellular immunoglobulin-like domains. *Mol. Cell Neurosci.* **6**, 97-105
95. Urfer, R., Tsoulfas, P., O'Connell, L., Shelton, D. L., Parada, L. F., and Presta, L. G. (1995) An immunoglobulin-like domain determines the specificity of neurotrophin receptors. *EMBO J.* **14**, 2795-2805
96. Wiesmann, C., Ultsch, M. H., Bass, S. H., and de Vos, A. M. (1999) Crystal structure of nerve growth factor in complex with the ligand-binding domain of the TrkA receptor. *Nature* **401**, 184-188
97. Arevalo, J. C., Conde, B., Hempstead, B. L., Chao, M. V., Martin-Zanca, D., and Perez, P. (2000) TrkA immunoglobulin-like ligand binding domains inhibit spontaneous activation of the receptor. *Mol. Cell Biol.* **20**, 5908-5916
98. Arevalo, J. C., Conde, B., Hempstead, B. I., Chao, M. V., Martin-Zanca, D., and Perez, P. (2001) A novel mutation within the extracellular domain of TrkA causes constitutive receptor activation. *Oncogene* **20**, 1229-1234
99. Xu, Y. (2002) Sphingosylphosphorylcholine and lysophosphatidylcholine: G protein-coupled receptors and receptor-mediated signal transduction. *Biochim. Biophys. Acta.* **1582**, 81-88
100. Soga, T., Ohishi, T., Matsui, T., Saito, T., Matsumoto, M., Takasaki, J., Matsumoto, S., Kamohara, M., Hiyama, H., Yoshida, S., Momose, K., Ueda, Y., Matsushime, H., Kobori, M., and Furuichi, K. (2005) Lysophosphatidylcholine enhances glucose-dependent insulin secretion via an

orphan G-protein-coupled receptor. *Biochem*. *Biophys*. *Res*. *Commun*. **326**(4):744-51

101. Maudsley, S., Pierce, K. L., Zamah, A. M., Miller, W. E., Ahn, S., Daaka, Y., Lefkowitz, R. J., and Luttrell, L. M. (2000) The beta(2)-adrenergic receptor mediates extracellular signal-regulated kinase activation via assembly of a multi-receptor complex with the epidermal growth factor receptor. *J. Biol. Chem*. **275**, 9572-9580
102. Lee, F. S., and Chao, M. V. (2001) Activation of Trk neurotrophin receptors in the absence of neurotrophins. *Natl. Acad. Sci. U. S. A*. **98**, 3555-3560
103. Lee, F. S., Rajagopal, R., Kim, A. H., Chang, P. C., and Chao, M. V. (2002) Activation of Trk neurotrophin receptor signaling by pituitary adenylate cyclase-activating polypeptides. *J. Biol. Chem*. **277**, 9096-9102
104. Masuda S, Murakami M, Takanezawa Y, Aoki J, Arai H, Ishikawa Y, Ishii T, Arioka M, Kudo I.(2005) Neuronal expression and neuritogenic action of group X secreted phospholipase A2. J. Biol. Chem. 280(24):23203-14
105. Scott GA, Jacobs SE, Pentland AP. (2006) sPLA2-X stimulates cutaneous melanocyte dendricity and pigmentation through a lysophosphatidylcholine-dependent mechanism. J. Invest. Dermatol. 126(4):855-61.
106. Blondeau, N., Lauritzen, I., Widmann, C., Lazdunski, M., and Heurteaux, C. (2002) A potent protective role of lysophospholipids against global cerebral ischemia and glutamate excitotoxicity in neuronal cultures. J. Cereb. Blood Flow Metab. 22, 821-834

論文の内容の要旨

応用生命工学専攻
平成 22 年度博士課程入学
氏　　名　　烏漢其木格
指導教員名　　北本　勝ひこ

論文題目

A study on the mechanism whereby lysophosphatidylcholine enhances neurotrophin-induced signals

（神経栄養因子シグナルに対するリゾホスファチジルコリンの増強作用に関する研究）

Introduction

Neurotrophins, including nerve growth factor (NGF) and brain-derived neurotrophic factor (BDNF), are essential regulators of neuronal differentiation, survival, plasticity, and other associated physiological actions of neurons throughout the entire life. By binding to their receptors TrkA (for NGF), TrkB (for BDNF), and p75 (for both), NGF and BDNF activate avariety of signals such as Ras-mitogen-activated protein kinase (MAPK), phosphatidylinositol 3-kinase-Akt, and phospholipase Cγ pathways. Our research group previously demonstrated that secretory phospholipase A_2 ($sPLA_2$), a group of enzymes that catalyze the hydrolysis of the *sn*-2 ester bond of membrane phospholipids to release free fatty acids and lysophospholipids, shows neurotrophin-like activity, i.e. induction of neurite outgrowth in PC12 cells, and protection of cerebellar granule neurons (CGNs) from apoptosis, mimicking the actions of NGF and BDNF. Subsequent studies showed that the neurotrophin-like actions of $sPLA_2$ are mediated through the release of one of the lysophospholipids, lysophosphatidylcholine (LPC). Indeed, LPC added to the cultures of PC12 and CGNs recapitulated the neurotrophin-like activity of $sPLA_2$. In this study, I have demonstrated that LPC promotes neurotrophin-Trk receptor signals in PC12 cells and in CGNs. I have also analyzed the underlying mechanism and confirmed that LPC specifically enhances NGF-induced signals through the extracellular domain of TrkA in PC12 cells, and BNDF-induced signals through TrkB in CGNs. Results from the neurite outgrowth assay in PC12 cells suggested that LPC at least partially potentiates NGF-induced differentiation of PC12 cells. It was unlikely that these processes were mediated by G

protein-coupled receptors G2A and GPR4, although they have been implicated in the biological actions of LPC in previous studies. Taken together, the findings obtained in this study might provide important evidences for the investigation of the mechanism by which LPC displays neurotrophin-like effect.

Chapter 1. Lysophosphatidylcholine promotes NGF-induced MAPK and Akt signals by enhancing the activation of TrkA in PC12 cells

LPC is one of the major lysophospholipids generated from the hydrolysis of phosphatidylcholine (PC) by $sPLA_2$. In our previous studies, LPC generated by $sPLA_2$ was found to induce neurite outgrowth in PC12 cells. Since NGF also induces neuronal differentiation, I tested if a cross-talk between NGF- and LPC-induced signals exists in PC12 cells by examining the effect of LPC on NGF-induced MAPK and Akt phosphorylation. I found that LPC significantly enhances NGF-induced MAPK and Akt phosphorylation. Other lysophospholipids, such as lysophosphatidic acid, lysophosphatidylethanolamine, and lysophosphatidylserine, did not display similar effect. Quantitative RT-PCR analysis showed that LPC upregulates the expression level of NGF-induced immediate early genes, c-*fos* and *NGF-IA*, which are necessary for the initiation and maintenance of differentiation. Neurite outgrowth assay showed that LPC partially potentiates NGF-induced differentiation of PC12 cells. Next, the signaling pathway by which LPC potentiates NGF-induced MAPK and Akt phosphorylation in PC12 cells was characterized. Phosphorylation of both MEK and TrkA, the upstream cellular components of MAPK, was enhanced by LPC. In contrast, LPC did not show any effect on MAPK phosphorylation induced by other growth factors, epidermal growth factor (EGF) and basic fibroblast growth factor. In accordance, EGF receptor phosphorylation induced by EGF was not increased by LPC. Furthermore, Akt phosphorylation induced by insulin-like growth factor-1 (IGF-1) was not affected by LPC. Collectively, these results indicate that LPC specifically promotes NGF-induced MAPK and Akt phosphorylation through enhancing the activation of TrkA.

Chapter 2. Lysophosphatidylcholine potentiates BDNF-induced MAPK and Akt signals through stimulating the activation of TrkB in cerebellar granule neurons

BDNF plays critical roles in regulating the survival and functions of neurons, particularly those in the brain, through binding to its receptor TrkB. BDNF is known to support the survival of cerebellar granule neurons (CGNs), the most abundant neurons in the brain, through the activation of Ras-MAPK pathway. Cultured CGNs are suitable model for studying the cell survival, since they undergo apoptosis when shifted to the culture medium containing low concentration of potassium (LK). IGF-1 is also known to protect CGNs from LK-induced

apoptosis through PI3K-Akt cascade. Previously, our research group showed that LPC protects CGNs from LK-induced apoptosis, mimicking the actions of BDNF and IGF-1, although the mechanism has not been identified. In this Chapter, I studied the effect of LPC on BDNF-induced MAPK and Akt phosphorylation in TrkB-transfected CHO-K1 cells and in CGNs. I first confirmed that MAPK was not phosphorylated upon treatments with BDNF, LPC, or both, in the wild type and vector-transfected CHO-K1 cells. In TrkB-transfected CHO-K1 cells, BDNF slightly induced phosphorylation of MAPK, which was significantly enhanced by LPC. In CGNs, although LPC alone did not induce phosphorylation of MAPK and Akt, it significantly elevated phosphorylation of MAPK and Akt induced by BDNF, but not by IGF-1. Furthermore, BDNF-induced TrkB phosphorylation was increased by LPC, suggesting that LPC promotes BDNF-induced MAPK and Akt signals through enhancing the activation of TrkB. Although LPC failed to further potentiate the effect of BDNF in rescuing CGNs from apoptosis, the results presented here, together with those shown in Chapter 1, indicate that LPC specifically enhances neurotrophin-Trk receptor signaling cascades.

Chapter 3. Analyses of the role of lysophosphatidylcholine on NGF-induced TrkA signal

Results shown in Chapter 1 demonstrated that TrkA, but not EGFR, is responsive to the effect of LPC. To further understand the mode of action of LPC on TrkA, I aimed to analyze the domain(s) of TrkA involved in the effect of LPC. To this end, I first analyzed receptor phosphorylation in TrkA-, EGFR-, or TrkA/EGFR chimera-transfected cells. However, spontaneous phosphorylation of TrkA occurred in transfected cells, and this was not further increased by NGF and/or LPC treatments, which hampered further analysis.

I next tested the effect of NGF, EGF, and LPC on the downstream signal, MAPK phosphorylation, in the same experimental system. I found that the wild type and vector-transfected CHO-K1 cells do not respond to NGF and EGF, i.e. MAPK was not phosphorylated upon NGF and EGF treatments, since no functional TrkA and EGFR were expressed in CHO-K1 cells. In TrkA-transfected cells, NGF weakly induced MAPK phosphorylation, and it was significantly increased by LPC. In EGFR-transfected cells, EGF induced MAPK phosphorylation, but this was not affected by LPC. These results indicate that transfected TrkA and EGFR behaved as those in PC12 cells. Next, the domain(s) of TrkA involved in the effect of LPC was analyzed by examining MAPK phosphorylation in TrkA/EGFR chimera-transfected CHO-K1 cells. TrkA/EGFR chimeras C1, C2, C3, and C4 were constructed by swapping the extracellular (ED), transmembrane (TMD), and intracellular (ID) domains between TrkA and EGFR. In C1 (TrkA ED/EGFR TMD+ID chimera)- or C3 (TrkA ED+TMD/EGFR ID chimera)-transfected cells, LPC enhanced MAPK phosphorylation triggered by NGF, as was seen in the TrkA-transfected cells. In C2 (EGFR ED/TrkA TMD+ID

chimera)- or C4 (EGFR ED+TMD/TrkA ID chimera)-transfected cells, MAPK was strongly phosphorylated upon EGF treatment, but this was not further enhanced by LPC. These results indicate that the ED, but not TMD and ID, of TrkA is responsible for the effect of LPC in enhancing NGF-induced MAPK phosphorylation.

As described in Introduction, LPC is generated through the hydrolysis of PC by $sPLA_2$. I next examined the effect of $sPLA_2$ addition on NGF-induced MAPK phosphorylation. I found that exogenously-added $sPLA_2$ enhances NGF-induced MAPK phosphorylation at a comparable level to LPC. This suggests that LPC generated *in situ* by the hydrolysis of plasma membrane PC acts synergistically with NGF.

Accumulating evidence suggests the involvement of G protein-coupled receptor, G2A and GPR4, in the biological actions of LPC. In addition, our research group previously found that $sPLA_2$-induced neuritogenesis in PC12 cells was mediated by G2A. I therefore examined if G2A and GPR4 regulate the effect of LPC on NGF-induced MAPK phosphorylation in PC12 cells. However, overexpression of neither G2A nor GPR4 affected the enhancement of NGF-induced MAPK phosphorylation by LPC, indicating that the action of LPC on NGF-induced MAPK phosphorylation is not mediated by G2A and GPR4.

It is well accepted that NGF induces dimerization and autophosphorylation of TrkA, thereby activating the downstream signaling events. Recently studies have shown, however, that the majority of TrkA preforms dimers in the endoplasmic reticulum before reaching to the cell surface; NGF activates the preformed, yet inactive, TrkA dimer on the cell surface. To examine if LPC regulates the dimerization state of TrkA, I performed crosslinking experiment using the divalent crosslinker bis[sulfosuccinimidyl] suberate. In accordance with the study, I succeeded in detecting TrkA dimer in TrkA-transfected PC12 cells irrespective of NGF addition. No increase in the amount of TrkA dimer was detected by LPC addition, indicating that LPC does not affect dimerization of TrkA.

Conclusion

Although various biological activities have been attributed to LPC, the precise mechanism is not fully understood. Results in this study have demonstrated that LPC enhances NGF-induced MAPK and Akt signaling pathways via the extracellular domain of TrkA. Similar effect was observed in BDNF-TrkB signaling. Further analyses suggested that LPC might display neurotrophin-like effect either by promoting NGF-induced MAPK and Akt signaling cascades, or through activating additional signaling pathway independently of NGF-TrkA. Deciphering the molecular mechanism of action of LPC might provide an important clue for the development of a new therapeutic method for neurodegenerative diseases.

Acknowledgments

First of all，I would like to express my greatest gratitude to my supervisor Professor Katsuhiko Kitamoto for giving me such a cherishable opportunity to study in the Laboratory of Microbiology, The University of Tokyo, and for his support and continuous encouragement throughout my work. I want to extend my thankfulness to Mrs. Kitamoto for warm reception in their house. Also, I would like to express my greatest appreciation to Dr. Manabu Arioka who gave me the chance to work with this project, and directly guided this work from the beginning to the end. Thanks for all his constructive guidance and corrections during all my studies in this laboratory. It is a pleasure to thank Dr. Jun-ichi Maruyama for his attentions and questions which made this work more accurate, and for always being kind.

I would like to express my thankfulness to Associate Prof. Hiroyuki Adachi from Graduate School of Agricultural and Life Sciences, Department of Biotechnology, The University of Tokyo, for his kindness and generous help in the work about apoptosis assay in CGNs.

A special thank of mine goes to Ms. Asako Itakura who instructed me to start this work from zero spending her precious time. Thanks for all her careful teaching and generous help. Also, I would like to thank the co‐authors Dr. Masato Tanaka and Ms. Yuri Matsuki, from Tokyo Denki University for their contributions to the paper in this thesis.

I would like to thank all members in the Laboratory of Microbiology, The University of Tokyo, especially members in the third building, for their company. All your kindness and help let me worked in a harmonious atmosphere during these years. Although I could not have more chance to talk with you, I will remember all of you forever. In addition, thank all staff in the Office for International Cooperation & Exchange and Student center for their help.

Then, I want to thank my friend Dr. William Valentine who is working as a researcher in

The University of Tokyo, for his discussion and important advices for the work about TrkA receptor by sparing his precious time. I also want to thank Professor Dehua Chang from Tokyo Women's Medical University for her invitation to visit the wonderful Institute of Advanced BioMedical Engineering and Science (TWIns) and exciting lecture about cell sheet engineering for myocardial tissue reconstruction. All these gave me a great encouragement. In addition, I have to thank my friends from Graduate Schools of Medicine and Pharmaceutical Sciences, The University of Tokyo, for their active talking, interesting questions, and advices for the work about TrkA/EGFR chimeras.

Now, I want to mention my deepest gratitude to the Watanuki International Scholarships Foundation for the scholarship for these years, to Japan Student Services Organization for the scholarship in the first year, to the supports from The University of Tokyo, and to Yamamoto Japan-China Academic Exchange Foundation for all the supports. Without all these help, I would be unable to complete my study here. All these kept me working hard. I also thank the University of Tokyo for giving me such a chance to study here, and for the beautiful Oiwake International Student's house. Thank all staff in this house for being so kind and talkative.

I would like to express my special gratefulness to Dr. Cristiane Akemi Uchima, Ms. Lin Zhu, and Ms. Yihan Huang for their voluble friendship, and warm concerns like families. Their understanding and help always encouraged me to continue. I cherish many holidays we spent together, too. Besides, I want to say thanks to Dr. Yujiro Higuchi and Dr. Cristopher S. Escano for their cheerful friendship. I also would like to thank my supervisor for my master degree and many of my friends in Inner Mongolia for their worm concerns and continues encouragement.

Finally, I would like to express my greatest and deepest thankfulness to my family, especially to my mother, to my boyfriend as well, for their enormous love.

2013-03 **烏漢其木格**